INTERACTIONS OCCURRING BETWEEN HALIDE IONS AND AQUEOUS AMMONIA UNDER ULTRA VIOLET LIGHT WITH LOW PRESSURE MERCURY LAMPS

by

Yvette Beckles

A dissertation submitted to the Graduate Faculty in Civil Engineering in partial fulfillment of the requirements for the degree of Doctor of Philosophy, The City University of New York

2007

ProQuest Information and Learning Company
300 North Zeeb Road
P.O. Box 1346
Ann Arbor, MI 48106-1346

This manuscript has been read and accepted for the
Graduate Faculty in Engineering in satisfaction of the
dissertation requirement for the degree of Doctor of Philosophy.

Professor Vasil Diyamandoglu

Date — Chair of Examining Committee

Dean Mumtaz Kassir

Date — Executive Officer

Professor John Filos

Professor Reza Khanbilvardi

Professor Haralambos Vasiliadis

Professor Urs Jans

Supervisory Committee

THE CITY UNIVERSITY OF NEW YORK

Abstract

INTERACTIONS OCCURRING BETWEEN HALIDE IONS AND AQUEOUS AMMONIA UNDER ULTRA VIOLET LIGHT WITH LOW PRESSURE MERCURY LAMPS

by

Yvette Beckles

Adviser: Professor Vasil Diyamandoglu

Ultraviolet (UV) technology is currently applied as a viable alternative in drinking water and wastewater applications, namely: disinfection and advanced oxidation processes (AOP). Nevertheless, little is known about the interactions that may occur between indigenous water constituents when exposed to UV irradiation. Such interactions may occur as secondary reactions, resulting in changes to effluent streams that might not meet mandatory regulations.

The indigenous water constituents investigated in this research included the interactions of individual halide ions, i.e. bromide (Br^-) chloride (Cl^-) and iodide (I^-) with ammonia (NH_3). The findings revealed that Br^- and Cl^- promote ammonia photo-oxidation in both acidic (pH 5) and alkaline (pH 8 – 10) solutions. I^- was unable to enhance the oxidation

of ammonia. The solution pH and oxygen concentration were depressed during ammonia oxidation while the halide ion concentrations remained unchanged. The extent to which halide ions were able to augment ammonia oxidation was found to be dependent on the type and concentration of the halide ion, as well as the initial solution pH. Nitrite (NO_2^-) and nitrate (NO_3^-) were produced as the major final stable products with the yields being associated with the solution pH during the irradiation. Bromate (BrO_3^-) and sulfur hexafluoride (SF_6) were used as electron (e^-) scavengers to demonstrate that e^- may be scavenged from the Charge Transfer to Solvent (CTTS) state of halide ions and that during ammonia photo-oxidation, e^- are generated.

Irradiation of a wastewater sample spiked with ammonia and its pH adjusted to 10 showed that ammonia oxidation in the presence of halide ions (chloride) occurs simultaneously with TOC degradation by UV irradiation. Approximately 30% of both TOC and ammonia degraded after 360 minutes of irradiation, while approximately 88% of the dissolved oxygen was consumed after 120 minutes of irradiation. Nitrite and nitrate were formed in the irradiating solution.

A reaction scheme proposed for the NH_3/Cl^- system and simulation of the reactions, demonstrated that the scavenging of electrons from the CTTS state of irradiated halide ions, forming an additional supply of hydroxyl (OH) and superoxide (O_2^-) radicals in solution was responsible for the enhanced rate of NH_3 oxidation observed.

Foreword

A number of advanced oxidation processes (AOP) employ low-pressure mercury lamps in conjunction with ozone and/or hydrogen peroxide to generate a copious supply of hydroxyl radicals, used to oxidize contaminated wastes. While several commercial-scale AOP technologies are available, there has been little research to assess the significance of secondary reactions occurring between indigenous water constituents when exposed to high doses of UV light. This research specifically examines the interactions that occur between halide ions (chloride and bromide) and ammonia to consider how these interactions may affect the effluents of UV systems exposed to high doses of UV light.

In order to observe the effects of these interactions on a bench scale, low-pressure mercury lamps (emitting at 254 nm and 185 nm) without the use of ozone and hydrogen peroxide was employed. Hydroxyl radical generation (which characterizes AOP technologies) in the water will occur due to the 185 nm wavelength, but on a smaller scale than when ozone and hydrogen peroxide are utilized.

INTERACTIONS OCCURRING BETWEEN HALIDE IONS AND AMMONIA UNDER UV LIGHT WITH LOW PRESSURE LAMPS

TABLE OF CONTENTS

No.		Page
1.	Introduction	1
2.	Thesis Objectives	4
3.	Literature Review	5
	3.1. Sources and occurrence of inorganic halogenated water constituents	5
	3.1.1. Halide ions	5
	3.1.2. Bromate	8
	3.2. Sources and occurrence of ammonia in water	11
	3.3. Photochemistry of water	11
	3.4. Photochemistry of Halide ions	12
	3.5. Photochemistry of Bromate	18
	3.6. Photochemistry of aqueous ammonia	20
4.	Hypothesis	27
5.	Methods and Materials	28
6.	Results and Discussion	33
	6.1. UV irradiation of halide ions with Low-pressure Mercury Lamps	33
	6.2. UV irradiation of Aqueous Ammonia	36
	6.3. UV irradiation of halide ions in the presence of ammonia	41

6.3.1. Halide Ions enhance ammonia oxidation 41

6.3.2. Effect of halide ion concentration, DO and pH 48

6.3.2.1. Effect of Initial Solution pH 48

6.3.2.2. Effect of Halide Ion Concentration 52

6.3.2.3. Influence of Dissolved Oxygen 71

6.3.2.4. Influence of UV Wavelength 75

6.4. Electron Generation during Ammonia photo-oxidation 77

6.4.1. Oxidation Reduction Potential of NH_3 Irradiated Solutions 77

6.4.2. Scavenger Studies to Verify the Electron Availability in NH_3 Irradiated Solutions 82

6.4.3. UV Irradiation of Bromate in NH_3 Solutions 87

7. Reaction Scheme and Simulation of the Cl^- / NH_3 system 102

7.1. Development of Reaction Scheme for Cl^- / NH_3 system 102

7.2. Simulation and Sensitivity Analysis 104

8. Conclusions 119

Appendices 121

Appendix A

TABLE I – Reaction Scheme for Cl^- / NH_3 system 121

Appendix B 126

Tables of Simulated Results 126

Tables of Selected Experimental Results 140

Bibliography 152

LIST OF TABLES

Table		Page
3.1	Typical Concentrations of Chloride in Various Source Waters	6
3.2	Summary of Bromide Concentration in Natural Water	7
3.3	Summary of Bromate Formation in Ozonation Plants	9
3.4	Ammonia Concentrations in Water in Selected Countries	11
3.5	Halide ion Properties Relative to CTTS Spectroscopy	14
5.1	Analytical Conditions for Ion Chromatograph	30
5.2	Expected Method Detection Limit	30
6.1	Photo-oxidation of Aqueous Ammonia in the Presence of Bromide Ions at Initial Solution pH 5.6	53
6.2	k_{obs} and % Conversion of Ammonia for Various X^-/N Ratios	63
6.3	Effect of NH_4^+ Concentration on BrO_3^- Photodecomposition	93

LIST OF FIGURES

Figure		Page
5.1	Sample Chromatogram of Four Anions	31
6.1	UV Irradiation of Halide Ions	34
6.2	UV Irradiation of Ammonia Solutions at Initial pH 8 and 10	39
6.3	Initial (a) and Final (b) Chromatograms for Ammonia Irradiation at pH 5.8	40
6.4	Comparison between the Halide Ions in forming NO_3^- during NH_3 Oxidation	42
6.5	Comparison of NH_3 Oxidation at (a) pH 8 and (b) pH 10 Under: (i) Dark (ii) UV Light and (iii) UV Light and Br^- or Cl^-	44
6.6	UV Irradiation of I (2 mg/L) in the Presence of NH_3 (NH_4^+ = 1.6 mg/L) at Initial pH of 5.7 and Adjusted to pH 10.4 after 60 minutes	47
6.7	Photo- products Generated from the UV Irradiation of Br^- (2.28 mg/L) in the Presence of Ammonia (1.6 mg/L as N) at Various Initial pH	50
6.8	pH Profiles of UV Irradiated Solutions of Halide Ions in the Presence of NH_3	51
6.9	Photokinetics of Br^- / NH_4^+ System in Producing Nitrate and Depressing pH	54
6.10	Effect of Halide Ion Concentration on NH_3 Oxidation	

	with Low-Pressure Mercury Lamps	56
6.11	Halide Ion Concentration in UV Irradiated Solutions Containing NH_3	58
6.12	Effect of Halide Ion to Ammonia-Nitrogen Molar Ratio on the Pseudo First-Order Representation of NH_3 Decay in the Presence of Halide Ions, k_{obs}	61
6.13	% Conversion of Ammonia as a Function of k_{obs}	62
6.14	Nitrite Conversion to Nitrate at Various X^-/N Ratios	67
6.15	pH Adjustment to Achieve Greater NH_3 Oxidation Cl^- = 115 mg/L, NH_3-N = 7.58 mg/L	68
6.16	UV Irradiation of Wastewater Containing Organics, Ammonia and Chloride Ions	70
6.17	Kinetic Profiles of Dissolved Oxygen in Irradiated NH_3-N (1.6 mg/L) Solutions Containing Halides	73
6.18	Effect of Dissolved Oxygen on NH_3 Oxidation and the Products of NH_3 Oxidation	74
6.19	UV Irradiation of a Cl^- /NH_3 solution with Sleeves Designed to Block the Transmission of 185 nm Wavelength	76
6.20	Kinetics of ORP and pH for Irradiated Aqueous Solutions of (i) NH_3 and (ii) NH_3 with Cl^- = 20 mg/L	79
6.21	pE – pH Diagram for Irradiating NH_3 and NH_3/Cl^- Solutions	81
6.22	Sulfate Formation in UV Irradiated SF6 Solutions (i) in the absence of NH_3 (ii) in the presence of NH_3-N = 1.6 mg/L	84

6.23 UV Irradiation of Br^- (2.22 mg/L) and Cl^- (7.4 mg/L) in the Absence and Presence of NH_3 (1.6 mg/L as N) 86

6.24 UV Irradiation of BrO_3^- in the Absence and Presence of NH_4^+ 90

6.25 First-Order Representation of BrO_3^- Photodecomposition without (k_{1obs}) and with (k_{2obs}) NH_4^+ 91

6.26 Effect of Initial BrO_3^- Concentration (C_0) on its Rate of Photodecomposition 92

6.27 First-Order Representation of BrO_3^- Photodecomposition at Different Initial Concentrations 92

6.28 Effect of NH_4^+ Concentration on BrO_3^- Photodecomposition 94

6.29 Effect of pH on the Photodecomposition of BrO_3^- in the Presence of NH_4^+ (Br:N = 1.5) 96

6.30 Influence of BrO_3^--Br/N Ratio on Kobs for BrO_3^- Decay 97

6.31 NO_3^- Formation and pH Change Resulting from BrO_3^- Photodecomposition in the Presence of NH_4^+ 99

6.32 BrO_3^- Decomposition with (i) UV (ii) UV and NH_3-N = 1.6 mg/L (iii) UV, NH_3-N = 1.6 mg/L and Cl^- = 10 mg/L 100

6.33 Relationship between the Br/N Ratio Applied and % Conversion of NH_4^+-N to NO_3^--N after 1 hr 101

7.1 Simulated and Experimental Kinetic Profiles for UV Irradiated Ammonia Solutions 107

7.2 Comparison of Simulated and Experimental NO_3^- Formed during UV Irradiation of Ammonia and Chloride Ions 110

7.3 Comparison of Experimental and Simulated Kinetic Profiles of NH_3-N (1.6 mg/L) Oxidation in the Presence of Cl^- = 20 mg/L for Different Scavenger Rates 112

7.4 Comparison of Experimental and Simulated Kinetic Profiles of NH_3-N (1.6 mg/L) Oxidation in the Presence of Cl^- = 20 mg/L for Different CTTS Formation Rates 116

7.5 Comparison of Experimental and Simulated Kinetic Profiles of NH_3-N (1.6 mg/L) Oxidation in the Presence of Cl^- = 20 mg/L for Different CTTS Formation Rates and Cl Scavenging from NO_3^- 117

7.6 Comparison between Combined Simulated and Experimental Results for NH_3-N (1.6 mg/L) Oxidation in the Presence of Cl^- = 20 mg/L for Different CTTS Scavenging Rates. 118

1.0 INTRODUCTION

Ultraviolet (UV) irradiation is the application of light of wavelengths 1 nm to 400 nm. UV technology is widely used in drinking water and wastewater treatment for disinfection and advanced oxidation processes (AOP). The lamps employed include:

i. Low-pressure mercury lamps (LPML) emitting primarily at 253.7 nm, although small amounts of emissions may also occur at 184.9 nm if the lamp is made from clear fused quartz or synthetic fused silica.

ii. Medium pressure mercury lamps can emit over the UV wavelength range 170 – 400 nm.

Although LPML applications are mostly employed in disinfection, their effectiveness in Advanced Oxidation Processes (AOP) for reduction of volatile and semi-volatile organic compounds, and removal of water contaminants e.g. *N*-nitrosodimethylamine has already been demonstrated (EPA/625/R-98/004, December 1998, Sharpless and Linden 2003).

LP applications for AOP usually incorporate processing with ozone, and/or hydrogen peroxide in order to improve the rate of contaminant reduction by generating an adequate supply of hydroxyl radicals ($^{\bullet}OH$). While the use of UV in water treatment is expanding, too few studies exist on the interactions that may occur when common water constituents are exposed to UV light. Such studies are important for effective UV process control and effluent quality control.

This thesis specifically addresses the interactions that occur between halide ions, namely chloride (Cl^-) and bromide (Br^-) when irradiated with low-pressure lamps in the presence of ammonia (NH_3). The monovalent ionic states of the halogen elements (fluoride, chloride, bromide and iodide) are prevalent in source waters used for drinking water treatment, chloride being the most abundant halide of incoming raw water to drinking water facilities. While the halide ions are not harmful to health in drinking water, their presence in source waters of drinking water treatment facilities can result in the generation of some harmful by-products.

Several species of inorganic halogenated water contaminants can occur in drinking water, as a result of drinking water treatment, however only a few are currently regulated by the EPA. In particular, ozonation used for disinfection and oxidation can produce considerable quantities of bromate through direct reaction with bromide ions. Bromate has long been recognized as a genotoxic carcinogen and the EPA has imposed a Maximum Contaminant Level (MCL) of 10 μg/L for this drinking water contaminant.

In estimating the levels of exposure of bromate from drinking water in the Netherlands (van Dijk-Looijaard and van Genderen, 2000) it was found that the relative contribution of drinking water to total exposure approached 100%. By comparison, the exposure level of bromate from drinking water served to 11 communities in the U.S. (noted for the highest bromate levels reported from 1998 to 2003, www.ewg.org/tapwater/contaminants was 61.2%.

Level of Exposure = (average yearly concentration / MCL) x 100

Bromate minimization strategies currently employed by ozone users, include reduction of ozone dose, ammonia addition and pH depression, but an effective yet economical removal strategy is still elusive. In order to meet health-based goals for bromate while maximizing the advantages of ozone in drinking water treatment, bromate removal strategies will have to be adopted. UV has been assessed as the only disinfectant that does not result in the formation of disinfection by-products. However, its potential to transform species that are ubiquitous to water, especially in AOP has not been investigated.

2.0 THESIS OBJECTIVES

The objectives of the research are as follows:

(a) Demonstrate that halide ions enhance the oxidation of NH_3 under low-pressure UV light.

- The influence of pH, dissolved oxygen (DO) and halide ion concentration effects on NH_3 oxidation in the presence of halide ions will be explored.

(b) Describe a reaction pathway for NH_3 oxidation in the presence of halide ions by:

- Utilizing the results of (a) above.
- Showing that electrons (e^-) are generated during NH_3 oxidation, by means of an electron scavenger and a water contaminant that is known to react readily with electrons (i.e. bromate).
- Simulation of the NH_3 / Cl^- UV-system using where available, the reactions and rate constants reported in the literature.

3.0 LITERATURE REVIEW

3.1. Sources and Occurrence of Selected Inorganic Halogenated Water Constituents

3.1.1. Halide Ions

Halide ions (namely chloride and bromide) are ubiquitous to source waters employed for drinking water purposes and are also found in significant quantities in some wastewaters. These ions are relatively stable in flowing water and are not known to have detrimental health effects. The USEPA and EU have set a secondary standard of 250 mg/L for chloride in drinking water, since elevated concentrations result in a salty taste. Variable quantities of halides in water exist as a result of natural processes (seawater intrusion, weathering of geological formations, etc.) and anthropogenic activities (chemical manufacture, mining of potassium and coal, etc.). Chloride is the most abundant halide of incoming raw water to drinking water facilities, with typical concentrations depicted in Table 3.1.

Chloride and bromide exhibit a strong correlation. In a survey of 35 drinking water companies in the U.S. the average Cl^-/Br^- ratio of incoming source water was 333 (Krasner et al., 1989) with a range of 100 to 667 (Krasner et al., 1993). The pre-anthropogenic Cl^-/Br^- ratio in groundwater in the United States has been

reported in the range of 40 for the continental interior to 300 in coastal regions (Davis et al., 2001). The Cl^-/Br^- ratio has been found to be a useful parameter in predicting anthropogenic and marine/evaporitic chloride occurrence in water (Rao et al., 2005). Magazinovic et al., 2004 have also shown that Br and Cl ions exhibit high linear correlation in surface and ground waters although the regression coefficients varied slightly from one location to another. Table 3.2 shows the ranges of bromide concentrations present in natural waters in various locations around the world (adapted from Magazinovic et al., 2004).

Table 3.1 Typical Concentrations of Chloride in Various Source Waters (Hanes et al, 1970)

SOURCE OF WATER	TYPICAL CHLORIDE CONCENTRATION (mg/L)
Rainwater	0 – 2
Upland surface water	0 – 12
Unpolluted river water	0 – 15
Spring water	0 – 25
Deep well water	0 – 50
Seawater	20,000

TABLE 3.2 Summary of Bromide Concentration in Natural Water

Water Source	Country	Bromide (mg/L)	Reference
Reservoirs	United States	0.006 – 0.083	Amy et al., 1993
	France, UK, Spain	0.030 – 0.070	Legube, 1996
Surface waters	United States	0.002 – 0.426	Westerhoff et al., 1994
	UK	0.100 – 0.120	Bourgine et al., 1993
	Germany	0.006 – 0.280	Haag and Hoigne et al., 1982
	France	0.055 – 0.202	Lefebvre et al., 1995
	Poland	0.400 – 0.700	Olsinska, 1994
	Israel	2.000	Rebhun, et al., 1988
	Australia	0.139 – 4.13	Magazinovic et al., 2004
Ground waters	United States	0.002 – 2.690	Westerhoff et al., 1994
	England	0.026 – 2.226	Houghton, 1946
	France	0.190 – 0.647	Lefebvre et al., 1995
	France, UK, Spain	0.040 – 0.140	Legube, 1996
	Australia	0.152 – 2.04	Magazinovic et al., 2004
Sea	Atlantic	65.000	Stumm and Morgam, 1981

Iodide ions occur the least in surface and ground waters (0.1 to 20 μg/L, Leitner, et al., 1998). Typical concentrations are usually <10 μg/L although they have been reported to reach levels greater than 50 μg/L due to seawater intrusion (von Gunten, 2003).

3.1.2. Bromate

Bromate may be present in drinking water originating from the raw water sources and by formation when source waters (both surface and ground waters) containing bromide ions are treated with ozone. While the bromide ion is not considered to be harmful in the concentrations found in drinking water, bromate pose serious health concerns. Bromate is classified as a potential human carcinogen (von Gunten, 2003 and WHO, 1993). As such, the USEPA and the European Union have established maximum contaminant limits (MCL) for this contaminant in drinking water at 10 µg/L (USEPA, 1998; EU, 1998). In addition, the USEPA in its Stage 1 Disinfectants and Disinfection by-products Rule has recommended a maximum contaminant level goal (MCLG) of zero for bromate. Even at current regulatory levels, it is a challenge for several utilities (with incoming raw water Br^- >50 µg/L) utilizing ozone to control bromate generation during typical treatment conditions (Westerhoff, P. 1994). Bromate generation during normal drinking water treatment conditions with ozone can range between < 2 – 150µg/L (Glaze et al., 1993 and von Gunten et al., 1996). A summary of bromate formation in full-scale ozonation plants in Europe and the U.S. is provided in Table 3.3.

TABLE 3.3 Summary of Bromate Formation in Ozonation Plants (adapted from von Gunten, 2003)

Country	No. of plants	Br^- range (µg/L)	BrO_3^- range (µg/L)	No. of Plants > 10 µg/L BrO_3^-	References
France	10	12 – 658	<2 –19	2	Lefebvre et al., 1995
France	32	<20 – 200	<2–19.6	2	Legube, 1996
Germany	4	30 – 150	<1 – 12	1	Sacher et al., 1995
Switzerland	86	<5 – 50	<0.5–20	2	von Gunten / Salhi, 2000
Canada	12	N/A	0.4–5.98	0	Health Canada, 1998
USA	24	2 – 180	0.1 – 40	3	Daw, 2000
USA	Pilot plant research	300 – 1400	8 – 180		Krasner et al., 1991
UK	2	N/A	10 – 20	2	Hutchinson et al., 1995

Bromate formation is encouraged by high ozone exposures (von Gunten et al., 2000). Among several bromate minimization strategies proposed for ozone users, ammonia addition and pH depression (usually < 6) are applicable in drinking water treatment. Even though a 50% reduction in bromate generated may be achieved with either minimization strategy, these methods were found to be incapable of reducing the bromate formed during the initial phase of ozonation (Pinkernell and von Gunten, 2001). Limitations also exist on their applicability in that pH depression is costly in high alkalinity waters and ammonia addition is only effective up to a certain NH_3 concentration (0.2 mg/L) above which, further BrO_3^- minimization does not take place, thus restricting its use in waters containing medium to high levels of ammonia.

The use of some advanced oxidation processes (AOP) such as O_3/γ-irradiation and O_3/H_2O_2/ γ-irradiation can also increase the formation of bromate in bromide-containing waters (von Gunten and Oliveras, 1998). In addition to bromate forming in ozone treated waters iodate may also form if iodide is present in the raw water. However, iodate is not considered to be problematic since it is retransformed endogenically back to iodide. Chloride is not oxidized by ozone (von Gunten, 2003).

Meunier et al. (2006) recently investigated a drinking water treatment strategy employing the sequential use of low-dose ozone (0.5 mg/L) and UV. While this strategy was found to be effective for disinfection and bromate minimization, taste and odor problems were only solved with a higher ozone dose (1 mg/L), which lead to higher bromate formation. Bromate removal strategies after ozonation may have to be considered if regulatory levels are further reduced to meet the recommended Maximum Contaminant Level Goal (MCLG). One of the objectives of this study was to investigate the effect of ammonia (NH_3) oxidation under UV irradiation with LPML in accelerating the decomposition of BrO_3^-. This may be a potential bromate removal strategy for ozonated waters containing bromide ions and medium to high ammonia concentrations (> 0.2 mg/L) since ammonia is not readily removed by conventional treatment systems.

3.2 Sources and Occurrence of Ammonia in Water

Ammonia may be present in source waters (lakes, rivers, and groundwater) due to biological degradation of nitrogenous organic matter, fertilizers and industrial waste

discharges. Table 3.4 shows the ranges of concentrations of ammonia in treated, surface and ground waters in selected countries.

TABLE 3.4 Ammonia Concentrations in Water in Selected Countries

COUNTRY	AMMONIA CONCENTRATION RANGE (mg/L AS N)	NO. OF SITES TESTED	REFERENCE
Bangladesh	2.27 – 19.93[t]	35	Anawar et al., 2003
Canada	< 0.02 – 0.65[g,s]	19	Health Canada, 1987
Vietnam	< 2 – 25[t]	8	Duong et al., 2003
U.S.A.	0.002 – 2.69[g] 0.002 – 0.426[s]	101	Westerhoff et al., 1994
g – ground water	s – surface water		t – treated water

Westerhoff et al. (1994) surveyed 101 U.S. drinking water utilities and found that ammonia concentrations in the source waters ranged between 0.04 – 0.69 mg-N/L and had corresponding Br^- concentrations ranging from 0.002 to 2.69 mg/L.

3.3 Photochemistry of Water

The work of Boyle et al., (1969) has demonstrated that solvated electrons (e_{aq}^-) are generated in pure water when relatively low energy UV photons are applied. It was determined that the minimum energy required for hydrated electron formation was 6.5eV (i.e. 190 nm). The quantum yield (Φ) of e_{aq}^- was estimated as 0.0127 (Sauer et al., 2004). Others have proposed different mechanisms for the water ionization process, but it is generally accepted that solvated electrons, as well as the hydroxyl radical (OH) and hydrogen atom (H) are all formed when UV light or other forms of radiation are applied

to neat water (Bartels and Crowell, 2000; Hart and Anbar, 1970). The quantity of each species formed is dependent on the nature of the radiating source. For example, water will homolyze mainly into hydroxyl radicals and hydrogen atoms under vacuum-UV at $\lambda \leq 172$ nm (Heit et al, 1998). The gross reaction of water radiolysis is given by:

$$H_2O + h\nu \rightarrow e_{aq}^- (2.7), H (0.6), OH (2.8), H_2O_2 (0.7), H^+ (3.2), OH^- (0.5)$$

where the G-values are given in parentheses (i.e. G-value = number of changed molecules per 100 eV (1.6×10^{-17} J) absorbed energy). In the photodecomposition of dilute aqueous solutions, these radicals may play a significant role in the photo-reduction of some water constituents.

3.4 Photochemistry of Halide Ions in Water

Under UV irradiation, halide ions (X^-) in aqueous solutions have been shown to exhibit broad absorption spectra (referred to as charge-transfer-to-solvent or CTTS spectra) in the UV region (Stein and Treinin, 1958). It should be noted that these states are non-existent in the gaseous state. The CTTS states are transient and correspond to the transfer of an electron from the p-shell of the halide into unoccupied orbitals of the solvent (Sobolewski and Domcke, 2003). These unoccupied orbitals constitute the polarization well formed by the surrounding water molecules (Long et al., 1994). In water association studies with diatomic sodium chloride (NaCl) it was found that full dissociation of the salt in forming the ions, Na^+ and Cl^- was not achieved until nine water molecules were added (Yamabe et al., 2000). The first solvent shell or polarization well is therefore formed by at least nine water molecules surrounding the halide ions (Ohtaki, and Radnai, 1993).

The properties of halide ions that are comparative to CTTS spectroscopy are given in Table 3.5 (source: Blandamer and Fox, 1969; Sauer et al., 2004) below. As can be seen from the table, the greater the ionic radius in going from chloride to iodide, the lower the energy required for ionization of the halide and correspondently longer wavelengths of light necessary. The maximum energy of absorption for a CTTS band (E_{max}) is a measure of the difference between the energies of the excited state and the ground state (Blandamer and Fox, 1970). The CTTS state is not a property of the isolated ion, but rather is induced by the surrounding water molecules (Borgis and Staib, 1996). Elementary reaction channels may therefore follow CTTS formation: direct ejection of the electron into a solvent cavity away from the parent atom, germinate recombination of the electron and the parent atom, formation of a transient atom-electron pair.

TABLE 3.5. Halide ion properties relative to CTTS spectroscopy

ION	**Ionic radius (Å)**	**Ionization Potential**		**Energy of absorption maximum, E_{MAX} for a CTTS Band (kcal/mol.)**
		(kcal/mol)	**Photolysis Wavelength (nm)**	
Chloride	1.64	83.67	185	155.8
Bromide	1.80	77.91	229, 185	143.7
Iodide	2.05	70.99	254	126.4

Models have been developed to describe CTTS spectra (Blandamer and Fox, 1970). The confined model describes CTTS as a potential energy well formed by nearby solvent

molecules. The energy needed to transfer an electron from zero potential and zero kinetic energy into this well is composed of two parts: the ionization potential (IP) and the kinetic energy of the electron within the well. Hence $E_{max} = IP + h^2/8mR_e^2$ where h is the Planck's constant, m is the mass of an electron and R_e is the radius of the potential energy well or orbital of the excited state (Blandamer and Fox, 1970).

Earlier work conducted by Jortner et al., (1964) suggested that the dissociation of the CTTS state led to the formation of a photochemical cage of the halide atom (X_{aq}) with the ion-expelled solvated electron (e_{aq}^-).

$$X^- + h\nu \rightarrow X_{aq}^- \rightarrow [X_{aq} + e_{aq}^-] \quad (1)$$

(excited ion, CTTS state) *(radicals in solvent cage)*

The species identified in parentheses, are formed as radical pairs in close proximity and are often referred to as radicals formed in a "solvent cage", since the solvent temporarily encapsulates the radicals, causing them to remain as colliding neighbors before they either diffuse apart or are recombined.

Sauer et al (2004) using femtosecond (fs) time-resolved laser spectroscopy, observed that electron photo-detachment from aqueous ions occur via two different mechanisms operating independently:

- The dissociation of a CTTS state creates a narrow distribution of electrons around the parent radical or atom. Kinetic studies and molecular dynamics simulations of halides suggest that an attractive mean force potential exist between the electron and the atom (Kloepfer et al., 2002; Kloepfer et al., 2000).

- The generation of solvated electrons by direct photo-ionization: Direct ionization of monovalent anions may or may not occur depending on the excitation energy (Barthel and Schwartz, 2003); the higher the excitation energy the greater the quantum yield for electron detachment.

The following equations depict the phenomenon of electron photo-detachment in halide ions according to Sauer et al., 2004:

Dissociation of a CTTS state:

$$X^- + h\nu \rightarrow X^{-*} \rightarrow [X + e^-]_{cage} \quad (2)$$

(excited ion) *(radicals dissociated from CTTS state)*

Direct photo-ionization:

$$X^- + h\nu \rightarrow X^{-*} \rightarrow X + e_{aq}^- \quad (3)$$

(excited ion) *(free radicals)*

The work of Long et al., 1994 also suggests that solvated electrons are formed from a photo-ionized state instead of CTTS excitation. An energy representation of the CTTS potential well and the excitation processes associated with the CTTS states of halide ions were presented as follows (Long et al., 1994):

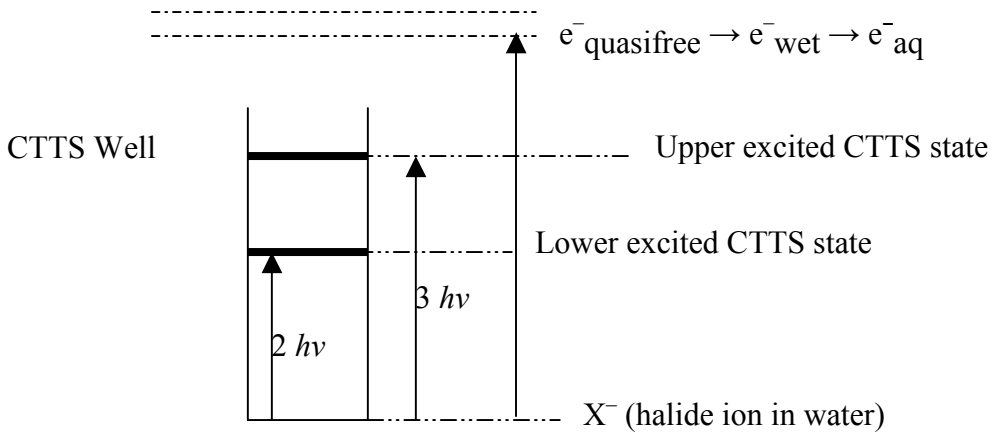

Transient CTTS spectra are universal to the halide ions in polar fluids. The kinetics of the CTTS electron is dependent on the wavelength (and therefore the photon-energy) of the incident radiation. The formation of CTTS spectra for I^- was observed from wavelengths (Long et al., 1994) as high as 625 nm (1.9 eV) and 450 nm (2.75 eV) for bromide. The CTTS state for chloride was not detected at 400 nm but its absorption lie further (lower) in the UV range of wavelengths, since the CTTS spectra is blue-shifted due to a decrease in ion radius (as observed with Br^- and I^-). Indeed, CTTS excitation has been studied for Cl^- at 193 nm (Sauer et al., 2004) and 185 nm (Dainton and Fowles 1965).

Light intensity had a noticeable effect on the CTTS states of I^- (Long et al., 1994). Two-photon excitation of iodide (I^-) resulted in the formation of the upper excited CTTS state, which relaxed in <50 fs to the lower excited CTTS state. The latter then relaxed in 80 fs to the ground state of I^-. Three-photon excitation of I^- was found to result in photo-ionization and the generation of aqueous electrons. This intensity dependence was

claimed to be responsible for I^- being promoted to the upper CTTS state or undergoing direct photo-ionization.

The radical formation process in equations (2) and (3) above competes with the recombination process back to the aqueous ion in solution (Jortner et al., 1964). Radical recombination may take place by either of the following processes (Noyes, 1955):

Primary Recombination where the radicals formed have not yet been separated by solvent molecules

Diffusive (secondary) Recombination where the radicals are encapsulated by solvent molecules but are still in close proximity

Bulk Recombination where radicals have escaped secondary recombination and have achieved homogeneous distribution within the solvent. When there are no scavengers present, these radicals will ultimately recombine via this process.

A photochemical cage recombination efficiency, also known as the "photochemical cage effect, F_{cP}" (Braden et al., 2001) is defined as the ratio of the cage recombination rate constant to the sum of the rate constants for all cage processes, i.e.

$$F_{cP} = k_c / (k_c + k_d)$$

where k_d and k_c are the forward and backward reaction rates respectively of the photochemical reaction producing the radical pair from the halide ion.

It should be noted that the cage effect formed by photochemical processes are not necessarily similar to those formed under thermal or diffusional collision for the same radical cage pair.

Cage effects are important in explaining a host of kinetic and reaction phenomena in photochemical and thermal reactivity in solution, including variations in products and yields. The Noyes' mathematical description of the cage effect, as presented in Braden et al., (2001) predicted that the cage effect increases as radical size increases and as radical mass decreases. One explanation offered was that radicals with lower mass would be less able to break out of the solvent cage due to lower momentum. The Noyes' cage effect theory can be expressed as:

$$k_d / k_c = (F_{cP}^{-1} - 1) \cong m^{1/2} / r^2$$

where m = mass of the radical, r = radius of the radical, F_{cP}, k_d and k_c are as previously defined.

3.5. Photochemistry of Bromate

The photodecomposition of aqueous bromate solutions has been studied using UV light, γ-radiation and high-energy electron beam irradiation (Buxton and Dainton, 1968; Siddiqui et al., 1996). The general consensus with respect to the mechanism of photodecomposition is that BrO_3^- decomposes via indirect photolysis where solvated electrons in the water are responsible for bond cleavage between bromine and oxygen atoms. Several intermediate oxy-bromine are formed prior to the final stable reduction product, the bromide ion. The reaction schemes proposed (Buxton and Dainton, 1968; Siddiqui et al., 1996; NDRL) are as follows:

Direct Steps in Bromate Photodecomposition

$BrO_3^- + e^-_{aq} \rightarrow BrO_2^\bullet + O^{2-}$ $\quad k_1 = 4.1 \times 10^9$; 3×10^9 $M^{-1}s^{-1}$

$BrO_2^\bullet + e^-_{aq} \rightarrow BrO_2^-$ $\quad k_2 = 1 \times 10^{10}$ $M^{-1}s^{-1}$

$BrO_2^- + e^-_{aq} \rightarrow BrO^\bullet + O^{2-}$ $\quad k_3 = 1.8 \times 10^{10}$; 1×10^{10} $M^{-1}s^{-1}$

$BrO^\bullet + e^-_{aq} \rightarrow BrO^-$ $\quad k_4 = 1 \times 10^{10}$ $M^{-1}s^{-1}$

$BrO^- + e^-_{aq} \rightarrow Br^- + O^-$ $\quad k_5 = 2.3 \times 10^{10}$; 2×10^{10} $M^{-1}s^{-1}$

Side-Reactions of intermediates formed

$2BrO_2^\bullet \rightarrow Br_2O_4^\bullet$ $\quad k_6 = 1.4 \times 10^9$ $M^{-1}s^{-1}$ and $K = 19M^{-1}$

$Br_2O_4^\bullet + OH^- \rightarrow H^+ + BrO_2^- + BrO_3^-$ $\quad k_7 = 7 \times 10^8 M^{-1}s^{-1}$

$BrO_2^- + OH \rightarrow OH^- + BrO_2$ $\quad k_8 = 1.9 \times 10^9$ $M^{-1}s^{-1}$

$BrO^\bullet + BrO_2^- \rightarrow BrO^- + BrO_2^\bullet$ $\quad k_9 = 3.4 \times 10^8$ $M^{-1}s^{-1}$

$2BrO + H_2O \rightarrow BrO^- + BrO_2^- + 2H^+$ $\quad k_{10} = 4.9 \times 10^9$ $M^{-1}s^{-1}$

$BrO^- + O^- \rightarrow BrO + O^{2-}$ $\quad k_{11} = 4.6 \times 10^9$ $M^{-1}s^{-1}$

$BrO^- + OH \rightarrow BrO + OH^-$ $\quad k_{12} = 4.5 \times 10^9$ $M^{-1}s^{-1}$

where: $BrO_2^\bullet$ - bromite radical $\quad BrO_3^-$ - bromate ion

$Br_2O_4^\bullet$ - peroxybromite radical $\quad BrO_2^-$ - bromite ion

$BrO^\bullet$ - hypobromite radical $\quad BrO^-$ - hypobromite ion

Br^- - bromide ion

During the course of bromate photodecomposition free bromine (OBr^- / HOBr) may be formed due to the generation of the hypobromite ion as an intermediate, in accordance with the equation below:

$OBr^- + H^+ \rightarrow HOBr$ $\qquad p\mathit{K}_a = 8.8$

Hypobromous acid reacts rapidly with aqueous ammonia forming three species of bromamines, viz: monobromamine (NH_2Br), dibromamine ($NHBr_2$) and tribromamine (NBr_3) (Inman and Johnson 1984; Hofmann and Andrews, 2001).

$HOBr + NH_3 \rightarrow NH_2Br + H_2O$ $\qquad k = 7.5 \times 10^7\ M^{-1}s^{-1}, 4 \times 10^7\ M^{-1}s^{-1}$

$HOBr + NH_2Br \rightarrow NHBr_2 + H_2O$ $\qquad \mathit{K}_{eq} = 4.4 \times 10^8$

$HOBr + NHBr_2 \rightarrow NBr_3 + H_2O$ $\qquad \mathit{K}_{eq} = 5.3 \times 10^6$

The extent to which these chemical reactions will occur under UV light in the BrO_3^- / NH_4^+ system and the fate of the bromamines generated, will be explored in examining the photoreduction of bromate in the presence of ammonia.

3.6. Photochemistry of Aqueous Ammonia

Wang et al (1994), Kim et al (2002), Klare et al., (2000) and Schmelling et al., (1995) reported that the simultaneous application of catalyst and UV light was necessary to effect NH_3 oxidation in solutions with a pH range 1 – 6, while only UV illumination was required in basic solutions.

In water, ammonia exhibits a pH-dependent equilibrium as follows:

$NH_4^+ \rightleftharpoons NH_3 + H^+$ $\qquad p\mathit{K}_a = 9.3$

Some studies (Bravo et al., 1993, Wang et al., 1994; Bonsen et al., 1997) have reported that ammonia oxidation rates are higher in alkaline solutions rather than neutral or acidic solutions. Zhu et al., 2005 further demonstrated that the pH-dependent equilibrium

between the ammonia species in water was responsible for the increased photocatalytic rate of ammonia oxidation with increasing pH. They found that the photocatalytic ammonia oxidation rates were proportional to NH_3 concentration, not total ammonia ($NH_3 + NH_4^+$) concentration.

Aqueous ammonia solutions can yield nitrite/nitrate as the final stable photolytic products under certain radiolytic and photolytic conditions (i.e. vacuum-UV, X-ray irradiation, gamma-irradiation, LPML) where the hydroxyl radical initiates the oxidation in radiolysis (Dwibedy et al., 1996) and produces the aminyl radical [NH_2]. The initiation reaction is given as,

$$NH_3 + {}^{\bullet}OH \rightarrow NH_2^{\bullet} + H_2O \qquad k = 1.0 \times 10^8\ M^{-1}s^{-1}$$

It should be noted that the species, NH_4^+ does not react with ${}^{\bullet}OH$, however, it may be slowly converted to the species, NH_3 by reaction with hydrated electrons (Shiraishi et al., 1994; Gonzalez and Braun, 1996).

$$NH_4^+ + e_{aq}^- \rightarrow NH_3 + H \qquad k = 1.6 \times 10^6\ M^{-1}s^{-1}$$

In the absence of oxygen, the aminyl radical ($NH_2^{\bullet}$) dimerize to form hydrazine [N_2H_4] (Laszlo et al., 1998). The reaction of $NH_2^{\bullet}$ in the presence of O_2 forms the aminylperoxyl radical [$NH_2O_2^{\bullet}$] and hydrazine is not a radiolysis product. The aminylperoxyl radical subsequently deprotonates and isomerizes to form $NO^{\bullet}$ (and H_2O) and in the presence of the superoxide radical [$O_2^{\bullet -}$] there is rapid formation of peroxynitrite, $ONOO^-$ (Laszlo et al., 1998).

$$NO^{\bullet} + O_2^{\bullet -} \rightarrow ONOO^- \qquad k = 3.8 - 19 \times 10^9\ M^{-1}s^{-1}$$

Peroxynitrite exhibits a pH-dependency of species in water:

$$ONOOH \rightleftharpoons ONOO^- + H^+ \qquad pK_a = 6.6 - 6.8$$

$ONOO^-$ / ONOOH decomposes by a combination of complex pathways to yield nitrite and nitrate as the final stable photolytic products. Peroxynitrous acid (ONOOH) is a reactive oxidizing species, decomposing by a first-order mechanism with nitrate/nitric acid as the major product. ONOOH also decays by O–O bond cleavage/cage recombination whereby the $NO_2^\bullet$ and $OH^\bullet$ radicals formed either escape the cage or are recombined forming nitrate/nitric acid (Halfpenny and Robinson, 1952; Mahoney, 1970). The experimental results of Hodges and Ingold (1999) Kirsch et al., (2003) and Lymar and Hurst (1998) confirm a 28% cage escape of $NO_2^\bullet$ and $OH^\bullet$ radicals. The schematic below represents the mechanisms.

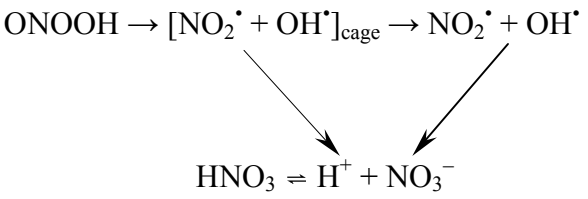

NO_2^-/NO_3^- proportions were found to vary with pH, where pH inflection points occurred approximately at 3.1, 5.8, 6.8, 8.0 and 11.9 (Kirsch et al., 2003). Generally, nitrate is the major product, at pH < 7 but nitrite formation increases intensely at the expense of nitrate at pH >7.3. The generation of the radicals, $NO^\bullet$ and $NO_2^\bullet$ during peroxynitrite decay is claimed to be responsible for the pH-dependent production of NO_2^-/NO_3^- via a series of intermediate reactions, forming pH-dependent species.

At low pH < 3 nitrite is not formed at the expense of nitrate and conversion of nitrite to nitrate results mainly from the dis-proportionation of nitrous acid. However, in the pH

range 3.1 to 5.5 some nitrite starts to form from peroxynitrite. At pH 5.8 a further step increase in nitrite generation occurs with a corresponding step decrease in nitrate levels due to the decomposition of peroxynitrate (O_2NOO^-, pKa = 5.5 – 5.9) to nitrite and oxygen, as shown below (Loegager & Sehested, 1993).

$$O_2NOO^- \rightarrow O_2 + NO_2^- \qquad k = 1.0\ s^{-1}$$

One route to peroxynitrate formation is the radical-radical reaction of $NO_2^\bullet$ and $O_2^{\bullet-}$ (Halfpenny & Robinson, 1952).

$O_2^{\bullet-} + NO_2^\bullet \rightarrow O_2NOO^-$ $\quad k = 4.5 \times 10^9\ M^{-1}s^{-1}$ (Halfpenny & Robinson, 1952)

At pH > 8.0, nitrite production surpasses that of nitrate generation, leaving nitrite as the major final product. At pH 9 – 10 yields of both nitrite and nitrate stabilize at values of 65% ± 5% and 35% ± 5% respectively.

The formation of hydrogen peroxide (H_2O_2) in gamma-irradiated solutions of ammonia was also observed, both in oxygenated and aerated systems (Dwibedy et al., 1996). Its yield was determined to be less than the expected value if it reacts only with hydrated electrons. Another pathway suggested for H_2O_2 consumption in irradiated ammonia solutions was reaction with $NH_2^\bullet$ radicals. In aerated solutions the H_2O_2 concentration reached a plateau of about 1 mg/L at an irradiation dose of

5×10^{-18} eV, but its concentration continued increasing at a significant rate in oxygenated ammonia solutions.

In considering the photochemistry of aqueous ammonia, not only the photochemistry of intermediates needs to be considered but also of the formed products. The photo-

reduction of nitrate in natural water results in nitrite as the major product, but the conversion was found to be a function of irradiation time and the presence of natural organic matter (Bems et al., 1999). Even in the presence of a photocatalyst, i.e. titanium dioxide, the photoreduction of nitrate was not promoted but instead acted as a catalyst in re-oxidizing nitrite to nitrate (Bems et al., 1999). The photolysis of nitrate has been shown to produce the hydroxyl radical in quantities that are important to the degradation of dissolved organic aquatic contaminants (Brezonik and Fulkerson-Brekken 1998). Dissolved organic matter in surface waters was generally found to be more important scavengers of the hydroxyl radical than inorganic carbonate forms. However, it was reported that when nitrate undergoes UV photolysis in the presence of dissolved inorganic carbon, the yield of nitrite decreased at pH ≈ 8, but remained unchanged at pH 6 (Sharpless and Linden, 2001). The presumption was that aqueous carbon dioxide reacts with peroxynitrite ($ONOO^-$), a major intermediate in nitrite (NO_2^-) formation, thus reducing the formation of nitrite at the higher pH. Some of the important reactions involved in the photolysis of nitrate, in the presence of CO_2 (aq) are as follows (Sharpless and Linden, 2001):

- $NO_3^{*-} \rightarrow ONOO^-$ (isomerization of the excited-state NO_3^-)
- $NO_3^{*-} \rightarrow [NO_2^{\bullet} + O^{\bullet-}]$ (radicals formed in a solvent cage from excited-state NO_3^-)
- $[NO_2^{\bullet} + O^{\bullet-}] + H^+ \rightarrow NO_2^{\bullet} + OH^{\bullet} \rightarrow ONOOH$ (formation of hydroxyl radical and cage recombination)
- $ONOOH \rightleftharpoons ONOO^- + H^+$ $pK_a = 6.8$ (acid/base pair equilibrium)
- $ONOO^- \rightarrow NO_2^- + ½O_2$ (nitrite formation via intermediates)

- The radical, $NO_2^{\bullet}$ may also be directly reduced via the following two reactions.)
- $2NO_2^{\bullet} \rightarrow N_2O_4 + H_2O \rightarrow NO_2^- + NO_3^- + 2H^+$
- $NO_2^{\bullet} + O_2^{\bullet -} \rightarrow NO_2^- + O_2$

Nitrite undergoes photolytic decomposition under light in the wavelength region 200 – 400 nm, forming the radicals $NO^{\bullet}$ and $O^{\bullet -}$ but at pH < 12 $O^{\bullet -}$ readily protonates to $OH^{\bullet}$. In oxygenated solutions $NO^{\bullet}$ is oxidized to nitrate (Mack and Bolton, 1999).

It has long been shown that aqueous ammonia has the potential to accelerate the photodecomposition of certain water contaminants. In particular, Farkas and Klein (1948) showed that aqueous ammonia has the potential to accelerate the photodecomposition of bromate. The phenomenon was ascribed to the reactions of hypobromous acid (formed as an intermediate in the photo-degradation of aqueous bromate) with ammonia, forming the less absorbing Br^- species. This suggestion was neither verified nor fully investigated and relies on the assumption that BrO_3^- decays solely by light absorption under UV with low-pressure lamps. However, it was reported earlier that the general consensus with respect to the mechanism of photodecomposition is that BrO_3^- decomposes via indirect photolysis where electrons in the water are responsible for bond cleavage between bromine and oxygen atoms. Several intermediate oxy-bromine species are formed prior to the final reduction product, the bromide ion.

Chenthamarakshan and Rajeshwar (2000) also observed that ammonium ions in solution displayed remarkable ability in accelerating the photocatalytic reduction of Cr(VI) to

Cr(III). The role played by ammonia in this phenomenon was claimed to be that of proton supply. It was observed that during photocatalysis in the presence of NH_4^+, nitrate was formed and a substantial change in pH occurred due to the release of protons into solution.

While the preceding explanations provide an insight into the possible role played by ammonia in accelerating the photodecomposition of two independent water contaminants, additional studies are necessary to confirm these hypotheses and to determine whether a general behavioral concept may be applicable to ammonia's accelerating role in the photo-reduction of water contaminants.

4.0 HYPOTHESIS

It is hypothesized that:

I. Halide ions enhance the oxidation of ammonia under LPML by:

- The scavenging of e^- by O_2 (i.e. dissolved oxygen in the water) out of the CTTS states of halide ions, forming greater quantities of O_2^- in the irradiating water.
- Increasing the supply of OH radicals in the irradiating water.

II. The enhanced decay rate of the water contaminant BrO_3^- in the presence of NH_3 results from the combined effect of:

- Halide ions enhancing the photo-oxidation of NH_3.
- The photo-oxidation of NH_3 generates electrons (e^-) in sufficient quantities to accelerate the photodecomposition of bromate.

The hypothesis I above will be tested via the simulation of reactions pertinent to the Cl^-/NH_3 system obtained from the literature and the outcome compared with experimental results. Hypothesis II will be evaluated using the electron scavenger, sulfur hexafluoride (SF_6).

5.0. RESEARCH METHODOLOGY AND MATERIALS

5.1. Materials

Chemicals used in the preparation of solutions for irradiation were of analytical grade and were used as received. Chemicals used for calibration purposes were sourced from Sigma with a purity > 99.9% (Deisenhofen, Germany). All solutions were prepared from Milli-Q water, with TOC < 6 ppb.

5.2. Experimental Methods

Batch experiments were used to evaluate the photochemical reactions taking place. The photoreactions were conducted in a 5-L glass photo-reactor, which is unambiguously described in Talu and Diyamandoglu, 2004. The cylindrical glass reaction chamber has an internal diameter of 17cm, a height of 35cm and was covered with a 1 inch thick Teflon cover. Low-pressure (mercury) lamps (ACE, Model 12128) each with a total output of 3.5W, length 27cm and emitting light at both 254 nm and 185 nm, were individually suspended in quartz tubes each with an internal diameter of 2.15cm, length 34cm and wall thickness of 1.35mm.

Known concentrations of the halogenated water constituents and/or NH_3 were spiked into Milli-Q water up to a total volume of 5 liters and irradiated with four (4) of the UV low-pressure mercury lamps and having a combined light intensity of 5.27×10^{-6} E/l·s, (as measured by potassium ferrioxalate actinometry). An electric-powered, arc-shaped, stirrer blade that was axially poised at the bottom of the glass reactor provided mixing of the

aqueous contaminants during the photoreactions. Ozone that may be formed in the air spaces between the lamps and the quartz tubes was removed by suction and bubbled through an acidified potassium iodide solution (20g/L of KI and 3mg/L conc. H_2SO_4).

All experiments were conducted at a controlled temperature of 20^{o}C. During the course of the irradiation, pH (measured with a pH electrode; Model 465-25-90-K9, Mettler Toledo Process Analytical, Inc., Wilmington, MA), temperature and dissolved oxygen (measured with an Ingold oxygen sensor; Mettler Toledo Process Analytical, Inc., Wilmington, MA) were continuously monitored and samples were withdrawn at pre-determined time intervals (with wasting, approx. 20mL, occurring between sampling) and analyzed for the following constituents:

- Halide species (i.e. fluoride, chloride, bromide and iodide)
- Halite species (i.e. chlorite ions)
- Halate species (i.e. bromate ions and chlorate ions)
- Sulfate ions
- Aqueous nitrogen species (e.g. nitrate, nitrite, ammonia)

5.3. Analytical Procedures

The following instruments were employed in quantifying the constituents in the water samples:

(1) Ion Chromatograph – to analyze for bromide, chloride, iodide, bromate, chlorite, nitrate and nitrite anions in the samples. The Dionex DX 500 Chromatography system consists of the following components: AS 40 Automated Sampler, GP 40

Gradient Pump, CD 20 Conductivity Detector and Peaknet Software. The analytical conditions employed for oxy-anions and halide quantification are listed in Table 5.1. The method detection limits for the analytes are given in Table 5.2.

Table 5.1. Analytical Conditions for Ion Chromatograph

Method Parameter	***Method Specification***
Analytical Columns	Dionex Ionpac AG9-HC and AS9-HC, 4mm
Eluent	9.0 m*M* sodium carbonate (Na_2CO_3)
Eluent flow-rate	1.0 mL/min
Detection	Suppressed conductivity (ASRS-ultra 4mm; external water mode
Sample injection volume	200 μL

Table 5.2. Expected Method Detection Limit

Analyte	***Expected MDL (μg/L)***
Bromate (BrO_3^-)	1.73[a]
Bromide (Br^-)	1.78[a], 7.8[b]
Nitrate (NO_3^-)	7.7[b]
Nitrite (NO_2^-)	6.5[b]

Reference: a - *Dionex* Application Note 81, **b** - *Dionex* Application Note 133

A sample chromatogram, using the method outlined in Table 5.1 and showing the measured above-mentioned analytes is displayed in Figure 5.1 below.

Peak. Num.	Retention Time	Component Name	Concentration mg/L	Peak Height	Peak Area
2	5.65	BROMATE	0.284	8327	86970
6	9.85	BROMIDE	0.674	13493	238206
7	11.30	NITRATE	0.070	6843	120435
10	17.05	SULPHATE	4.311	87174	2511396
		Totals	5.339	115836	2957007

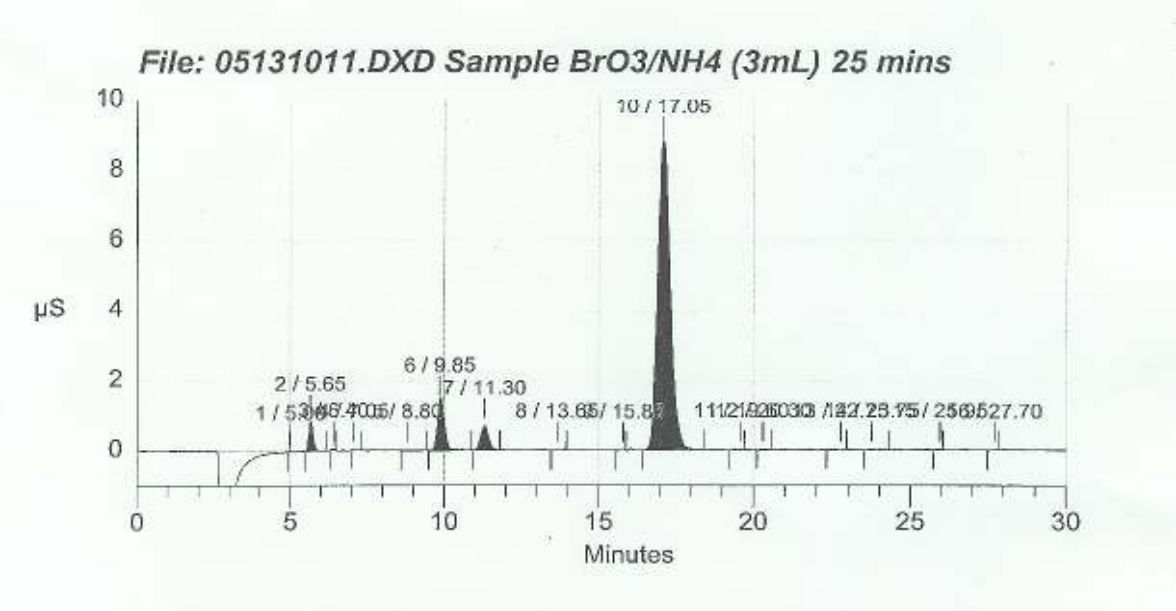

Figure 5.1. Sample Chromatogram of four Anions using method outlined in Table 5.1.

(2) Spectrophotometer – used to measure ammonia concentration by the colorimetric method. The method to be used is the indophenol blue method and is based on the reaction of ammonia in alkaline solution with phenate, producing a blue color in the presence of a strong oxidizing agent, like hypochlorite. A metal-containing catalyst like nitroferricyanide (nitroprusside) is used to speed the reaction. The method is simple and involves the addition and mixing of specified quantities of the reagents (i.e. phenol solution, nitroferricyanide and oxidizing agent) into a 10mL volume of sample. The indophenol blue color is allowed to develop for at least one hour, after which the absorbance is measured on the spectrophometer (HP8453 UV-visible spectrophotometer will be used). Concentration of ammonia is related to the absorbance and a standard calibration curve is therefore required.

6.0 EXPERIMENTAL RESULTS AND DISCUSSION

6.1. UV Irradiation of Halide Ions with Low-Pressure Mercury Lamps

The ionization wavelengths of Br^- and Cl^- are 229 nm and 185 nm respectively (Sauer et al, 2004) and therefore it is not expected that these ions will decay to any significant extent with the low-pressure mercury lamps emitting primarily at 253.7 nm, with only small emissions at 185 nm. Chloride and bromide ion oxidation by hydroxyl radicals (formed as a result of water irradiation) are analogous, forming the hydroxide and halide atom by a pH dependent equilibrium (von Gunten, 2003 and Ross et al., 1998).

$$Cl^- + OH \rightleftharpoons ClOH^- \qquad k_f = 4.3 \times 10^9\ M^{-1}s^{-1},\ k_r = 6.0 \times 10^9\ s^{-1}$$

$$ClOH^- + H^+ \rightleftharpoons Cl + H_2O \qquad k_f = 2.0 \times 10^{10}\ M^{-1}s^{-1},\ k_r = 1.6 \times 10^5\ s^{-1}$$

The steady-state concentrations of $ClOH^-$ and $BrOH^-$ are small because of the very fast reverse reactions. Consequently, the concentrations of Cl and Br will be very small and dependent on the pH; hence there should be negligible overall change in the concentrations of Cl^- and Br^-.

Solutions of each halide ion were irradiated in the pH ranges 5.72 – 5.98 and 9.79 – 10.08. The results depicted in Figure 6.1 showed no noticeable changes in pH and ion concentration of Br^- and Cl^- in either pH range. However, in the case of iodide (I^-) at an initial solution pH of 5.72, the pH of the irradiating iodide solution progressively increased while the concentration of iodide concurrently decreased. When the solution pH was adjusted to 9.79 the iodide concentration immediately increased as a result of iodine atoms scavenging electrons from the hydroxide ions (Ross et al., 1998).

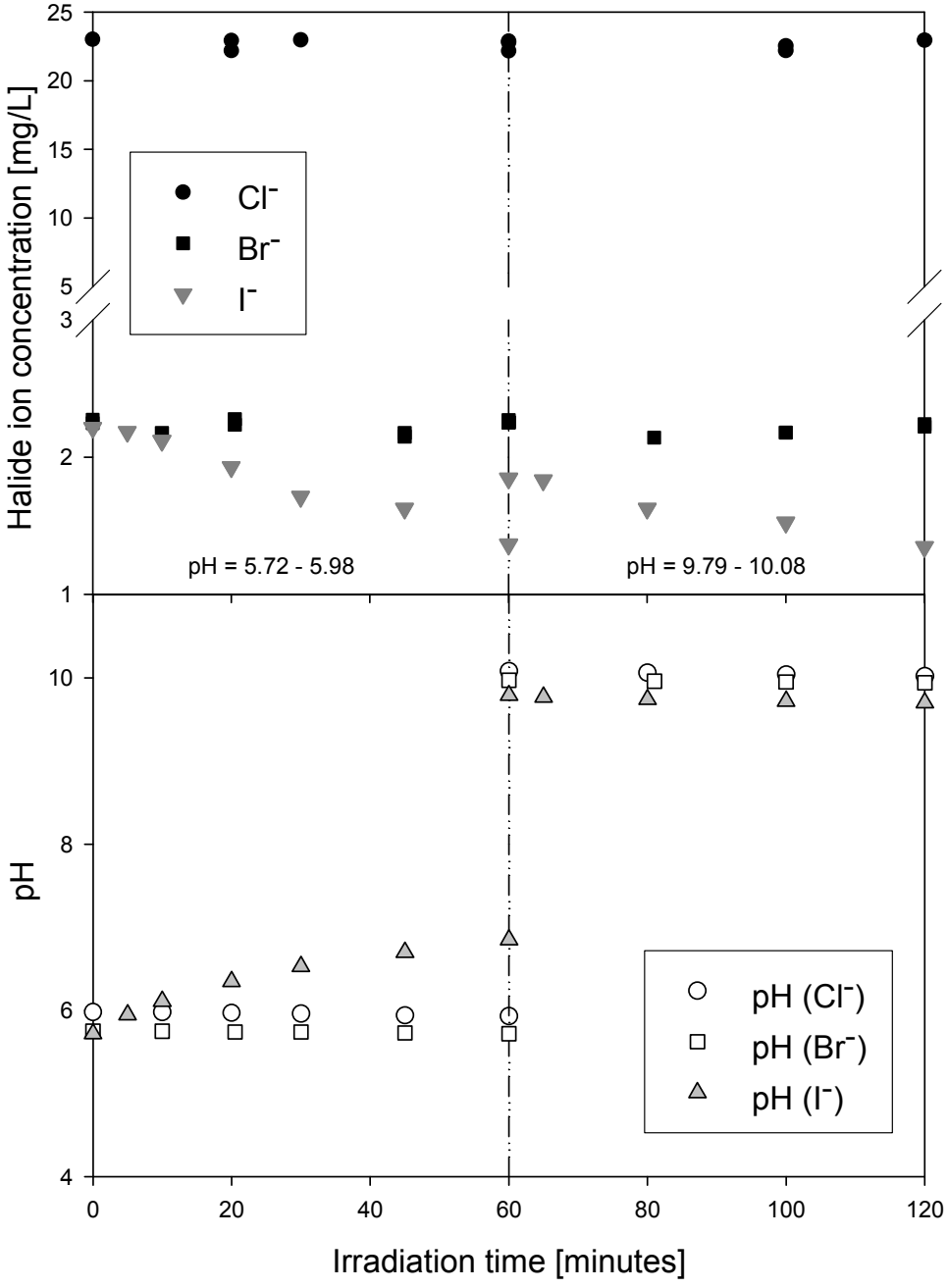

Figure 6.1 UV Irradiation of Halide Ions

$$I + OH^- \rightarrow I^- + OH$$

Upon the application of UV light, I^- decreased (at elevated pH) but the change in pH was inconspicuous because only a small molar concentration of hydroxide ions (i.e. ≤ 2.2 / 126.9 = 0.017 mM) is consumed in comparison to its concentration in the alkaline solution. The ionization wavelength for iodide is 254 nm (Sauer et al., 2004) and therefore it was expected that this ion would undergo direct photolysis decaying to the iodine atom.

These findings also support the theory of electron photo-detachment from halide ions (Blandamer and Fox, 1970). In the case of Cl^- and Br^- the electron photo-detachment from the aqueous anion occurs via the short-lived CTTS states (Sauer et al., 2004). Since there were no scavengers in the water to permanently remove the electrons in the CTTS band when the UV light is shut off, the ion concentration remains unchanged.

$$Br^- + h\nu \rightarrow [Br + e^-]_{CTTS}$$

$$[Br + e^-]_{CTTS} \rightarrow Br^-$$

and

$$Cl^- + h\nu \rightarrow [Cl + e^-]_{CTTS}$$

$$[Cl + e^-]_{CTTS} \rightarrow Cl^-$$

In the case of I^- electron photo-detachment takes place by direct ionization, forming the solvated electron and iodide atom as free radicals. Solvated electrons react with the H^+ (available in greater concentrations in acidic solutions) in accordance with the following reactions, increasing the pH of the solution as observed in the case of iodide:

$I^- + h\nu \rightarrow I + e_{aq}^-$

$I + I^- \rightleftharpoons I_2^-$

$H^+ + e_{aq}^- \rightarrow H$ and

$H + e_{aq}^- + H_2O \rightarrow OH^- + H_2$

As hydrated electrons are consumed, the concentration of iodide is depleted. It should be noted that the hydrated H^+ is unable to scavenge trapped electrons in the CTTS states (Hamill, 1968 and 1969) so in the case of Cl^- and Br^- only oxygen in the system can scavenge the trapped electron forming the superoxide radical (O_2^-). Since there are no sinks for O_2^-, the concentrations of Cl^- and Br^- remain unchanged in dynamic equilibrium according to the following reactions.

$O_2 + e_{aq}^- (\text{or } e^-) \rightleftharpoons O_2^-$

$X^- + hv \rightarrow [X + e^-]$

$X + e_{aq}^- \rightarrow X^-$

6.2 UV Irradiation of Aqueous Ammonia

Several studies (Wang et al., 1994; Kim et al., 2002; Klare et al., 2000; Schemelling et al., 1995) have supported the thought that only the NH_3 species of ammonia is oxidized since they only observed ammonia oxidation taking place in alkaline solutions. This species is predominant at pH > pK_a for ammonia (i.e. pK_a = 9.456 @20^{o}C). In verifying this observation for the experimental conditions employed, ammonia solutions at initial pH 8 and 10 were irradiated. Ammonia oxidation proceeded with greater percent conversion achieved at the higher initial solution pH 10. Figure 6.2 shows the kinetic profiles for ammonia decay

and nitrite/nitrate generation for the two pH values. As the initial solution pH increases from 8 to 10 the major final stable product changes from nitrate to nitrite. At initial solution pH 8 only nitrate was formed during ammonia oxidation, while nitrite was undetected as the pH of the solution was depressed. A slight decline in pH was also observed for the irradiating ammonia solution at initial pH 10 but both nitrite and nitrate were observed as the final products, nitrite being in excess.

In order to confirm that ammonia irradiation in acidic solution was not taking place under the experimental conditions tested, an aqueous solution of ammonia (in deionized water) at initial solution pH 5.5 was irradiated for almost two and one half hours but nitrate/nitrite formation was not observed as shown in Figure 6.3 (a) and (b). When analyzing for NO_2^- and NO_3^- with the ion chromatograph employed, the retention time range of these species in the column were 7.5 – 9.5 and 9.5 – 10.5 minutes respectively. If either of these species were formed their peaks would have been observable on the chromatographs at the respective retention times. It is therefore apparent that the ammonium (NH_4^+) species that predominates in acidic solution is not oxidized.

The literature reports that hydroxyl radicals forming the aminyl radical (NH_2) oxidize NH_3 and the reaction of NH_4^+ with OH radicals is too slow for observation (Neta et al., 1978).

$$NH_3 + OH \rightarrow NH_2 + H_2O$$

Aqueous electrons react with NH_4^+ but only at a slow rate of reaction.

$$NH_4^+ + e_{aq}^- \rightarrow NH_3 + H^\bullet \qquad k = 1.6 \times 10^6\ M^{-1}s^{-1}$$

This reaction is probably not important in the oxidation of ammonia with low-pressure mercury lamps. The reaction pathway to nitrite/nitrate involves oxygenated species formed by irradiation of water and the presence of dissolved oxygen.

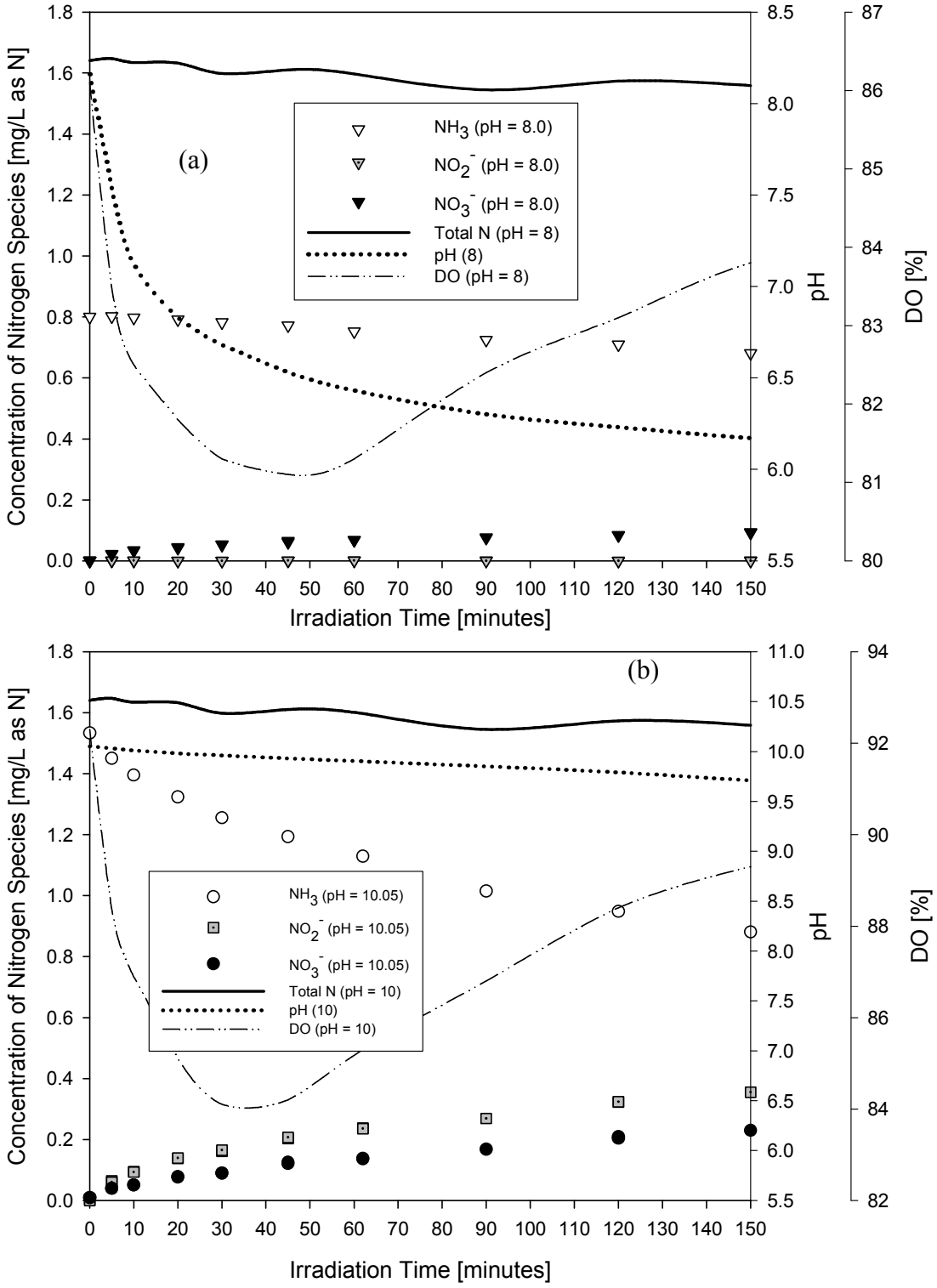

Figure 6.2 UV Irradiation of Ammonia Solutions at Initial pH 8 and 10

(a)

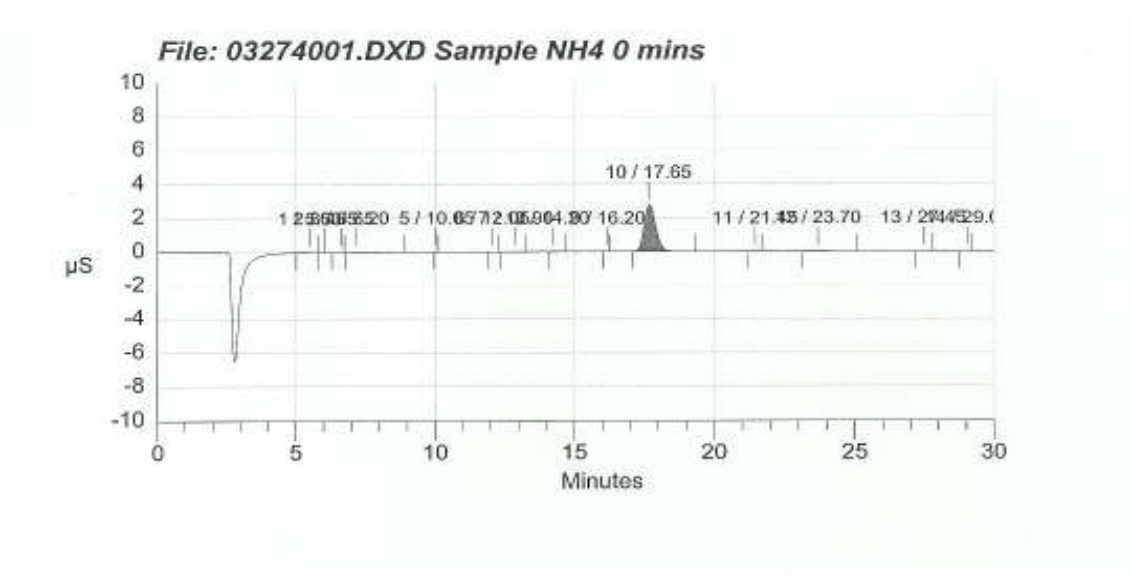

(b)

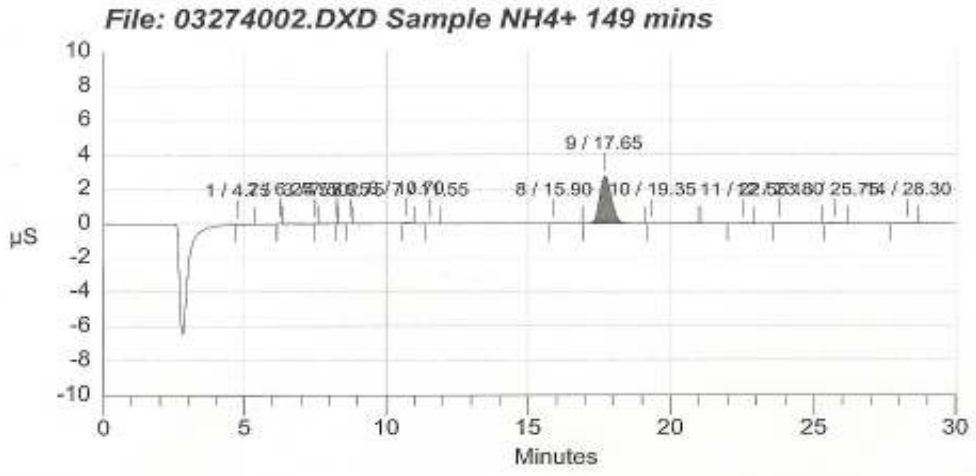

Figure 6.3. Initial (a) and Final (b) Chromatographs for Ammonia Irradiation at pH 5.8 for 149 minutes.

6.3 UV Irradiation of Halide Ions in the Presence of Ammonia

6.3.1 Halide ions promote the oxidation of NH_3 under UV light

Experiments were conducted to observe the effects of halide ion presence in UV irradiated ammonia solutions. It was found that the existence of halide ions in the ammonia solutions promoted the rate at which ammonia oxidation occurred under UV light under specified conditions.

In acidic solutions (pH range 5.5 – 5.8) experiments were set up to compare the rate of formation of NO_3^- / NO_2^- using different concentrations of halide ions. Concentrations were varied to compare on a molar basis as well as to reflect the typical concentrations found in source water used for drinking water. Large iodide concentrations were employed in order to see the anion on the chromatograph.

In acidic solutions where ammonia oxidation does not normally take place under UV light alone, it was found that NH_3 oxidation progressed to a limited extent in the presence of Cl^- and Br^-. Figure 6.4 shows the NO_3^- formation (NO_2^- was not formed at this pH) for various concentrations of Cl^- and Br^- at initial pH 5.5 – 5.8. The kinetic profiles of nitrate generation from NH_3 oxidation in the presence of Br^- / Cl^- depicted that smaller concentrations of Br^- were more effective in promoting NH_3 oxidation than Cl^- since larger amounts of nitrate were formed with smaller molar concentrations (compare Br^- = 2.22 mg/L with Cl^- = 1.0 mg/L which both correspond to a molar concentration of 0.028 mM). In the case of iodide, there was no formation of either NO_3^- / NO_2^- observed in acidic solution.

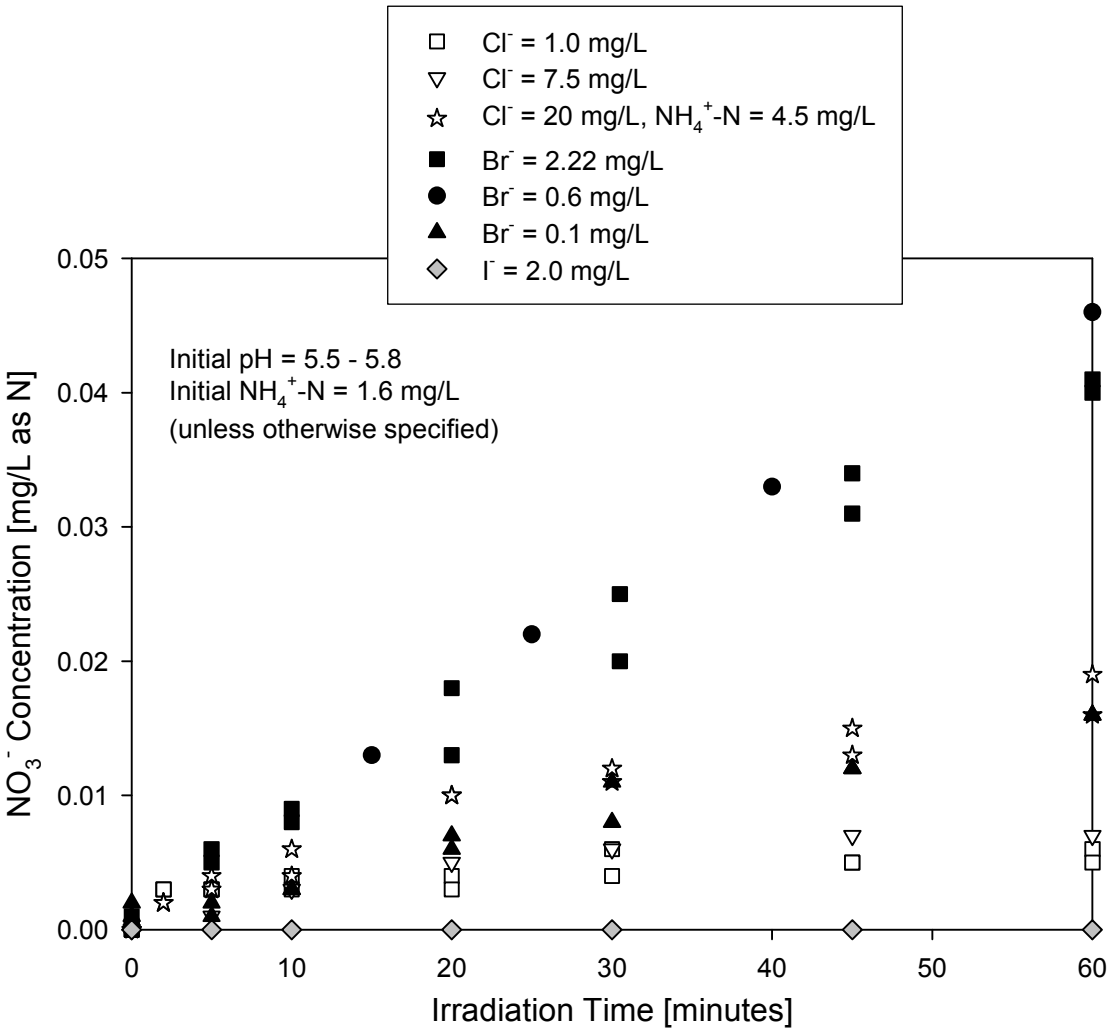

Figure 6.4 Comparison Between the Halide Ions in Forming NO_3^- During NH_3 Oxidation

Figure 6.5 (a) and (b) depicts the results of ammonia oxidation at initial solution pH 8 and 10 respectively under the following conditions:

(i) Dark

(ii) UV application only and

(iii) UV light employed in the presence of halide ions.

In the absence of light, ammonia oxidation did not take place at either pH values, the ammonia, nitrite and nitrate concentration kinetics remained flat. When UV irradiation was applied, ammonia oxidation ensued at both pH 8 and 10 with ammonia oxidation occurring to a greater extent at the higher pH of 10. This result is in agreement with Dwibedy et al., 1996 who indicated that higher concentrations of NH_3 (resulting from higher pH) lead to a better chance for NH_3 to scavenge OH radicals due to competition from other species (e_{aq}^-, H and OH themselves) in the irradiating water, ultimately resulting in higher product yields.

Although nitrate was formed at the two initial pH, nitrite formation was only observed at pH 10. It has been suggested (Dwibedy et al., 1996) that higher nitrite yield is the consequence of increasing concentrations of NH_3 and oxygen. The aminyl (NH_2) radical formed from the reaction of NH_3 with OH radicals is transformed to the aminylperoxyl radical (NH_2O_2) when O_2 is present in the system. Increasing concentrations of O_2 generates higher yields of nitrite since its reaction with NH_2 is favored over the dimerization reaction of NH_2.

$NH_2 + O_2 \rightarrow NH_2O_2$ (favored in the presence of O_2)

$NH_2 + NH_2 \rightarrow N_2H_4$ (favored in the absence of O_2)

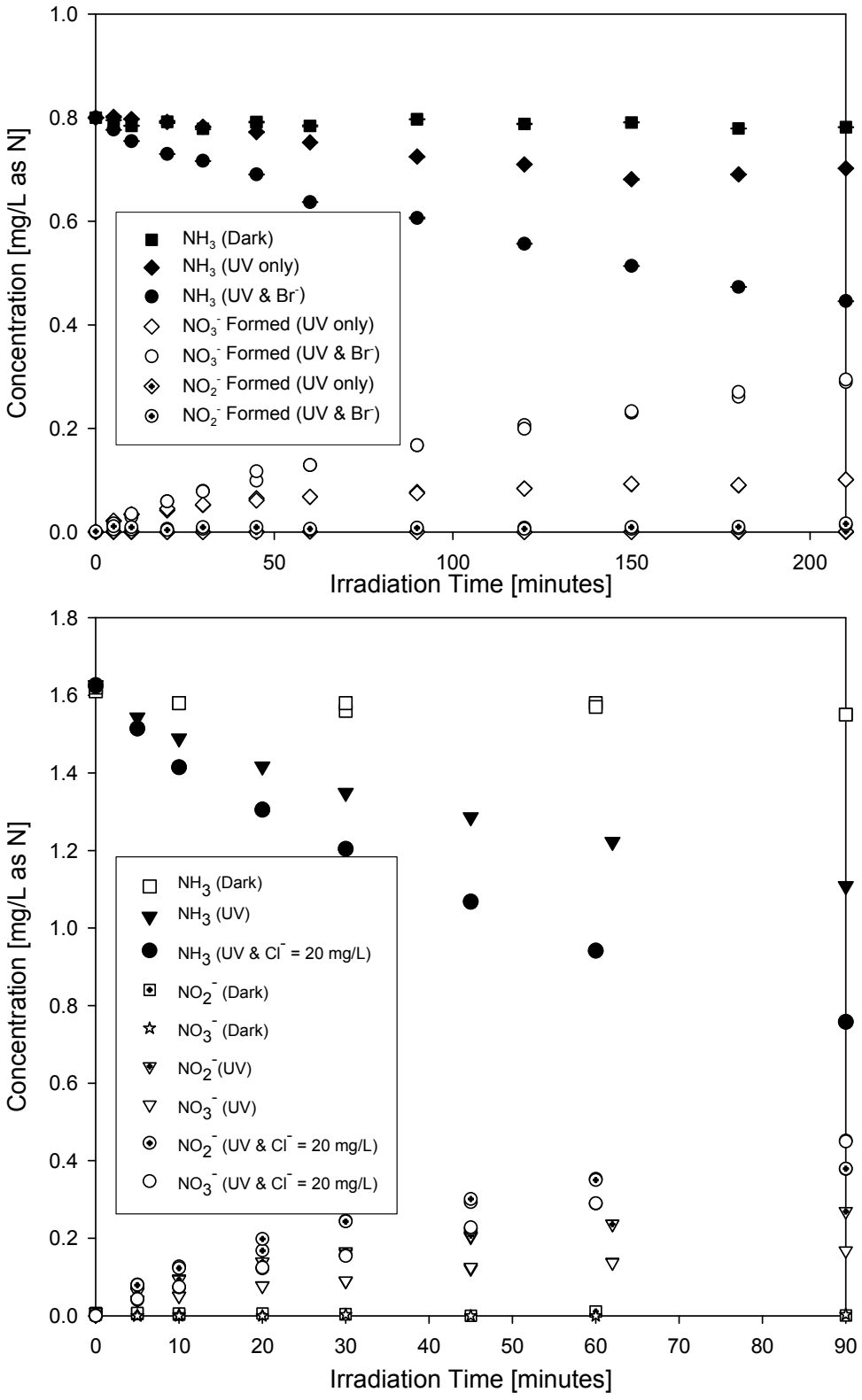

Figure 6.5. Comparison of NH_3 Oxidation at (a) pH 8 and (b) pH 10 under: (i) Dark (ii) UV Light and (iii) UV light and Br^- or Cl^-

The NH_2O_2 radical undergoes catalyzed de-protonation by a water or NH_3 molecule or OH^- ion (Laszlo et al, 1998) forming nitric oxide (NO) and in the presence of the superoxide ion (O_2^-) rapidly converts to peroxynitrite ($ONOO^-$), which is stable in alkaline solutions. The pH conditions determine the pathway for $ONOO^-$ decomposition and ultimately the yields of NO_2^-/NO_3^- (Kirsch et al., 2003).

The transformation of NH_3 to the final stable products, NO_2^- and NO_3^- therefore involves a series of intermediates that are interconnected by several redox and equilibria reactions where pH, NH_3, e_{aq}^-, O_2 and OH concentrations determine the product yield and probability of reaction (Gonzalez and Braun, 1996).

The effect of iodide ($[I^-]$ = 2.0 mg/L) on ammonia photo-oxidation was evaluated at an initial solution pH of 5.7 and NH_3-N of 1.6mg/L. Ammonia photo-oxidation did not occur under this pH condition, instead, the pH of the irradiating solution increased while the ion concentration decreased as shown in Figure 6.6. This result was also obtained when iodide was irradiated in the absence of ammonia. The solution pH was then adjusted to 10.4 with 10N NaOH and the irradiation continued for up to 3 hours. Immediately following the pH adjustment to 10.4 ammonia photo-oxidation proceeded, however, the accelerating effect of I^- on ammonia photo-oxidation was not observed at the iodide ion concentration employed. In addition, although nitrite and nitrate were formed as stable final products of NH_3 oxidation, nitrate had the major yield at the solution pH 10.4. This contrasts with Figure 6.5 (b) (ii) and (iii) where at pH 10, nitrite had the major yield. It was shown earlier that I^- undergoes direct photolysis under UV light of wavelengths 254 nm and below, hence the

process generates the iodine atom (I) in solution. The iodine atom scavenges electrons from both OH^- (shown earlier) and NO_2^- according to the following reaction, thus maintaining the I^- concentration relatively constant and depleting the nitrite concentration in solution.

$$I + NO_2^- \rightarrow I^- + NO_2$$

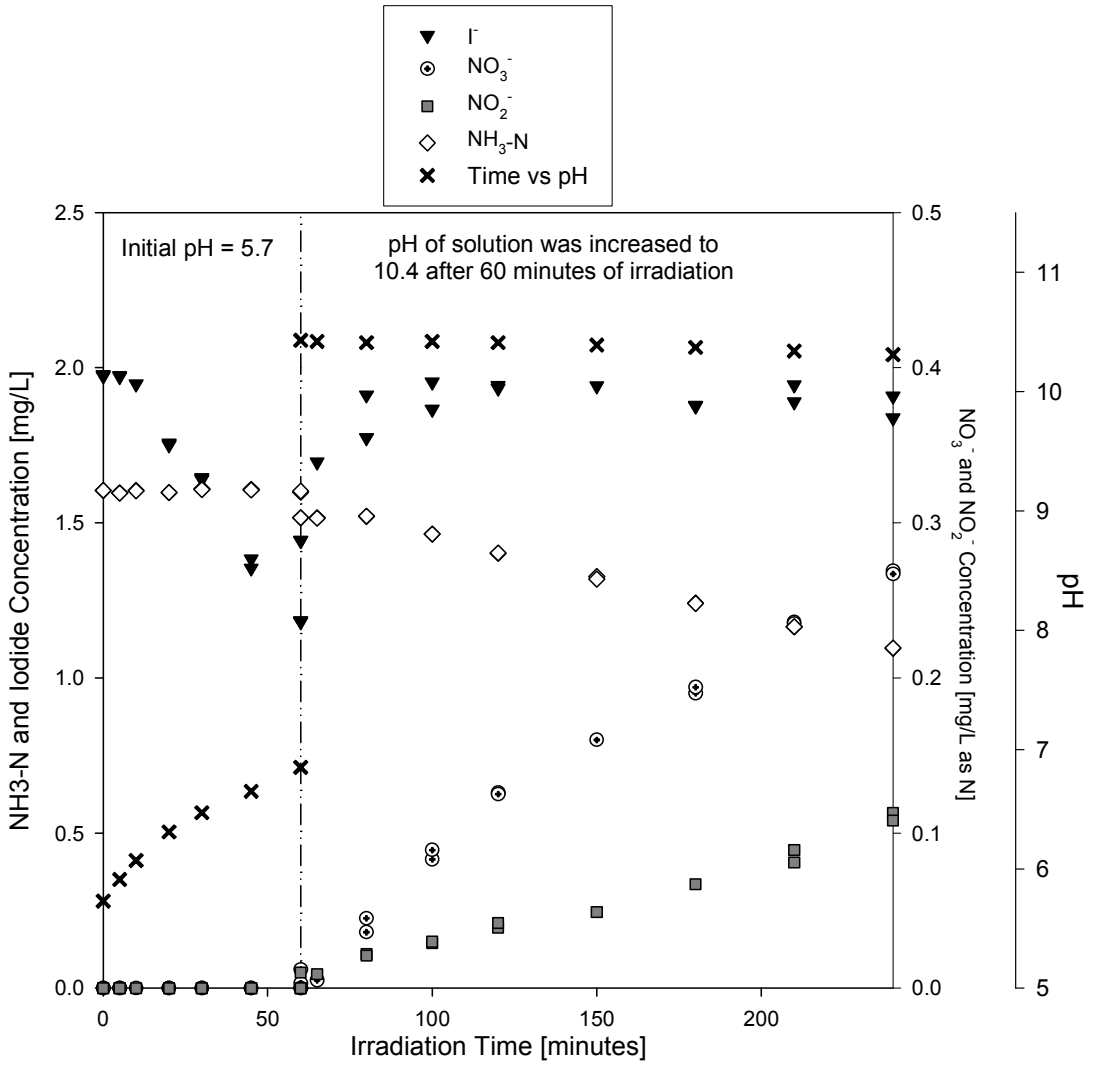

Figure 6.6. UV Irradiation of I^- (2 mg/L) in the presence of NH_3 (NH_4^+-N = 1.6 mg/L) at initial pH of 5.7 and adjusted to a pH of 10.4 after 60 minutes

6.3.2. Influence of pH, Halide Ion Concentration and DO on Ammonia Photo-oxidation

6.3.2.1. Effect of Initial Solution pH on Ammonia photo-oxidation in the Presence of Halide Ions

Wang et al. (1994), Kim et al. (2002), Klare et al. (2000) and Schmelling et al. (1995) reported that the final stable products of ammonia oxidation under UV irradiation were dependent on the initial pH of the irradiating solution and this was also observed when ammonia photo-oxidation occurred in the presence of halide ions. Ammonia solutions (1.6 mg/L as N) with initial pH 5.6, 8.6 and 11.3 were irradiated in the presence of 2.2 mg/L of bromide ions (see Figure 6.7). At pH 5.6, nitrate was the predominant final stable product of ammonia oxidation, whereas at initial solution pH 8.6, nitrite was observed initially but quickly dissipated as the pH of the irradiating solution dropped leaving nitrate as the final stable product. At pH 11.3, both nitrite and nitrate were observed as the final stable products and there was no significant decrease in pH.

The observation of pH depression, particularly in the pH range 5 – 10 implies that protons were released into solution as a result of ammonia oxidation. This observation is further elucidated when pH depression is compared with ammonia decay kinetics (Figure 6.8). In irradiated ammonia solutions containing bromide and chloride ions at pH 5.6 – 5.8 (where pH changes are easily distinguished due to the logarithmic nature of the pH scale) the pH of the solution progressively decreased as ammonia oxidation proceeded. While in ammonia / halide solutions at pH 10.0 – 10.4 the release of protons into solution was only discernable in the solution containing chloride ions, where the extent of ammonia oxidation was greatest.

The greater amount of protons released was enough to enable a significant degree of pH depression to be observed.

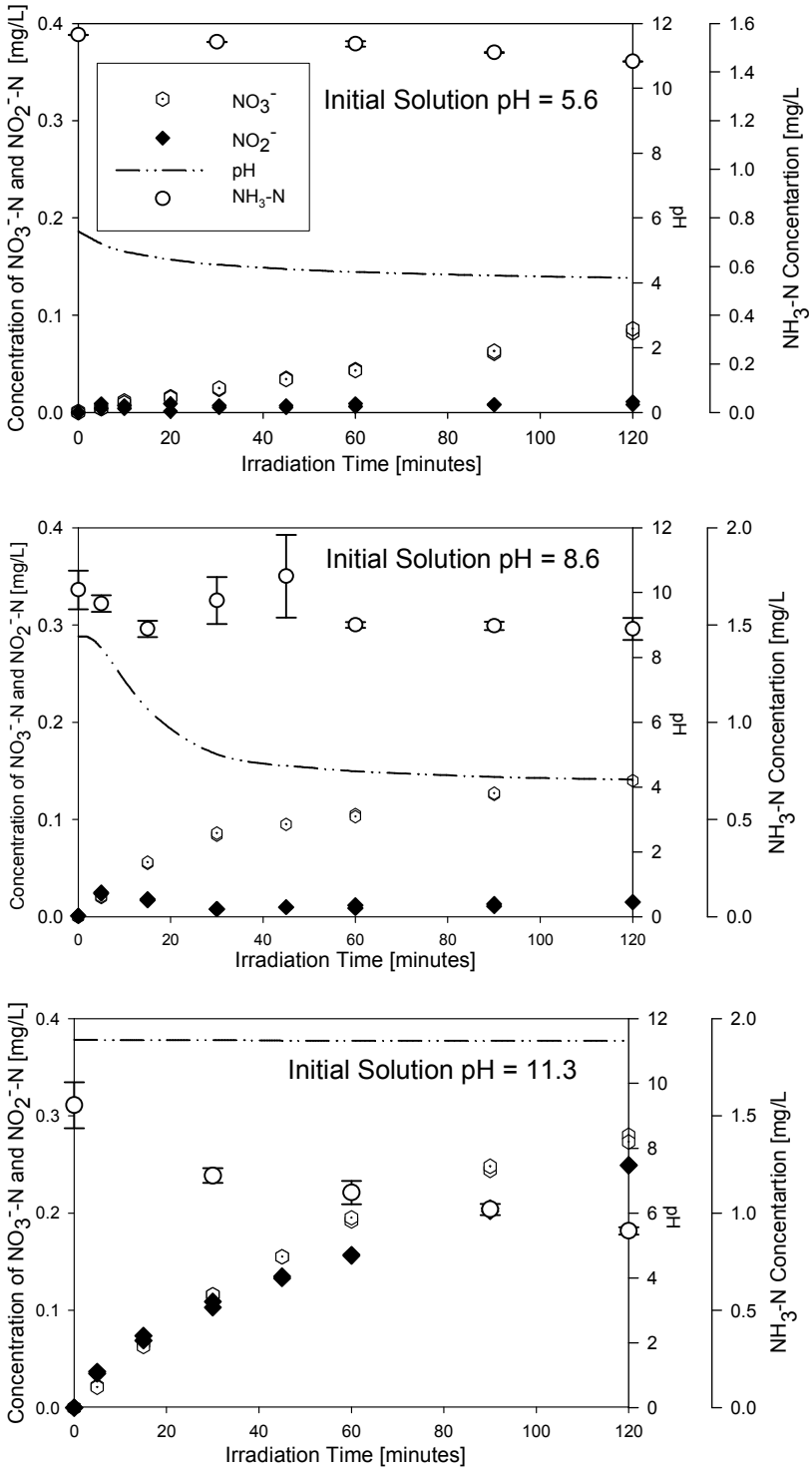

Figure 6.7. Photo-products Generated from the UV Irradiation of Br^- (2.28 mg/L) in the Presence of Ammonia (1.6 mg/L as N) at Various Initial pH

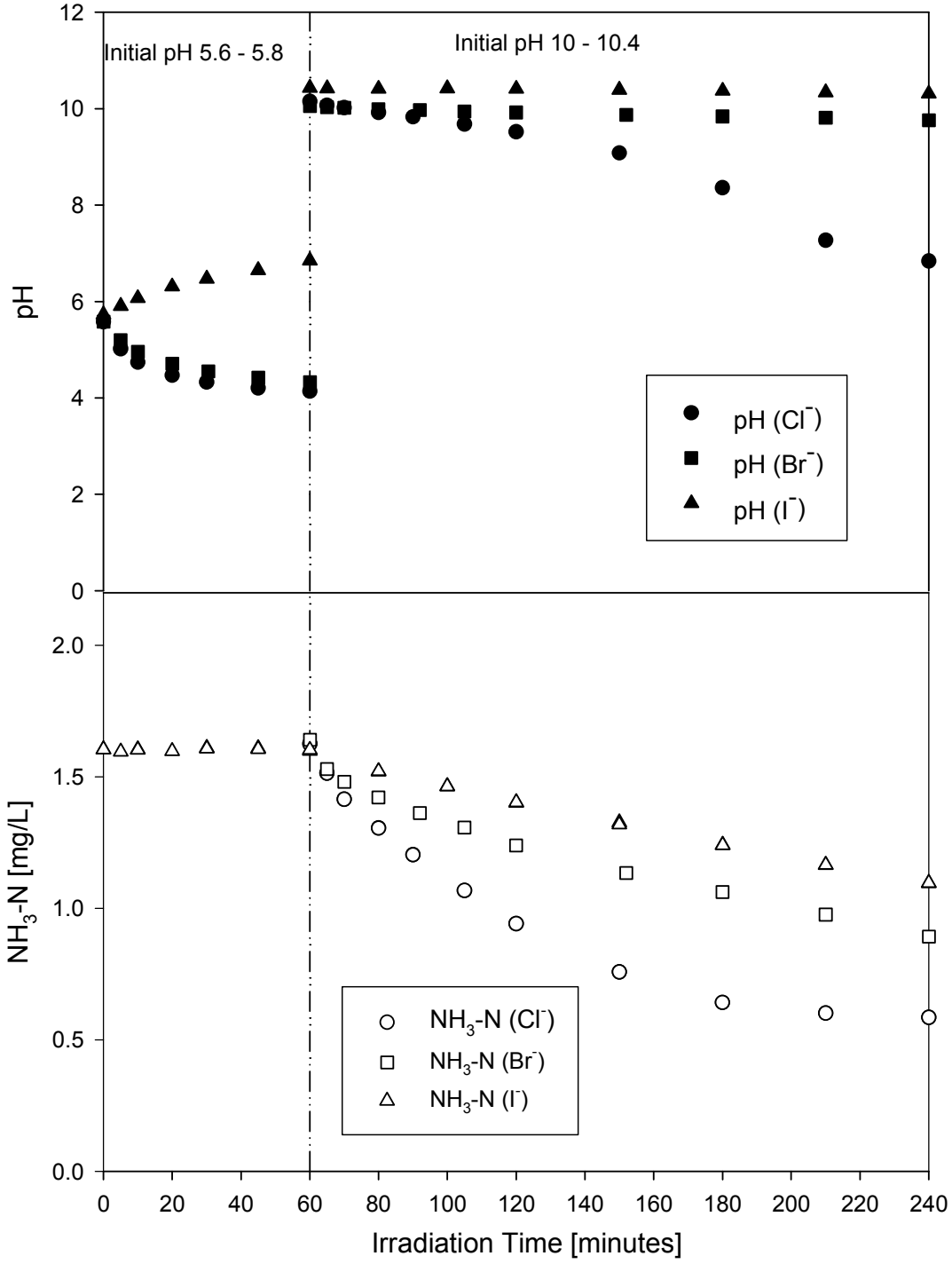

Figure 6.8. pH Profiles of UV Irradiated Solutions of Halide Ions in the Presence of NH_3

6.3.2.2. Influence of Halide Ion Concentration on the Extent of Ammonia Photo-oxidation

In addition to the initial pH of the irradiating solution, the extent to which NH_3 oxidation is augmented by the presence of halide ions was found to be dependent on the type and concentration of the halide ion employed. As mentioned earlier, the effect of various Cl^- and Br^- concentrations on ammonia oxidation in acidic solutions is illustrated in Figure 6.4. The same molar concentration of Cl^- and Br^- (0.028 mM) resulted in a greater formation of nitrate (i.e. the ammonia oxidation product generated at this pH) in the presence of Br^- compared to Cl^-. In addition, smaller molar concentrations of Br^- resulted in more nitrate generation than Cl^- implying that the presence of smaller quantities (in terms of molecules) of Br^- may be more effective in promoting ammonia oxidation than Cl^- in acidic solution.

In order to further investigate the effect of Br/N molar ratio on the extent of ammonia oxidation in acidic solution, a standard concentration of bromide ions (0.635 mg/L) was irradiated in the presence of three different concentrations of aqueous ammonia. The results are presented in Figure 6.9 and Table 6.1 below. The higher the Br/N ratio the greater the conversion of ammonia achieved but more NO_3^- was produced with the highest ammonia concentration used (i.e. the lowest Br/N ratio). It was shown earlier (Figure 6.4) that increasing the Br/N ratio by maintaining the same ammonia concentration but employing different Br^- concentrations also gave similar results in achieving greater ammonia oxidation.

TABLE 6.1. Photo-oxidation of Aqueous Ammonia in the Presence of Bromide Ions at Initial Solution pH 5.6

Initial Br^- Conc. [mg/L as Br]	Initial NH_4^+ Conc. [mg/L as N]	Br:N Molar Ratio	Changes After 1hr of Irradiation		
			pH Depression	Total NO_3^--N Formation (mg/L)	% Conversion of NH_4^+ to NO_3^-
0.635	0.03	3.713	0.30	0.015	50
0.634	0.19	0.585	0.43	0.025	13
0.634	0.80	0.139	0.64	0.046	6

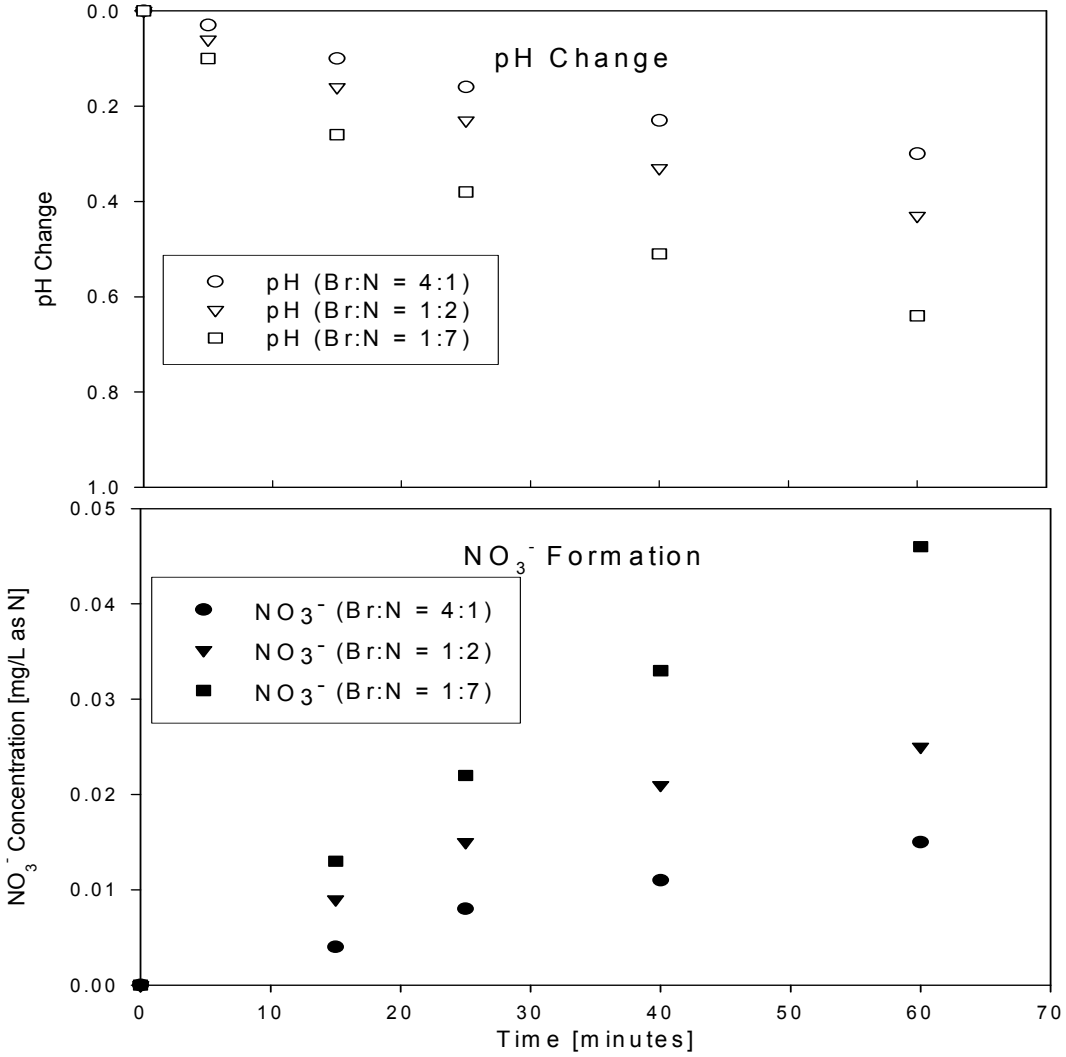

Figure 6.9. Photokinetics of Br^- / NH_4^+ System in Producing Nitrate and depressing pH

NH_3 solutions (NH_3-N = 1.6 mg/L) were irradiated in the presence of various halide concentrations at initial solution pH of 10 (Figure 6.10). The rate of NH_3 oxidation increased in the presence of Cl^- = 10 and 20 mg/L and Br^- = 5 mg/L over NH_3 oxidation without halide ions. At Cl^- = 10 mg/L (0.282 mM) and Br^- = 5 mg/L (0.063mM) the increase in the rate of NH_3 oxidation was comparable, suggesting that Br^- may be more effective in promoting ammonia oxidation than Cl^- in basic solution. Nevertheless, at Br^- = 2.2 mg/L (0.028 mM) no increase in the rate of NH_3 oxidation at initial solution pH 10 was observed. It should be noted however, at initial solution pH 8 there was an observed increase in the rate of NH_3 oxidation for Br^- = 2.2 mg/L over NH_3 oxidation without halide ions at initial solution pH 8 (see Figure 6.10).

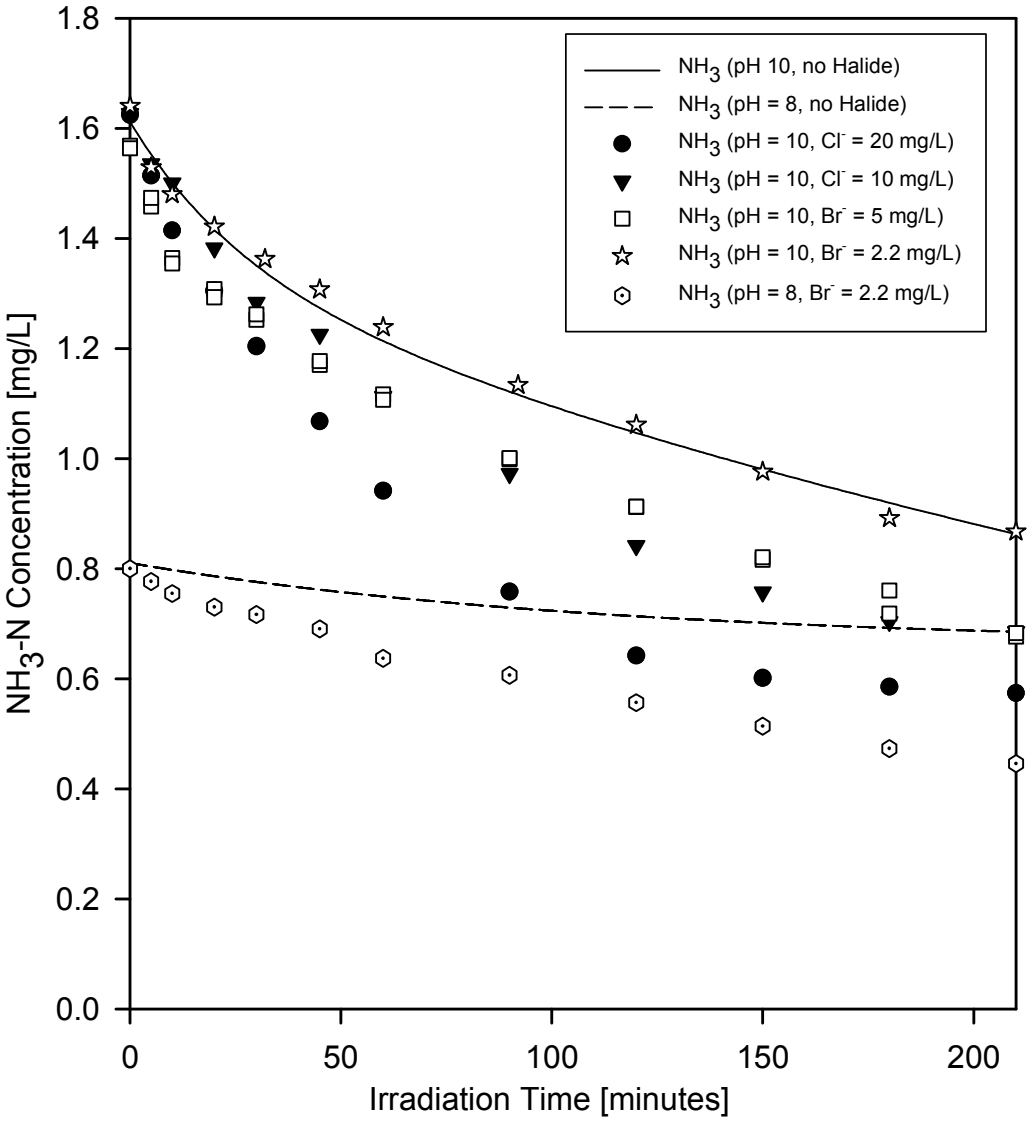

Figure 6.10. Effect of Halide Ion Concentration on NH3

Oxidation with Low Pressure Mercury Lamps

During the course of ammonia oxidation no change in the concentration of halide ions ensued. Figure 6.11 depicts the halide ion concentration kinetics for irradiating NH_3 solutions containing Cl^- = 20 mg/L, Br^- = 2.2 mg/L and I^- = 2.0 mg/L (pH and ammonia kinetic profiles are provided in Figure 6.8). Only in the case of iodide at pH 5.7 where it was observed that ammonia oxidation did not take place, the [I^- decayed during the 60 minutes of irradiation. When the pH of the irradiating solution was adjusted to 10.4 where NH_3 oxidation was observed [I^-] returned to its original level within minutes and remained unchanged upon further irradiation of the solution. The following reactions may have caused the iodide concentration to decline under UV irradiation in acidic solution but revert to its original level in alkaline pH.

$$I^- + h\nu \rightarrow I + e_{aq}^-$$

$$I + I^- \leftrightarrow I_2^-$$

$$I_2^- + I \rightarrow I_3^-$$

$$I_3^- + H \rightarrow 2I^- + H^+ + I$$

$$I + OH^- \rightarrow I^- + OH$$

$$I + NO_2^- \rightarrow I^- + NO_2$$

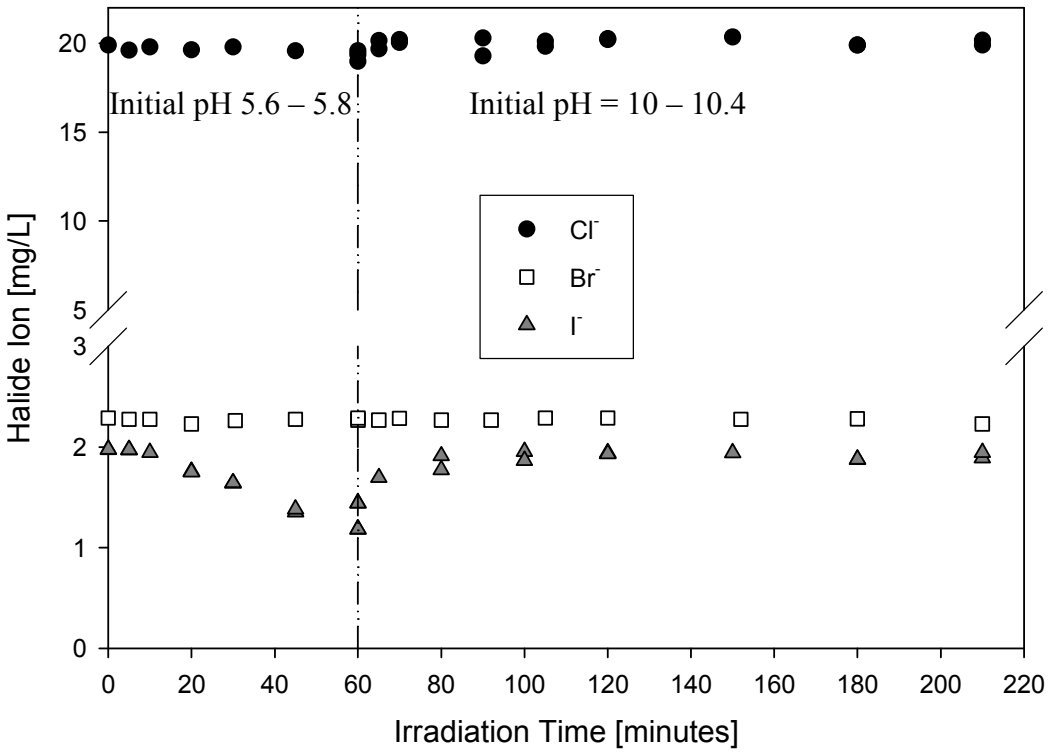

Figure 6.11. Halide Ion Concentration
in UV Irradiated Solutions Containing NH_3

The pseudo first-order rate of ammonia decay (k_{obs}) at initial pH 9.96 – 10.15 and in the presence of halide ions (Cl^- and Br^-) was plotted against the halide ion / ammonia-nitrogen molar ratio [X^-/N] in Figure 6.12. In general it was found that as X^-/N increased, k_{obs} also increased but the extent of the increase was dependent on the actual concentrations of halide ions and ammonia in the water. Point 1 represent k_{obs} for zero X^-/N. Points 2 to 4 represent ammonia and chloride concentrations that are respectively at least seven and five times smaller than ammonia and chloride concentrations used for points 5 to 7. Based on the slope of the plot of points 1 to 4, small changes in Cl^-/N is expected to result in a more significant increase in k_{obs} than points 5 to 7.

Table 6.2 also compares the changes in k_{obs} as X^-/N changed for the halide ions: Cl^-, Br^- and I^-. For a Br/N ratio of 0.241 which corresponds to the concentrations, Br^- = 2.2 mg/L and NH_3-N = 1.6 mg/L, it was seen that the pH of the initial solution had a profound effect on k_{obs}. There was a three-fold increase in k_{obs} as the initial solution pH increased from 5.7 to 8.64 and more than a five-fold increase as the pH was further increased to 10.05. It should be noted that although k_{obs} at pH 10.05 was greater than that without halide ions, this increased rate of ammonia decay was not preserved for very long and the percent conversion of ammonia soon leveled out to that of NH_3-oxidation without halide ions present at the prevailing pH (also see Figure 6.10).

Generally, as the k_{obs} for ammonia decay in the presence of Cl and Br ions increased, the percent conversion of ammonia was also enlarged as depicted in Figure 6.13. Using the bromide profile for comparison, it is seen that higher initial solution pH resulted in greater

ammonia conversion (points A and C) while lower initial ammonia concentrations gave higher % conversions of ammonia (compare points A and B, as well as C and F). Increasing k_{obs} by increasing Br concentration may also improve the percent conversion of ammonia as depicted by comparing points C and E. Nevertheless, higher k_{obs} did not always result in increased conversion of ammonia. When the bromide and ammonia concentrations are both increased (point D) so that the Br/N ratio is double that of C the higher k_{obs} did not cause an increase in the conversion of ammonia. This may be due to concentration effects.

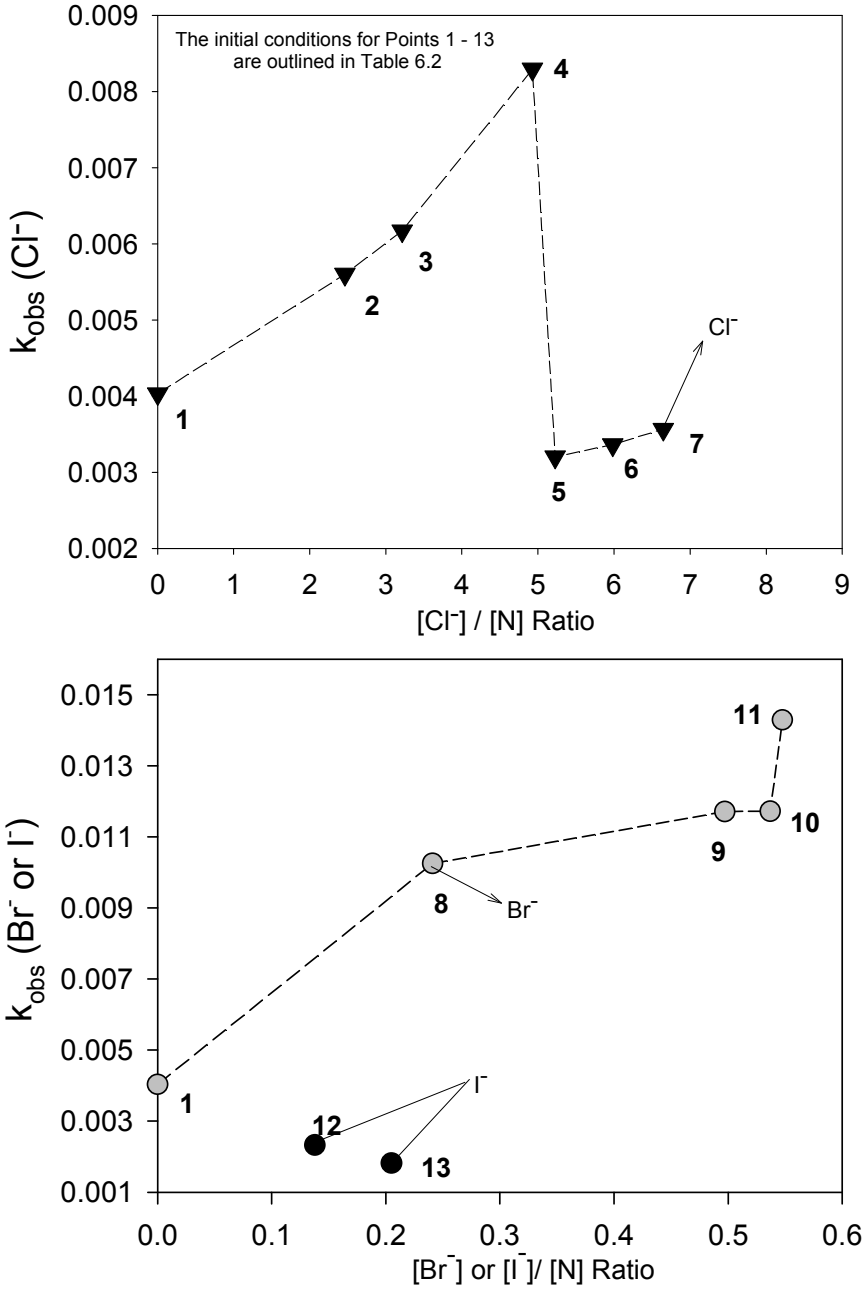

Figure 6.12. Effect of Halide Ion to Ammonia-Nitrogen Molar Ratio on the Pseudo First-Order Representation of NH_3 decay in the Presence of Halide Ions, k_{obs}

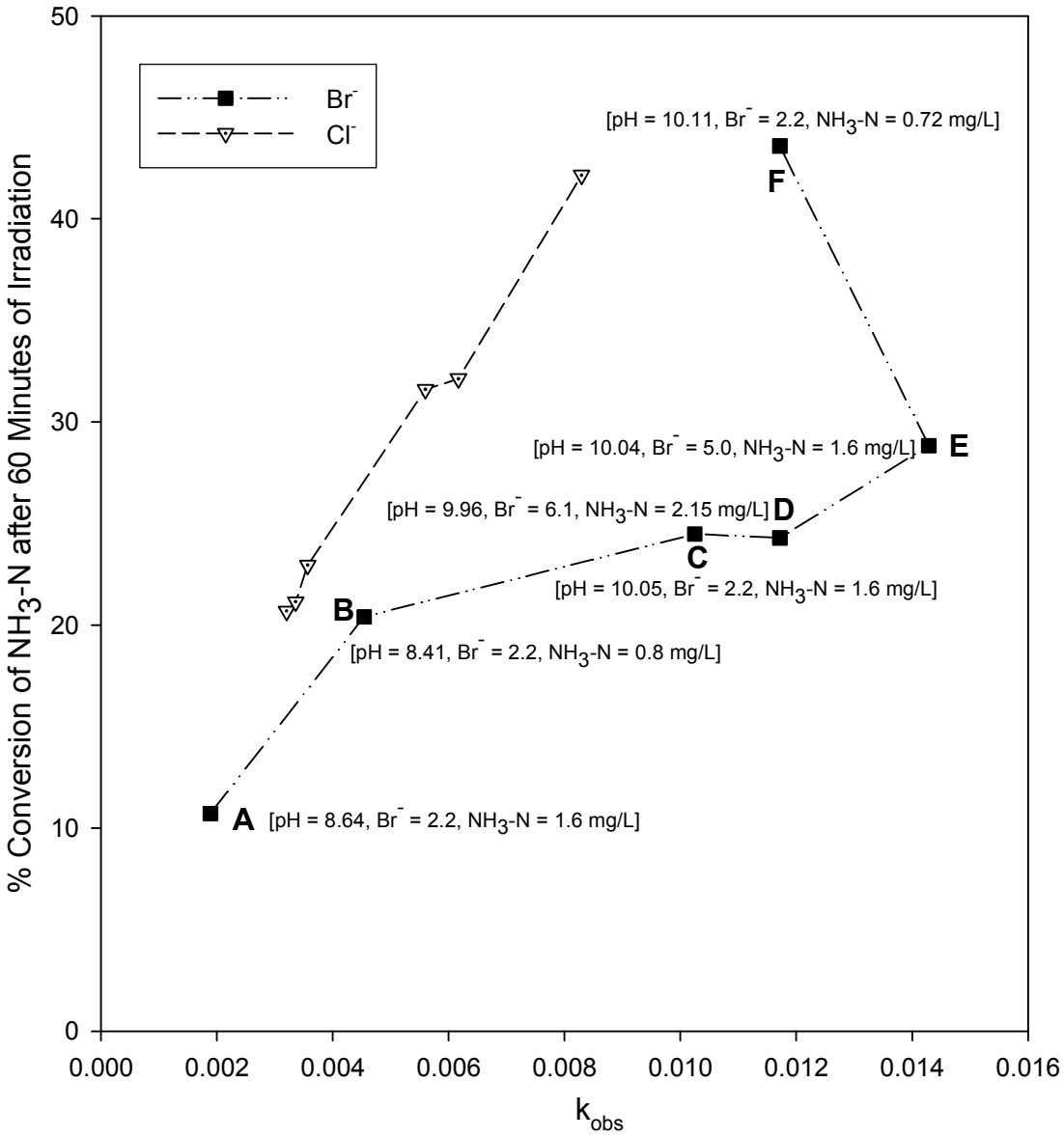

Figure 6.13. % Conversion of Ammonia as a Function of k_{obs}

TABLE 6.2. **k_{obs} and % Conversion of Ammonia for Various X^-/N Ratios**

Pt. on Fig. 6.12	Halide ion (X)	Ion conc mg/L	NH_3 conc (mg/L as N)	X^-/N Molar Ratio	Initial pH	k_{obs} (minute^{-1}) [r^2]	% Conversion of NH_3-N after	
							60 mins	120 mins
-	Br^-	2.2	1.60	0.24	5.70	5.91×10^{-4} [0.9889]	-	6.70
-	None	0.0	0.8	0.00	8.16	7.79×10^{-4} [0.9982]	5.97	11.30
-	Br^-	2.2	1.60	0.24	8.64	1.89×10^{-3} [0.9464]	7.31	9.69
-	Br^-	2.2	0.80	0.48	8.41	4.54×10^{-3} [0.9770]	20.40	30.44
1	None	0.0	1.60	0.00	10.05	4.03×10^{-3} [0.9711]	24.86	35.97
8	Br^-	2.2	1.60	0.24	10.05	1.03×10^{-2} [0.9567]	24.48	35.29
9	Br^-	2.2	0.72	0.54	10.11	1.17×10^{-2} [0.9912]	43.59	58.50
10	Br^-	5.0	1.60	0.55	10.04	1.43×10^{-2} [0.9950]	28.83	41.83
11	Br^-	6.1	2.15	0.50	9.96	1.17×10^{-2} [0.9976]	24.29	36.18
2	Cl^-	10.0	1.60	2.47	10.02	5.60×10^{-3} [0.9840]	31.60	48.26
3	Cl^-	12.0	1.47	3.22	10.02	6.17×10^{-3} [0.9914]	32.13	49.06
4	Cl^-	20.0	1.60	4.93	10.15	8.30×10^{-3} [0.9936]	42.15	60.56
5	Cl^-	115.0	7.58	5.98	10.09	3.36×10^{-3} [0.9929]	21.14	34.57
6	Cl^-	125.0	9.43	5.23	10.08	3.20×10^{-3} [0.9919]	20.68	33.62
7	Cl^-	146.0	8.66	6.65	10.09	3.57×10^{-3} [0.9911]	22.95	35.91
12	I^-	2.0	1.60	0.14	10.43	2.33×10^{-3} [0.9945]	12.43	22.61
13	I^-	4.06	2.18	0.21	9.98	1.82×10^{-3} [0.9950]	11.08	19.30

Figure 6.14 depicts the reaction kinetics for aqueous ammonia solutions at initial solution pH 10 containing: (a) Br^- = 2.2 mg/L, NH_3-N = 0.72 mg/L (b) Cl^- = 12 mg/L; NH_3-N = 1.6 mg/L, (c) Br^- = 6.1 mg/L; NH_3-N = 2.15 mg/L and (d) Cl^- = 125 mg/L; NH_3-N = 9.43 mg/L. Depending on the initial concentration of ammonia, NH_3 oxidation in basic solutions may generate protons to such an extent that the pH is eventually depressed with prolonged irradiation and the NO_2^- formed is readily converted to NO_3^-. It should be noted that in the absence of halide ions, NO_2^- remains as the major reaction product.

In Figure 6.14 (a) the ammonia concentration was too low to generate enough protons to depress the pH significantly and thus, NO_2^- conversion to NO_3^- was only minimal after 240 minutes of irradiation. With higher initial ammonia concentrations i.e. (b) (c) and (d) of Figure 6.14, pH depression was more pronounced with prolonged irradiation and the nitrite formed initially was ultimately converted to nitrate. This relationship between pH depression and NO_2^- to NO_3^- conversion is not understood, but the presence of halide ions seem to have a bearing on this phenomenon since it is not observed in the absence of halide ions, where nitrite remains as the final stable product even with prolonged irradiation.

Nevertheless, the following phenomenon should be noted in the NO_2^- to NO_3^- conversion phenomenon observed in the presence of halide ions.

- The increased oxidation of ammonia in the presence of halide ions may generate sufficient protons to depress the pH of the irradiating solution.
- As the pH is depressed, peroxynitrite ($ONOO^-$) converts to peroxynitrous acid (ONOOH) by pH equilibria and the following reaction takes place:

$$HO^{+} + NO_2^{-} \rightarrow NO_3^{-} + H^{+}$$

Maurer et al., 2003, have experimentally observed this formal transfer of the species, HO^{+} to NO_2^{-} forming NO_3^{-} in ONOOH acid solutions. The source of the HO^{+} ion is peroxynitrous acid and its transfer in the chemistry of peracids is common, the family of acids to which peroxynitrous acid belong (Maurer et al., 2003). This reaction however is not responsible for NO_2^{-} conversion to NO_3^{-} in the presence of halide ions, since the graphs of Figure 6.14 show that as the solution pH attains a value of the pK_a of ammonium/ammonia (pK_a = 9.4 @ 20^0C) and not the pK_a of ONOOH/ $ONOO^{-}$ (pK_a = 6.8) that NO_2^{-} depletion to NO_3^{-} ensues. The presence of the halide ions in the irradiating solution seems to influence NO_2^{-} conversion to NO_3^{-}.

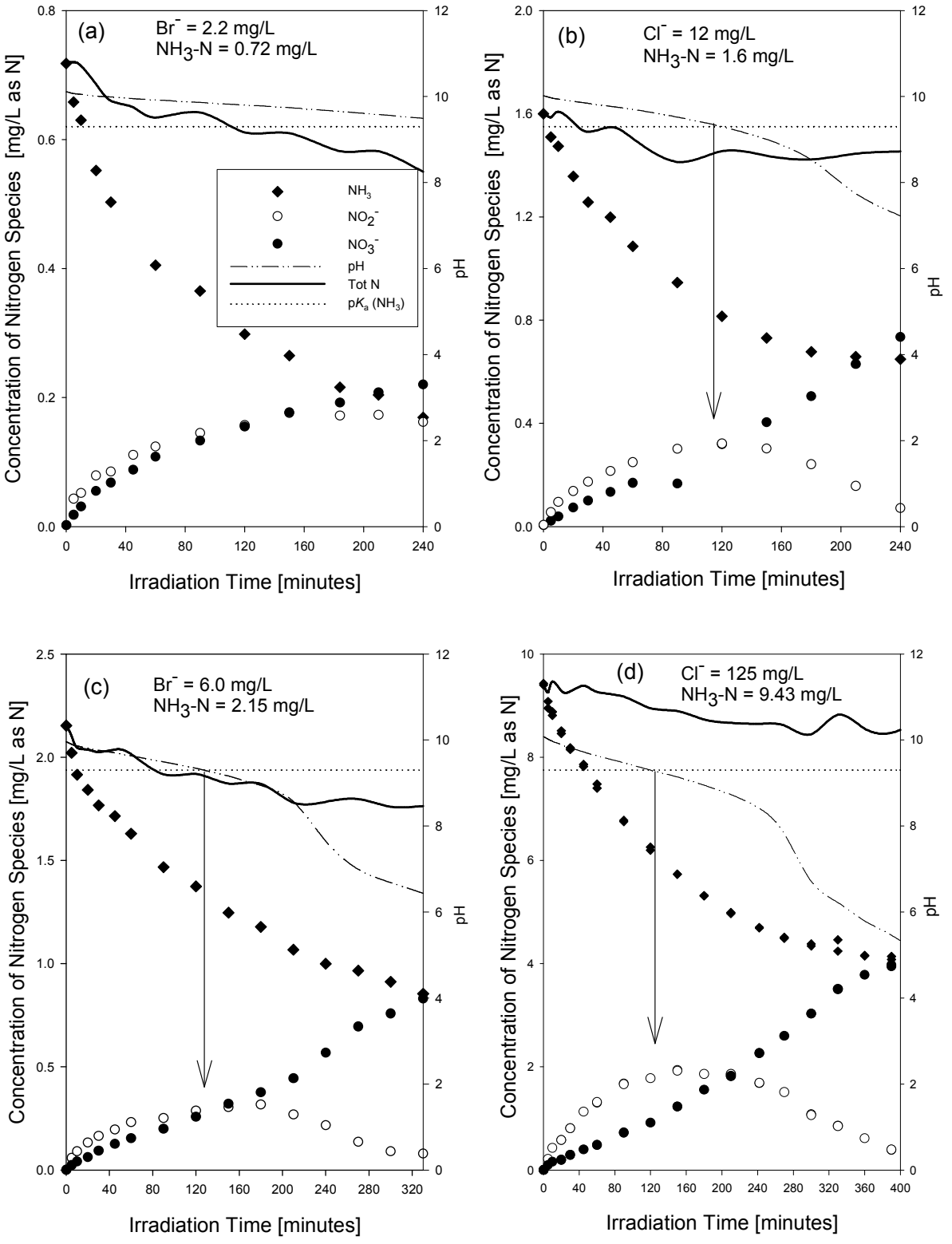

Figure 6.14. Nitrite Conversion to Nitrate at Various X^-/N Ratios

In order to observe the influence of pH adjustment on increasing the % conversion of ammonia in the presence of halide ions, the pH of a solution containing Cl^- = 115 mg/L and NH_3-N = 7.58 mg/L was adjusted back to 10 after irradiation for 330 minutes and the irradiation continued for an additional 400 minutes. pH adjustment was achieved by adding incremental drops of 10N sodium hydroxide (NaOH) solution to the irradiated ammonia/chloride solution after shutting off the UV lights.

Figure 6.15 depicts the kinetic profiles of ammonia decay and NO_2^-/NO_3^- formation. During the first 330 minutes sufficient oxidation of ammonia ensued to effect pH depression and the conversion of NO_2^- to NO_3^-. When the pH was adjusted back to 10 after shutting off the lamps there was observed changes in the concentrations of species in the reactor. After resuming the irradiation, the nitrate concentration was reduced initially while nitrite started to accumulate in the system. However, as the pH of the irradiating solution was again depressed, nitrite was subsequently converted to nitrate. There was a slight reduction in total nitrogen species in the reactor as the irradiation proceeded, most likely due to evolution of nitrogen gas formed via ammonia re-oxidation (Gonzalez and Braun, 1996).

Approximately 48% conversion of ammonia to NO_2^-/NO_3^- was achieved in the first 330 minutes of irradiation, while approx. 54% conversion was achieved during the second 330 minutes of irradiation. As the irradiation proceeded, the Cl^-/N molar ratio increased (the chloride ion concentration remains unchanged during the process) resulting in a corresponding increase in % conversion of ammonia.

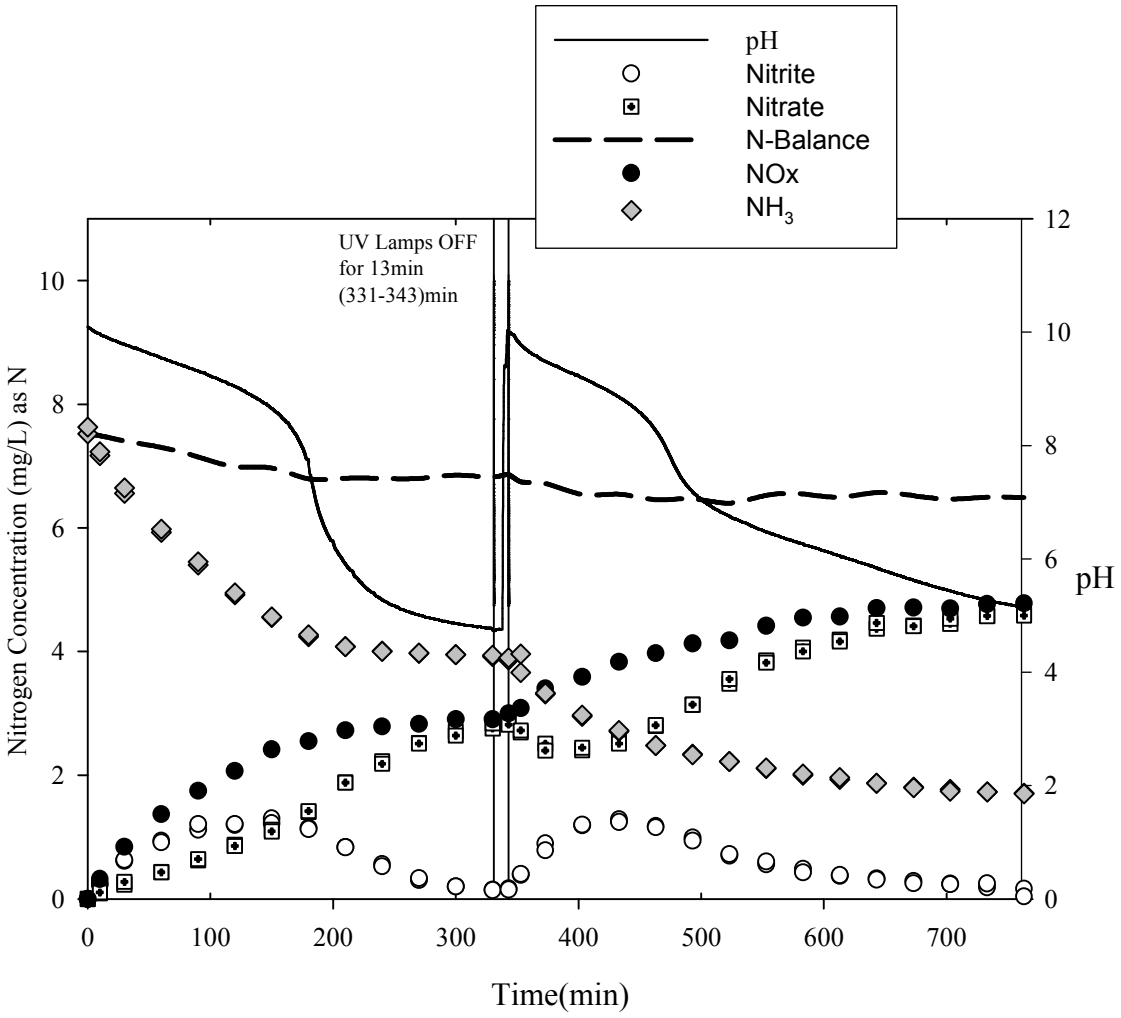

Figure 6.15. pH Adjustment to Achieve Greater NH_3 Oxidation

Cl^- =115 mg/L NH_3-N =7.58mg/L

A wastewater sample from the final settling tank of a municipal facility in New York City was utilized to determine whether the interactions between halide ions and ammonia will occur as secondary reactions in a UV process where the objective is to remove organic material from the water. The sample collected was first filtered through a 0.45 micron filter and then spiked with ammonia to a concentration of 13 mg/L. The pH was also elevated to 10 prior to irradiation. It should noted that pH adjustment is employed in the removal of some contaminants from waters, e.g. Smith and Frailey (1990) used pH adjustment to 10 – 11 for the degradation of color and chlorinated organics from Kraft Mill Beach Plant Effluents.

The results depicted in Figure 6.16 shows that ammonia oxidation occurred simultaneously with TOC degradation, forming nitrite and nitrate. A considerable amount of dissolved oxygen was consumed during the initial stages of the irradiation (approximately 88% after 120 minutes of irradiation) after which oxygenation of the water ensued due mostly to the continued mixing in the reactor. It should be noted that although the reactor was covered with a Teflon plate, its constituents were still exposed to air from holes drilled into the plate. TOC removal and ammonia decay were approximately the same (almost 30% degradation after 360 minutes of irradiation); however, the pH of the solution was only depressed to 9.5 within the 360 minutes of irradiation, due to the high alkalinity of the wastewater (initially 120 mg/L as $CaCO_3$).

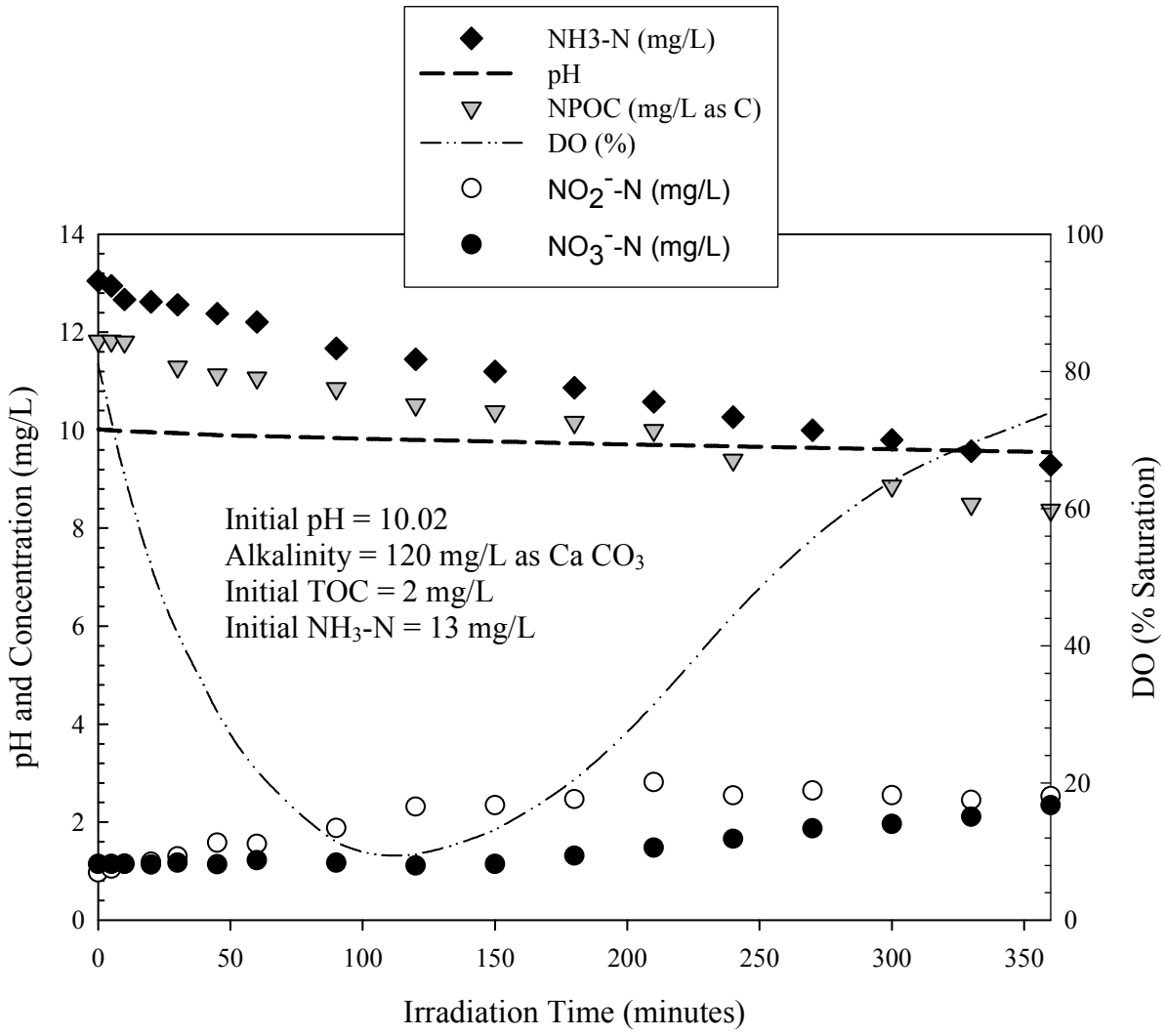

Figure 6.16. UV Irradiation of Wastewater Containing Organics, Ammonia and Chloride Ions

6.3.2.3. Influence of Dissolved Oxygen on the Photo-oxidation of Ammonia in the Presence of Halide Ions

When NH_3 oxidation occurs, there is an initial consumption of dissolved oxygen (DO) observed as the aminyl radicals react with O_2 (Dwibedy et al., 1996).

$$NH_2 + O_2 \rightarrow NH_2O_2$$

DO consumption for Br^- = 2.2 mg/L, Cl^- = 20 mg/L and I^- = 2 mg/L which were individually irradiated with NH_3-N = 1.6 mg/L, is shown in Figure 6.16. At initial solution pH 5.6 – 5.8 the initial consumption of DO is only observed for Br^- and Cl^-, while DO consumption during NH_3 oxidation was witnessed for all three halides at pH 10.05 – 10.43. In the case of Br^- and Cl^- at initial solution pH 5.6 – 5.8 and all three halides at pH 10.05 – 10.43, NH_3 oxidation ensued (refer to Figure 6.8, the pH and NH_3 decay profiles) and was probably responsible for the DO consumption observed. While DO is required for NH_3 oxidation, O_2 is generated during peroxynitrous acid decay (ONOOH) an intermediate formed during NH_3 oxidation and the mixing in the experimental reactor both contributed to the restoration of DO seen in Figure 6.17.

In the case of I^- in acidic solution, this initial DO consumption was not observed since NH_3 oxidation did not occur in its presence. The DO in the water increased to 100% saturation and was then depleted. At initial solution pH 10, where it was observed that NH_3 oxidation occurred (Figure 6.8) there was DO consumption.

The effect of DO on NO_X formation was observed when an ammonia/chloride solution was irradiated first in the absence of oxygen by bubbling helium through the reactor and then allowing a pulse of oxygen through the system. In the absence of the DO pulse, the

concentration of NH_3 decayed but the total N in the reactor was equivalent to the amount of NH_3 in the system (see Figure 6.18). NH_3 decays in the absence of oxygen as a result of the following reactions (Sutherland, 1979; NDRL) where nitrogen gas (instead of NO_X) is formed thereby depleting NH_3 in the system.

$$NH_3 + OH \rightarrow NH_2 + H_2O$$

$$NH_2 + NH_2 \rightarrow N_2H_4$$

$$N_2H_4 + OH \rightarrow N_2H_3 + H_2O$$

$$N_2H_3 + N_2H_3 \rightarrow 2NH_3 + N_2$$

When DO was introduced, NO_X was formed and total N was then equal to NH_3 plus NO_X. The presence of DO is therefore important for NO_X production. It has been suggested (Wang et al., 1994) that molecular oxygen is not important for rate-limiting NH_3 oxidation but rather, the reaction of NH_3 with oxygen free radicals is the more likely photo-oxidation pathway. It is generally accepted that NH_3 is oxidized by OH radicals to NH_2 radicals, which in turn are further oxidized by O_2 and O_2^- to NO_2^- and NO_3^-.

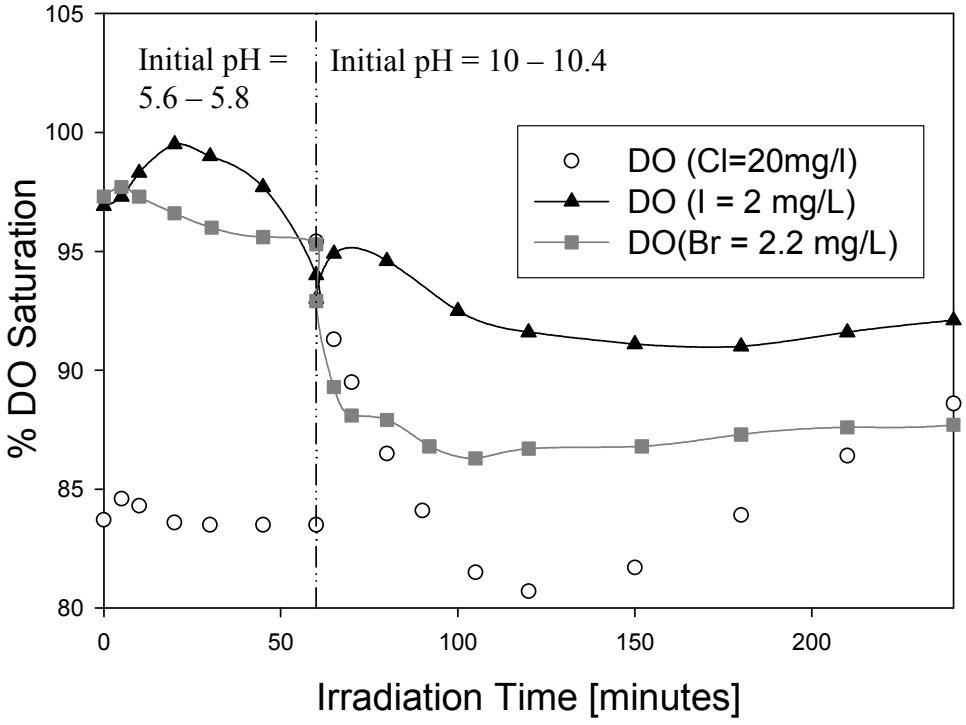

Figure 6.17. Kinetic Profiles of Dissolved Oxygen in Irradiated NH_3-N (1.6 mg/L) Solutions Containing Halides

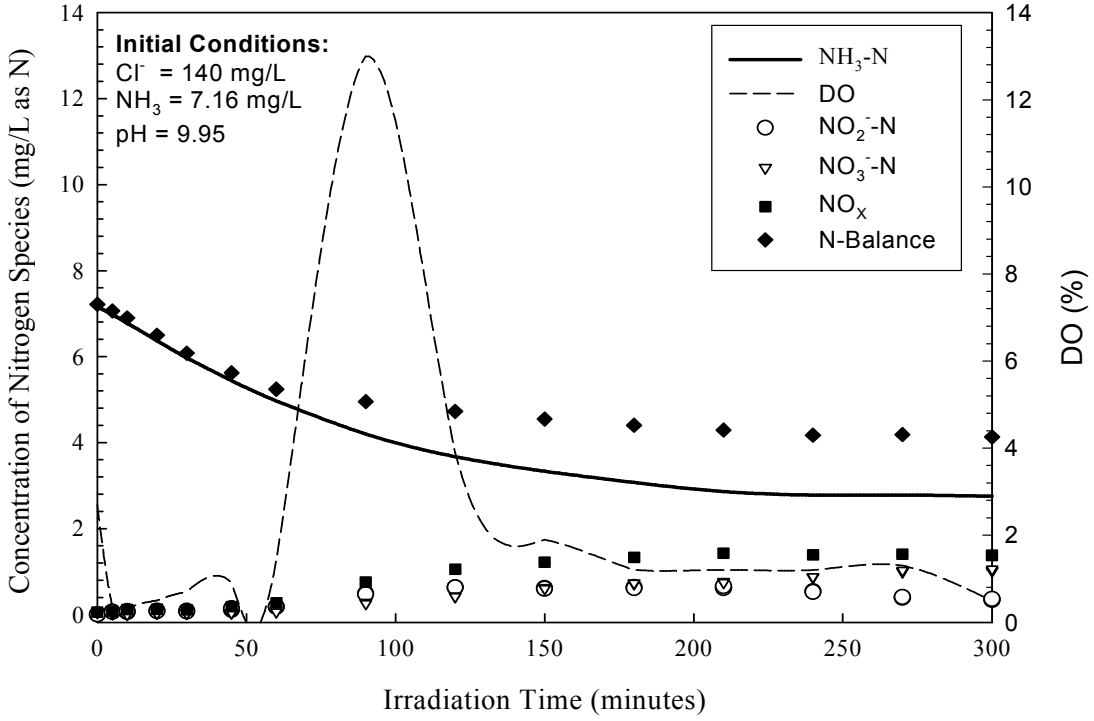

Figure 6.18. Effect of Dissolved Oxygen on NH_3 Oxidation and the Products of NH_3 Oxidation

3.1.1.1 6.3.2.4. Influence of UV Wavelength on the Halide Ion / Ammonia Process

In order to determine whether the ammonia oxidation process in the presence of halide ions occur as a result of the application of only the 254 nm wavelength or 185 nm wavelength emitted by the low-pressure lamps or a combination of both wavelengths, a solution containing Cl^- = 100 mg/L, NH_3-N = 2 mg/L and initial pH = 10.02 was irradiated using quartz sleeves (GE 218) that block the transmission of the 185 nm wavelength to the irradiated water. Figure 6.19 shows the kinetic profiles for the nitrogen species after irradiation for 360 minutes.

The ammonia oxidation process occurred only negligibly with 0.014 mg/L of NO_2^--N (i.e. 0.7% conversion of ammonia) and 0.018 mg/L of NO_3^--N (0.9% conversion of ammonia) formed at the end of the irradiation. The solution pH was depressed to 9.79 and 10% of the DO was consumed during the irradiation period.

Long et al., (1994) and Sauer et al., (2004) have suggested that the CTTS state of halide ions are created by two and three photon excitation. It was particularly noted that two- photon excitation of I^- results in the formation of an upper excited CTTS state while three-photon excitation of I^- results in photo-ionization and the generation of aqueous electrons. Since it was shown that the lamps employed was able to cause the photo-ionization of I^- it can be concluded that the intensity of the lamps employed enabled three-photon ionization of I^- to occur, but was capable of exciting Br^- and Cl^- to CTTS states. Based on the results of Figure 6.19 the wavelength of light that is mainly responsible for the creation of the CTTS states in Br^- and Cl^- was 185 nm, where two photon (combinations of 254 and 185 nm or two 185

nm photons) or three-photon (combinations of three 185 nm; one 254 and two 185 nm; or two 254 and one 185 nm photons) excitation occurs.

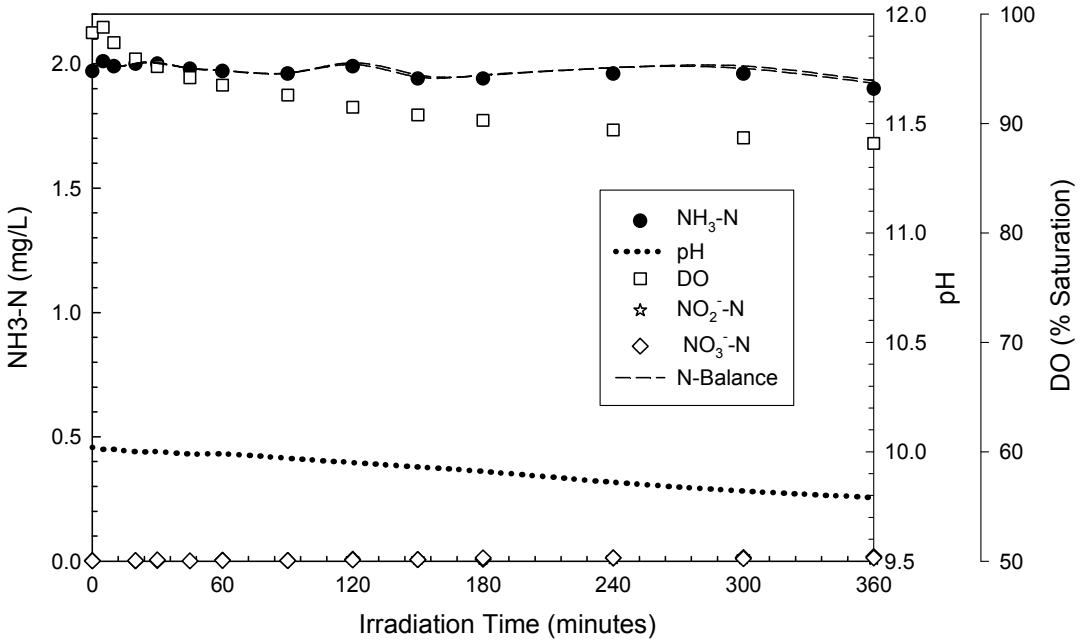

Cl^-=100 mg/L
NH_3= 2mg/L as N
pH = 10
4 UV lamps (GE 219) @ 20 ^oC

Figure 6.19. UV Irradiation of a Cl^- /NH_3 solution with Sleeves (GE 218) Designed to Block the Transmission of 185 nm Wavelength

6.4. Electron generation during NH_3 photo-oxidation

6.4.1. Oxidation Reduction Potential of Ammonia Irradiated Solutions in the Presence and Absence of Halide Ions

It was shown previously that ammonia oxidation generated protons and such reactions that involve a yield of protons frequently lead to electron production as well. The conventional way of writing the half-reactions for ammonium (NH_4^+) oxidation to nitrite and nitrate are as follows:

$$1/6\ NO_2^- + 4/3\ H^+ + e^- \rightarrow 1/6\ NH_4^+ + 1/3\ H_2O \ \ldots\ldots (E^0 = 0.898\ V)$$

$$1/8\ NO_2^- + 5/4\ H^+ + e^- \rightarrow 1/8\ NH_4^+ + 3/8\ H_2O \ \ldots\ldots (E^0 = 0.880\ V)$$

Similar equations involving the NH_3 species should apply if electrons are generated during the oxidation of the NH_3 species.

The ORP (oxidation-reduction potential) of a solution is a measure of the oxidizing / reducing power of the water and is defined as:

$$ORP = E_{system} = E^0 - (0.059/n) \times \log [\text{reduced species/oxidized species}]$$

Hence, although the charge balance of the half-reactions for ammonia oxidation sums to neutrality, the ORP during NH_3 oxidation will increase as the concentration of reducing species (i.e. species that are able to donate electrons) decreases.

ORP measurements were recorded for irradiated solutions of ammonia in the presence and absence of chloride ions and the results are presented in Figure 6.20. In both instances, as ammonia oxidation ensued, the ORP values increased as expected. However, as greater NH3 oxidation proceeded in the presence of Cl^- a more significant increase in ORP was observed

suggesting that the reducing power of the irradiating NH_3 solution was diminishing more rapidly in the presence of Cl^- than when Cl^- was absent.

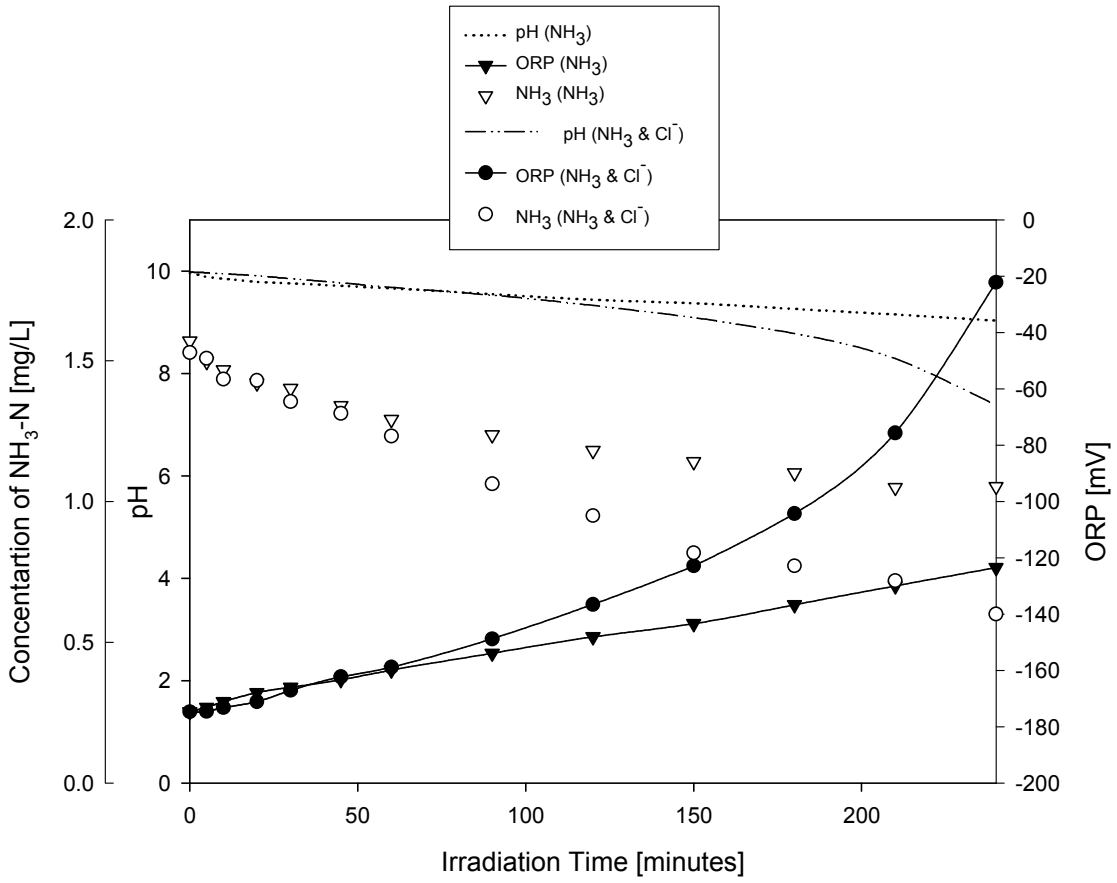

Figure 6.20. Kinetics of ORP and pH for Irradiated Aqueous Solutions of (i) NH_3 and (ii) NH_3 with Cl^- = 20 mg/L

Pourbaix (pE –pH) diagrams show the representation of the half-reactions involving protons and/or electrons. The term pE is a measure of the availability of electrons in solution and is defined as – log (e^-). The relationship between pE and ORP is given by,

$$pE = (FE_{system}) / (2.303\ RT)$$

F is Faraday's constant = 96,485 J/V-mole, R is the universal gas constant = 8.314 J/mol K and T is the temperature is degrees Kelvin.

Redox equilibria are depicted on the Pourbaix diagram by (a) horizontal lines that show the equilibrium involving only electrons (b) vertical lines where the reaction involves only protons and (c) diagonal lines that depict redox involving both protons and electrons. Figure 6.21 shows the pE – pH graph of the irradiating NH_3 and NH_3 / Cl^- solutions. The diagonal lines indicate that both protons and electrons are generated during ammonia oxidation and the linear regression reveals that the lines are virtually coincidental, as they should be and bears the relationship, pE = −pH + 7.

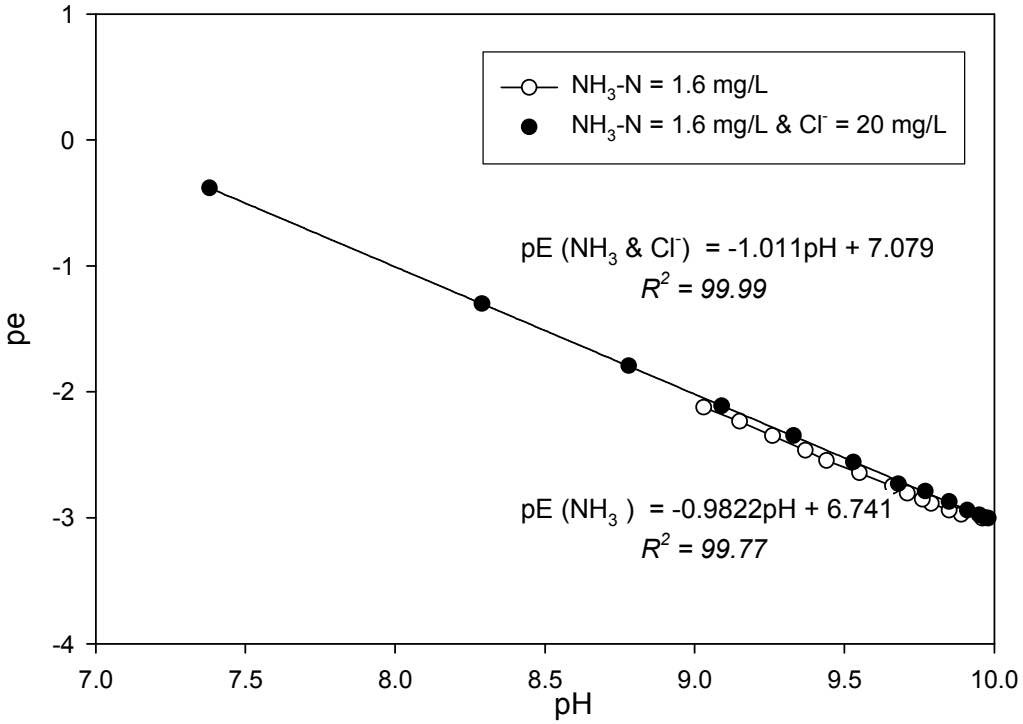

Figure 6.21. pE - pH Diagram for Irradiating NH_3 and NH_3/Cl^- Solutions

Half reactions involving the NH_3 species could therefore be written as:

$$1/6\ NO_2^- + 7/6\ H^+ + e^- \rightarrow 1/6\ NH_4^+ + 1/3\ H_2O$$

$$1/8\ NO_2^- + 9/8\ H^+ + e^- \rightarrow 1/8\ NH_4^+ + 3/8\ H_2O$$

6.4.2. Scavenger Studies to Verify the Electron Availability in NH_3 Irradiated Solutions in the Presence and Absence of Halide Ions

Dwibedy et al. (1996) showed that when aerated solutions of ammonia are irradiated, the reaction of NH_3 with OH radicals forms nitrite. In the photodecomposition of nitrite solutions, a few investigators have explored the possibility that hydrated electrons are formed, but their results were inconclusive (Fischer and Warneck, 1996; Mack and Bolton, 1999). The hypothesis that ammonia oxidation generates electrons in aqueous solution was verified using sulfur hexafluoride (SF_6) as an electron scavenger.

Asmus et al. (1968) has reported that SF_6 is chemically inert except with its reaction with dry electrons (e^-) or aqueous electrons (e_{aq}^-). Fluoride and sulfate ions are both produced as final end products in accordance with the following reactions.

$$SF_6 + e_{aq}^- \rightarrow F^- + SF_5$$

$$SF_5 + 4H_2O \rightarrow 5F^- + SO_3^{2-} + 7H^+ + OH$$

$$SO_3^{2-} + (OH, SF_5 \text{ or } H_2O_2) \rightarrow SO_4^{2-}$$

(SO_3^{2-} is oxidized by OH, SF_5 or H_2O_2 to SO_4^{2-})

In testing the hypothesis that the electrons generated during NH3 oxidation are available for reaction with other constituents in water, a 20 L batch solution of SF_6 at pH 10 was prepared

and irradiated in the presence and absence of NH_3. Higher production of sulfate ions was observed in the solution containing NH_3 where oxidation proceeded (Figure 6.22).

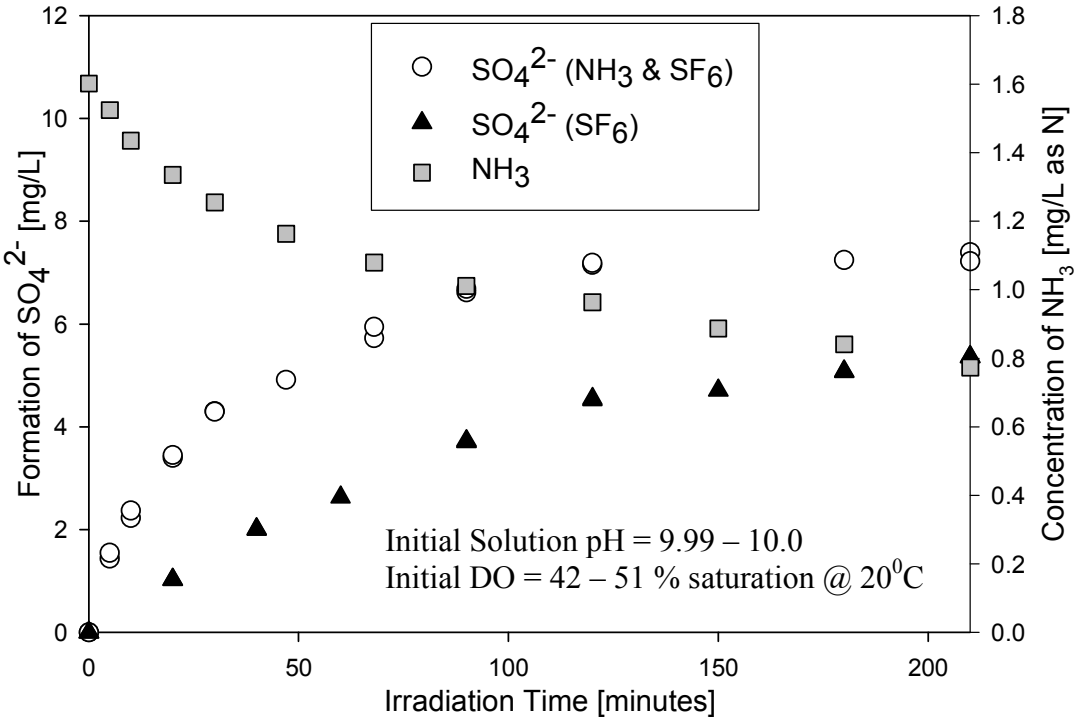

Figure 6.22. Sulfate Formation in UV Irradiated SF_6 Solutions
(i) in the absence of NH_3 (ii) in the presence of NH_3-N = 1.6 mg/L

When Br^- and Cl^- were each irradiated in the presence of SF_6 and dissolved oxygen (DO), the halide ion concentration was gradually depleted. However, when ammonia was present, no loss of halide ion occurred as shown in Figure 6.23. In order to determine whether the aqueous electrons reacting with SF_6 were sourced from the irradiated water or the halide ions, de-ionized water containing only dissolved SF_6 was irradiated. Only trace levels of the reaction products, fluoride and sulfate ions were detected following irradiation of about 10 hours. It is therefore expected that SF_6 scavenges aqueous electrons from the halide ions' photochemical cage, causing depletion of the halide ion concentration in the presence of SF_6, but when ammonia is present, oxidation occurs and e^- is generated while Br^- and Cl^- concentrations remain unchanged.

The reaction rates of SF_6 and DO with e_{aq}^- are similar, 1.65×10^{10} $M^{-1}s^{-1}$ and 1.9×10^{10} $M^{-1}s^{-1}$ respectively as reported in Hart et al. (1970). However, based on the results obtained herein, it can be surmised that the electron scavenging ability of both SF_6 and DO differ for the halide ions.

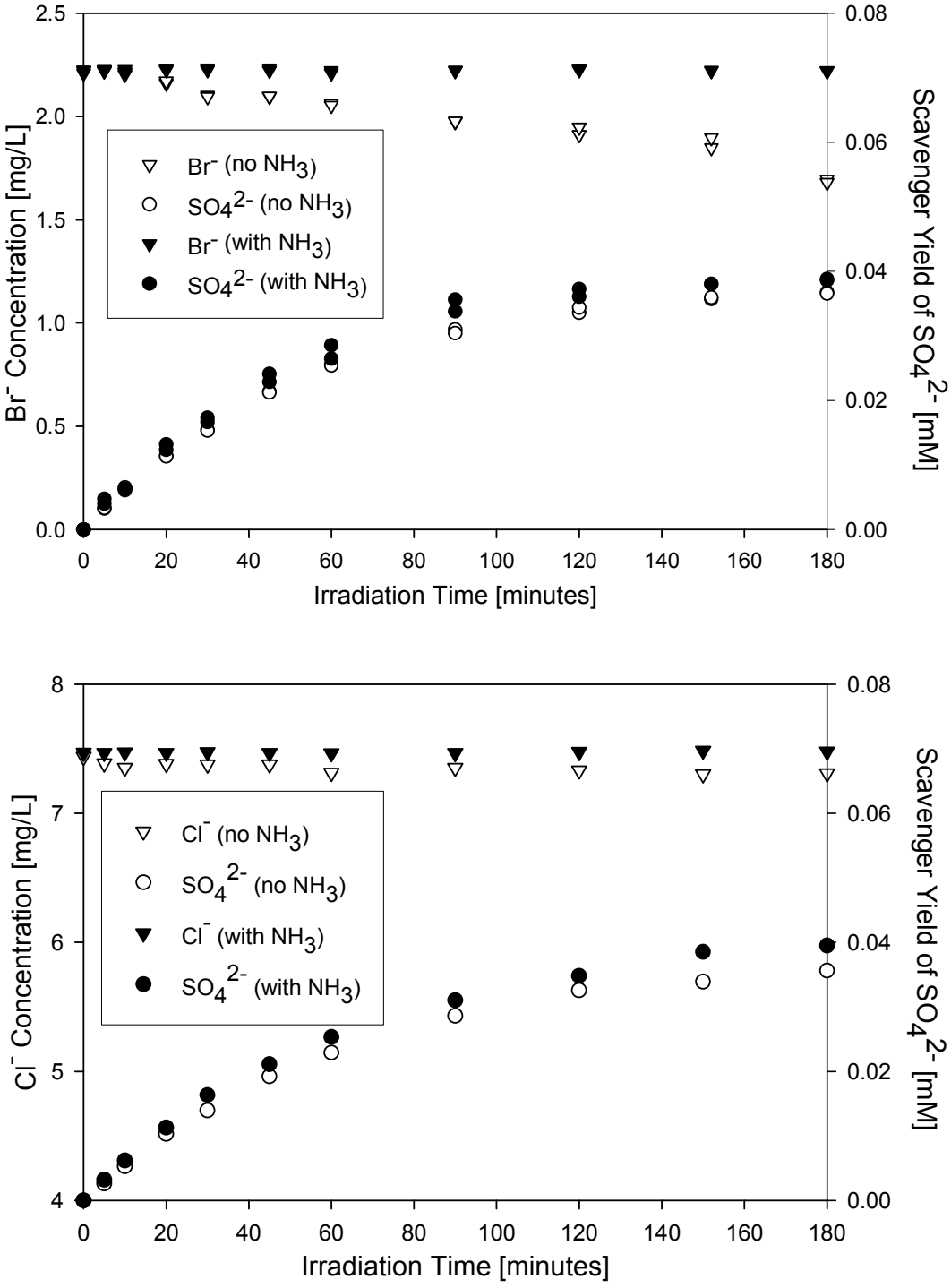

Figure 6.23. UV Irradiation of Br^- (2.22 mg/L) and Cl^- (7.4 mg/L) in the Absence and Presence of NH_3 (1.6 mg/L as N)

6.4.3. UV Irradiation of Bromate in the Presence of Aqueous Ammonia

Farkas and Klein (1948) were the first to observe the effect of ammonia on irradiating bromate solutions. They ascribed this phenomenon to the reactions of hypobromite ion, BrO^- (formed as an intermediate in the photodegradation of aqueous bromate) with ammonia, forming the less absorbing Br^- species at a faster rate. The following equation was provided as supporting evidence.

$$3BrO^- + 2NH_4^+ + 2OH^- \rightarrow 3Br^- + N_2 + 5H_2O$$

Farkas and Klein (1948) irradiated concentrated solutions of bromate (i.e. 0.1M) and observed that BrO^- was formed in greater quantities in the absence of ammonia than in its presence, but was depleted during the course of the irradiation. They predicted that this greater depletion of BrO^- in the presence of ammonia was due to its reaction with ammonia forming nitrogen gas. Nevertheless the products of ammonia oxidation were not measured to observe nitrogen gas formation.

This supposition was neither verified nor fully explored and relies on the assumption that BrO_3^- decays solely by light absorption under UV with low-pressure lamps. However, the maximum absorption wavelength for BrO_3^- occurs at 185 nm so direct photolysis of bromate with low-pressure lamps may not be its primary mechanism of photo-decomposition. The general consensus (Siddiqui et al., 1996; Buxton and Dainton, 1968) with respect to the mechanism of photodecomposition with low-pressure lamps is that BrO_3^- decomposes via indirect photolysis where electrons formed in the irradiated water are responsible for bond

cleavage between bromine and oxygen atoms. Several intermediate oxy-bromine species including BrO^- are formed prior to the final reduction product, the bromide ion.

It is hypothesized that the accelerated rate of photodecomposition of BrO_3^- in the presence of NH_3 is attributed to the release or increased availability of electrons as ammonia oxidation occurs. It was shown earlier that this additional supply of electrons is generated through the ammonia photo-oxidation system. The theory of electron availability during BrO_3^-/NH_3 photodecomposition is therefore a plausible explanation for the increased rate of bromate decay observed in the presence of ammonia. This phenomenon was further explored in much more diluted solutions (7×10^{-6} M and lower) than those employed by Farkas and Klein (1948).

First irradiating BrO_3^- alone in de-ionized water at pH 5.6 and then irradiating the same initial bromate concentration and solution pH in the presence of ammonia clearly indicated that aqueous ammonia has an accelerating effect on the rate of bromate photodecomposition. The results are shown in Figure 6.24 below. A Br balance was conducted by determining the $\sum$(Br) species, as a function of time and the results show that the major reaction end-product in dilute solutions is bromide. Nonetheless, there was no accumulation of hypobromite ion in the absence and presence of ammonia as observed by Farkas and Klein (1948).

In comparing the difference in the initial pseudo-first order rate (k_{obs}) for the photodecomposition of BrO_3^- in the presence and absence of ammonia, it was found that k_{obs}

was increased by over 100% when NH_4^+ is present (see Figure 6.25) than when ammonia was absent.

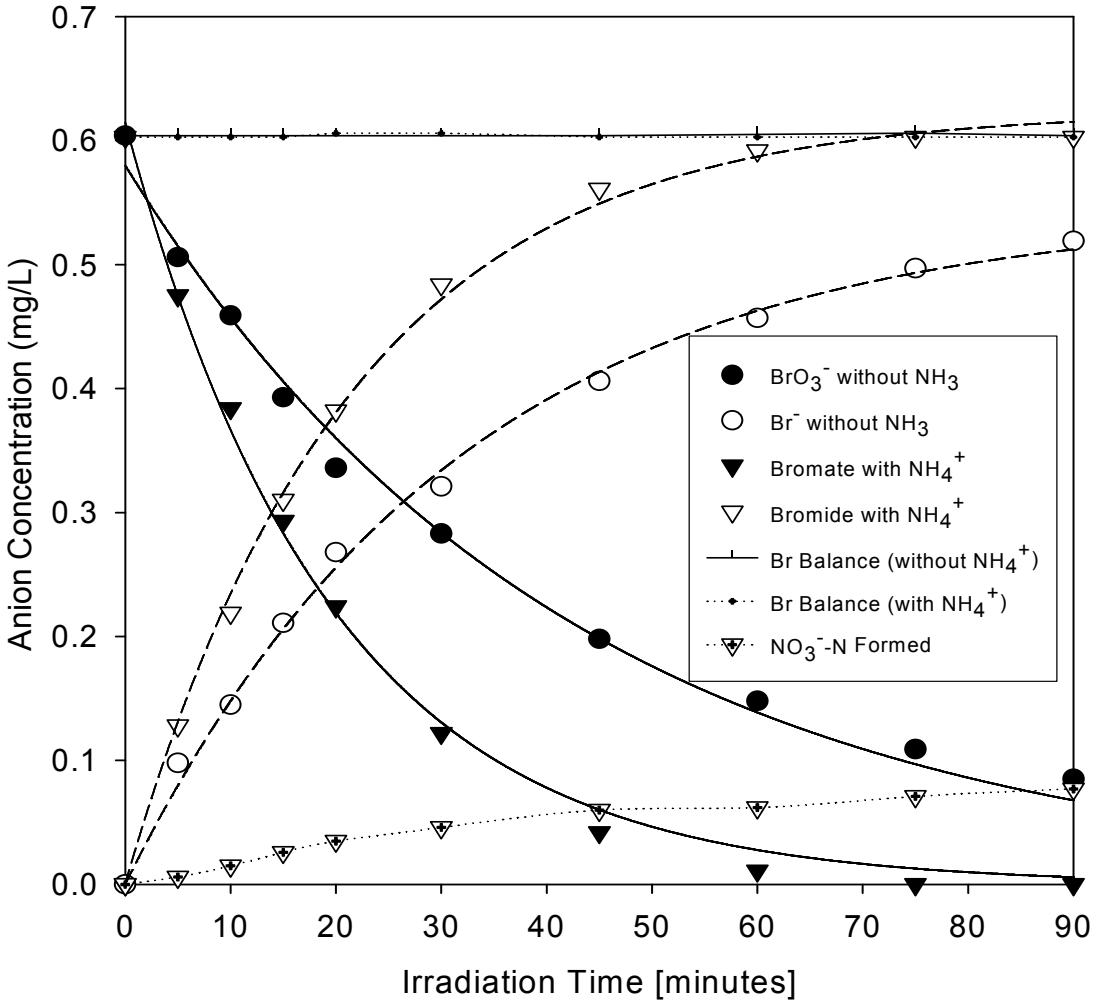

Figure 6.24. UV Irradiation of BrO_3^- in the Absence and Presence of NH_4^+

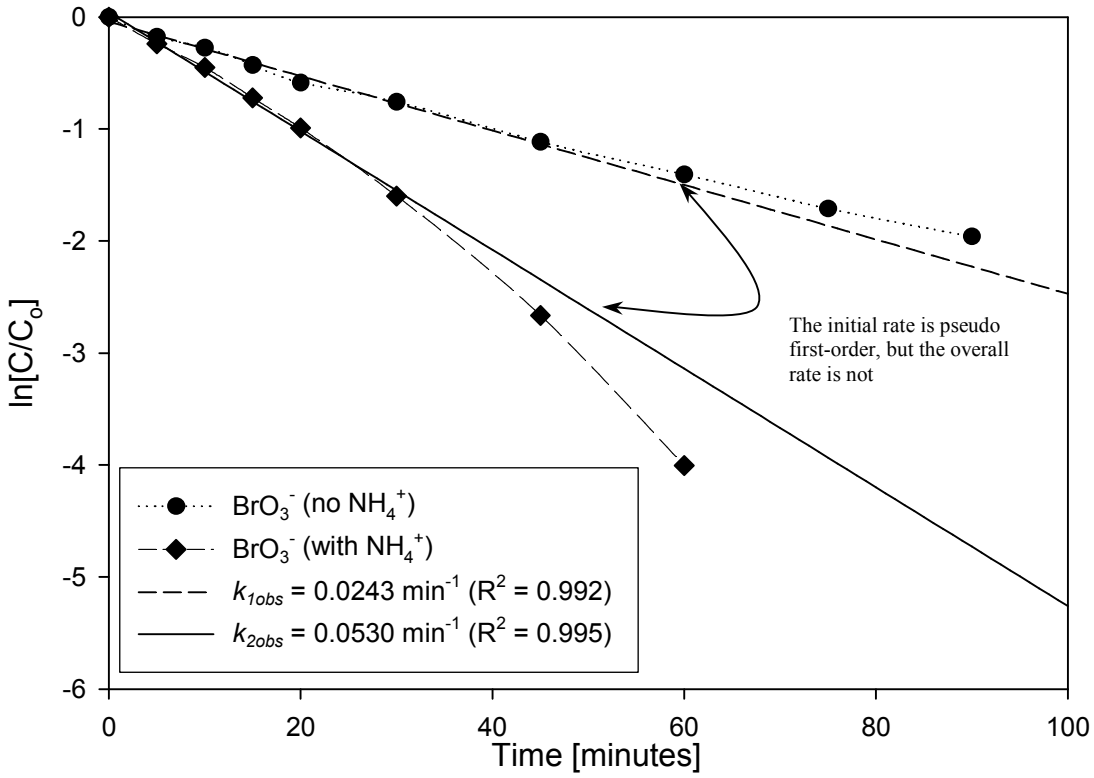

Figure 6.25. First-Order Kinetic Representation of BrO_3^- Photodecomposition without (k_{1obs}) and with (k_{2obs}) NH_4^+

The effect of initial concentrations of bromate was investigated and it was found that the rate of photodecomposition was only slightly affected by the initial concentration of bromate. Figure 6.26 show that the higher initial bromate concentration resulted in a slightly lower k_{obs} for bromate photodecomposition. In almost halving the initial BrO_3^- concentration, achieved an increase in the photodecomposition rate of a little more than 10%, shown in Figure 6.27.

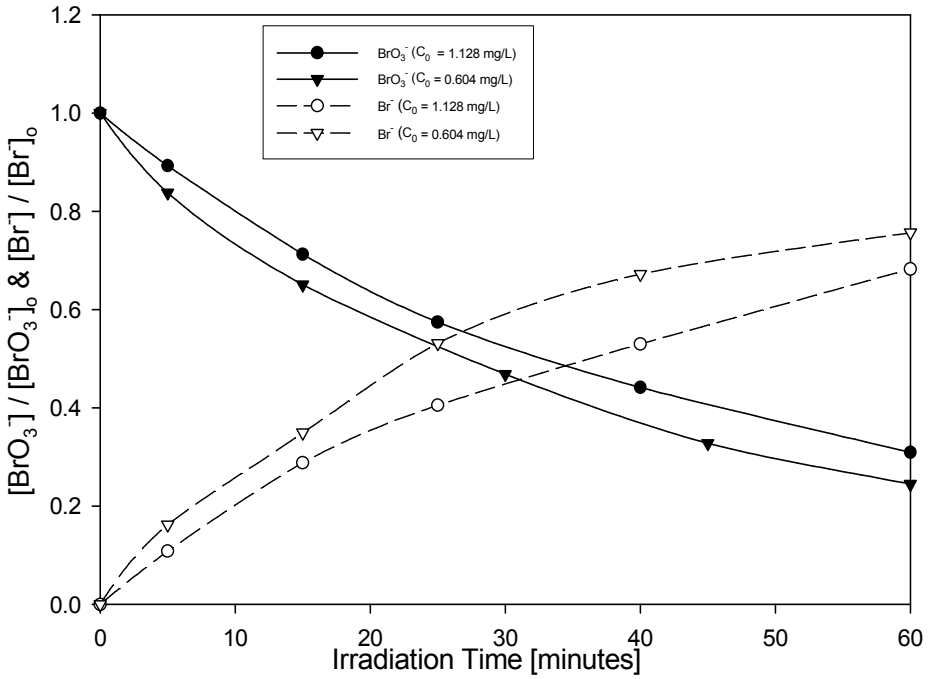

Figure 6.26. Effect of Initial BrO_3^- Concentration (C_o) on its Rate of Photodecomposition

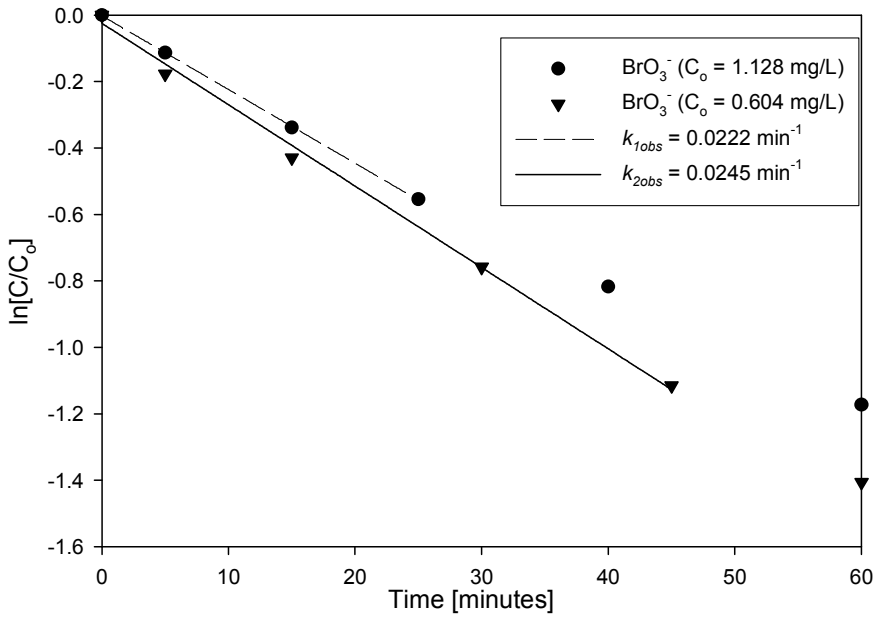

Figure 6.27. First-Order Representation of BrO_3^- Photodecomposition at Different Initial Concentrations

In evaluating the influence of ammonia concentration on the photodecomposition of bromate, four different initial concentrations of ammonia (1.26 mg/L, 0.39 mg/L, 0.22mg/L and 0.03 mg/L) were applied to the same initial concentration of bromate at pH 5.6, producing various Br:N initial ratios. The results are presented in Figure 6.28 and Table 6.3. All concentrations of ammonia were capable of significantly accelerating the rate of bromate photodecomposition, however, at Br: N < 1 the accelerating effect of ammonia tapered off after continuous irradiation for some time.

TABLE 6.3. Effect of NH_4^+ Concentration on BrO_3^- Photodecomposition

NH_4^+ -N [MG/L]	INITIAL BrO_3^- / NH_3 MOLAR RATIO AS Br / N	pH		NO_3^--N AFTER 1 HR	% Conversion of NH_4^+-N to NO_3^-	k_{obs} (MIN^{-1})
		Initial	1 hr after			
0.00	-	5.46	5.48	-	-	0.0243
0.03	5.561	5.53	5.13	0.024	80	0.0261
0.22	0.766	5.44	4.70	0.068	31	0.0462
0.39	0.435	5.52	4.65	0.087	22	0.0489
1.26	0.135	5.47	4.55	0.112	14	0.0530
0.80	0.207	3.20	3.17	0.080	10	0.0428
0.80	0.207	4.63	4.30	0.090	11	0.0484
0.80	0.207	8.50	5.28	0.185	23	0.0573

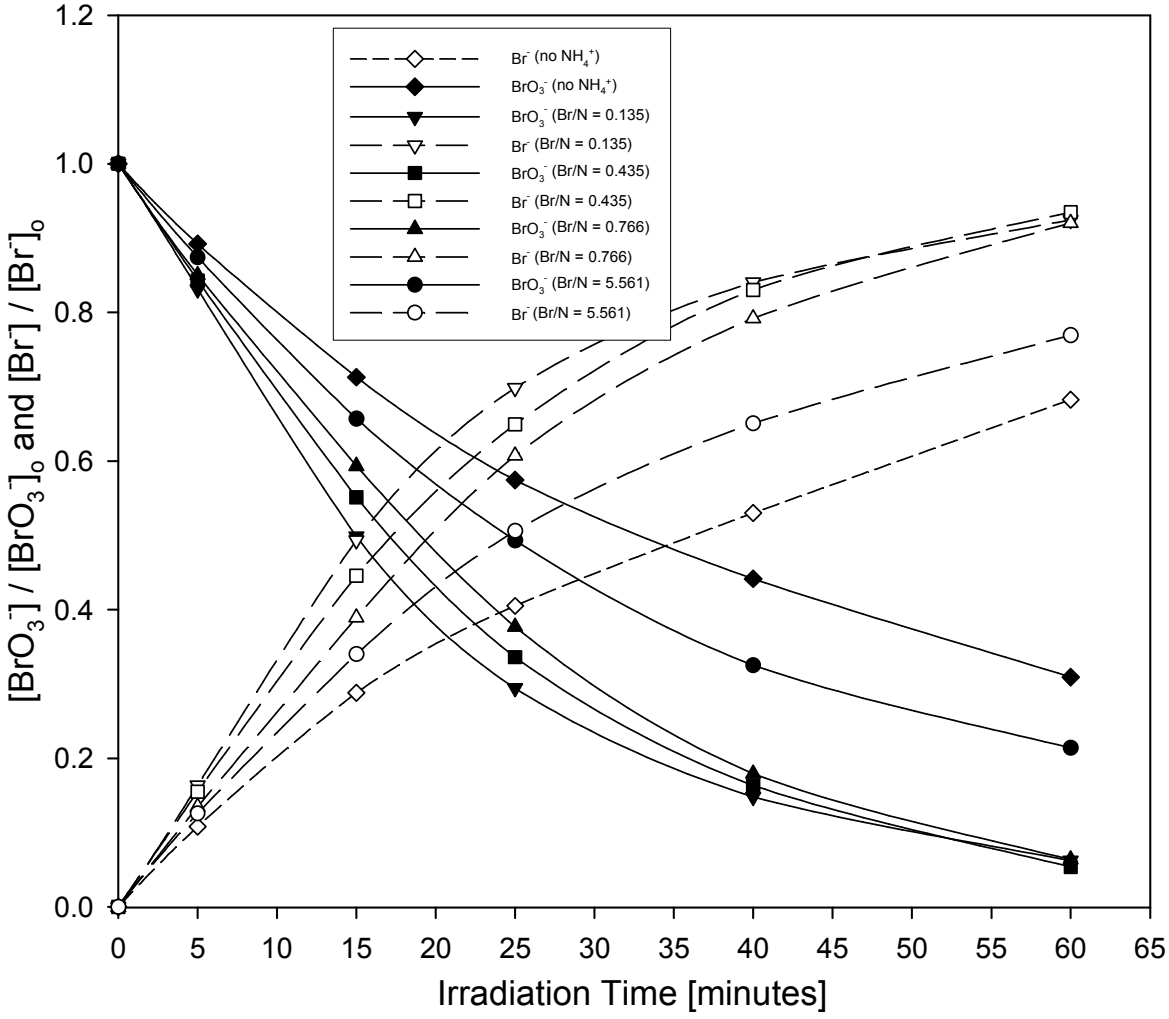

Figure 6.28. Effect of NH_4^+ Concentration on BrO_3^- Photodecomposition

In attempting to assess the effect of initial solution pH on the rate of bromate photodecomposition in the presence of ammonia, the same initial bromate and NH_4^+ concentrations were used for all experiments. Sodium hydroxide was used to increase the pH while sulfuric acid was applied to depress the pH.

As can be seen from Figures 6.29 and 6.30, a greater rate of photodecomposition is attained under alkaline conditions, at least within the initial stages of irradiation. This is in accordance with greater ammonia photo-oxidation occurring at elevated pH, as discussed previously. But since the pH is depressed during NH_3 photodecomposition, the accelerated rate of BrO_3^- photodecomposition wanes.

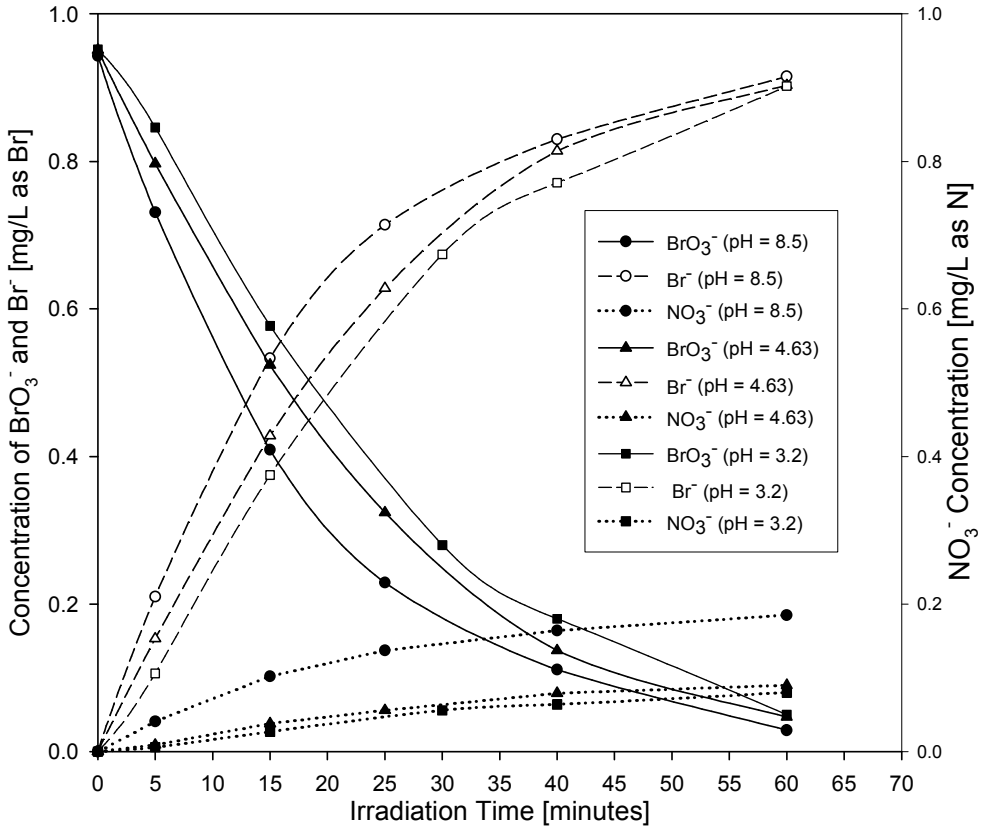

Figure 6.29. Effect of pH on the Photodecomposition of BrO_3^- in the Presence of NH_4^+ (Br:N = 1:5)

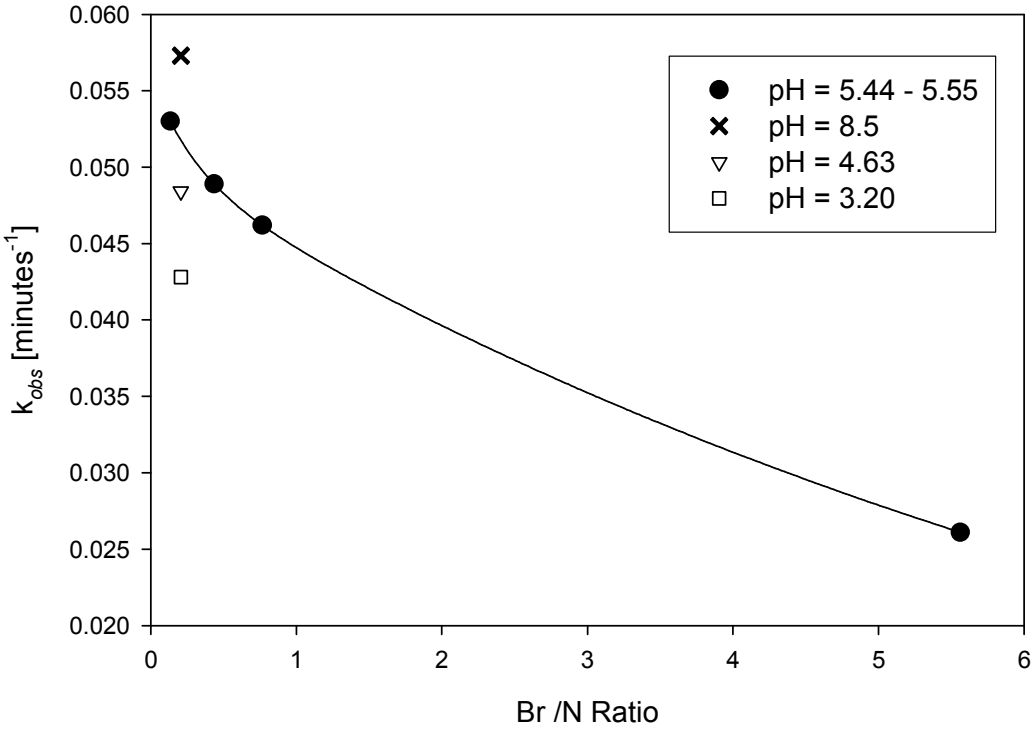

Figure 6.30. Influence of BrO_3^--Br/N Ratio on k_{obs} for BrO_3^- decay

During the photodecomposition of bromate in the presence of aqueous ammonia, it was found that nitrate formation occurred with a corresponding depression of pH. Figure 6.31 and Table 6.3 show the relation of nitrate formation with pH depression during the photodecomposition of bromate and ammonia.

In order to test whether bromate decay in the presence of ammonia results from the additional supply of electrons generated during ammonia oxidation, solutions of bromate at pH 10 were also irradiated in the presence of ammonia and chloride ions (a common constituent in source water). Since the presence of halide ions accelerates the decomposition of NH_3, there will be an even greater supply of electrons from NH_3/Cl^- oxidation for BrO_3^- scavenging. As shown in Figure 6.32 the fastest rate of bromate decay was achieved when both ammonia and chloride ions (Cl^- = 10 mg/L) were present. This result was expected since NH_3 oxidation occurred at a faster rate in the presence of both ammonia and chloride ions than ammonia alone, providing a greater supply of electrons for BrO_3^- scavenging. It can therefore be surmised that the faster rate of bromate decay in the presence of ammonia is a consequence of electron scavenging from the supply (availability) generated as ammonia oxidation proceeds.

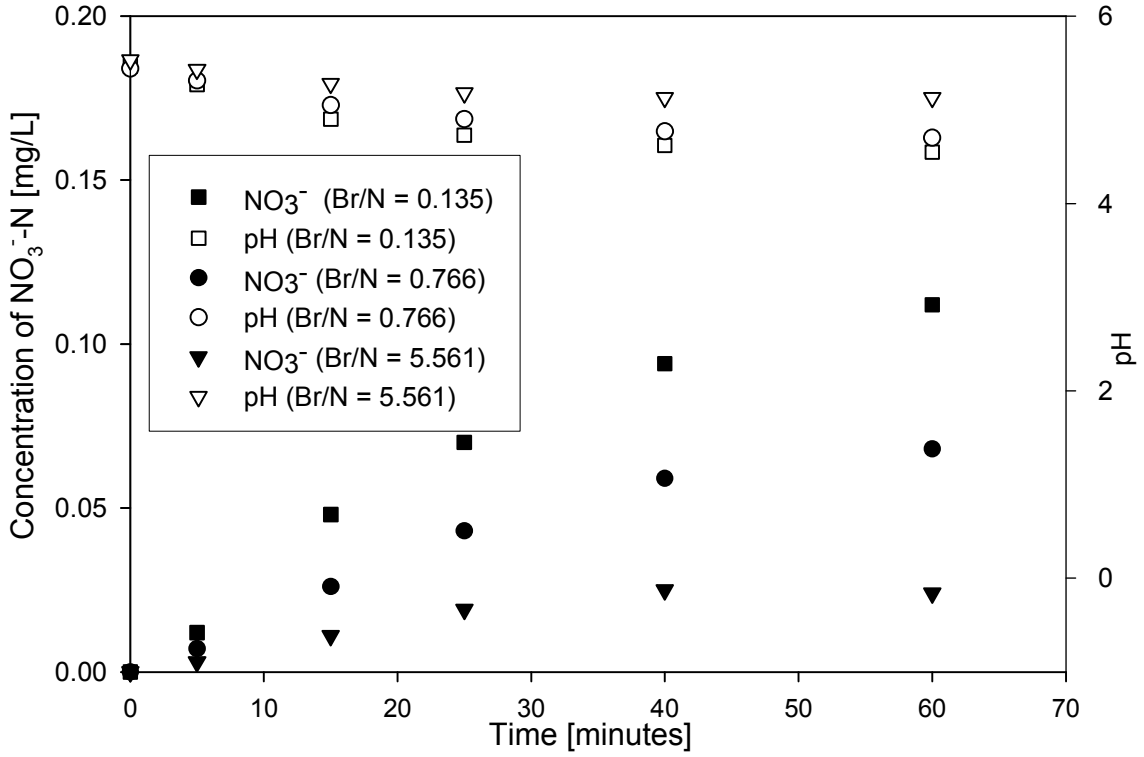

Figure 6.31. NO_3^- Formation and pH Change Resulting from BrO_3^- Photodecomposition in the Presence of NH_4^+

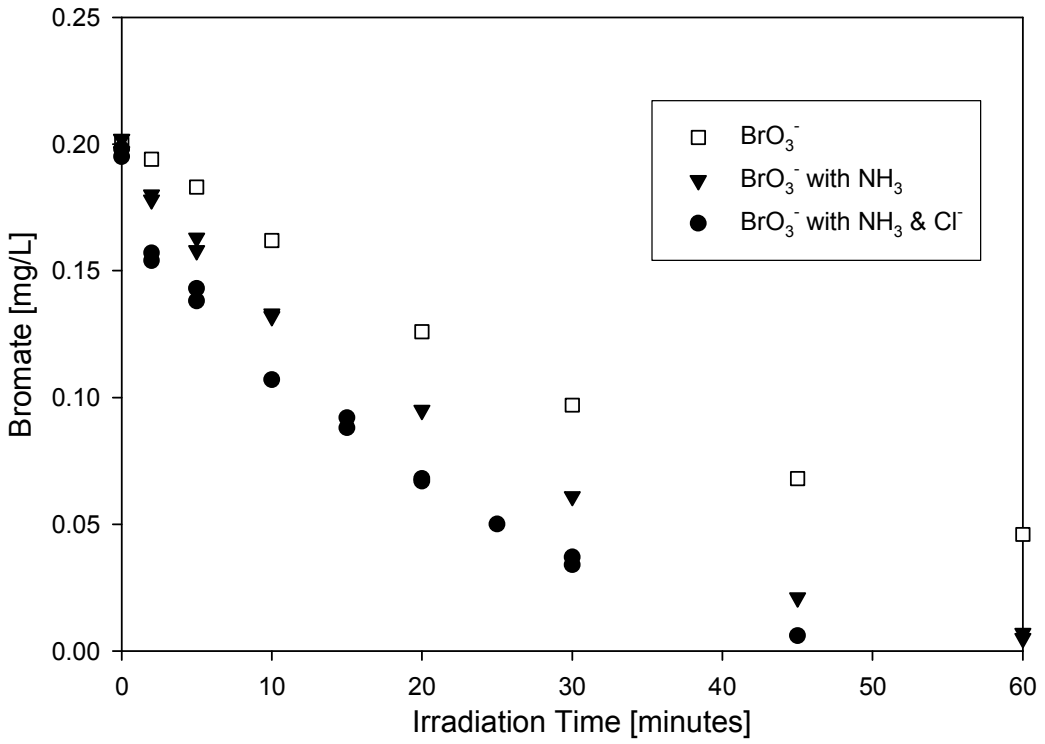

Figure 6.32. BrO_3^- Decomposition with (i) UV (ii) UV and NH_3-N = 1.6 mg/L (iii) UV, NH_3-N = 1.6 mg/L and Cl^- = 10 mg/L

In general, for increasing concentrations of ammonia, it was found that as the molar ratio [BrO_3^--Br/N] increases, the percent conversion of aqueous ammonia also increases, but there is greater nitrate formation as [BrO_3^--Br/N] is lowered (see Figure 6.33). Smaller concentrations of ammonia were more readily converted to nitrate, resulting in higher % conversion of NH_4^+ but having lower overall nitrate concentrations and effecting to a lesser extent, the increase in the rate of bromate decay.

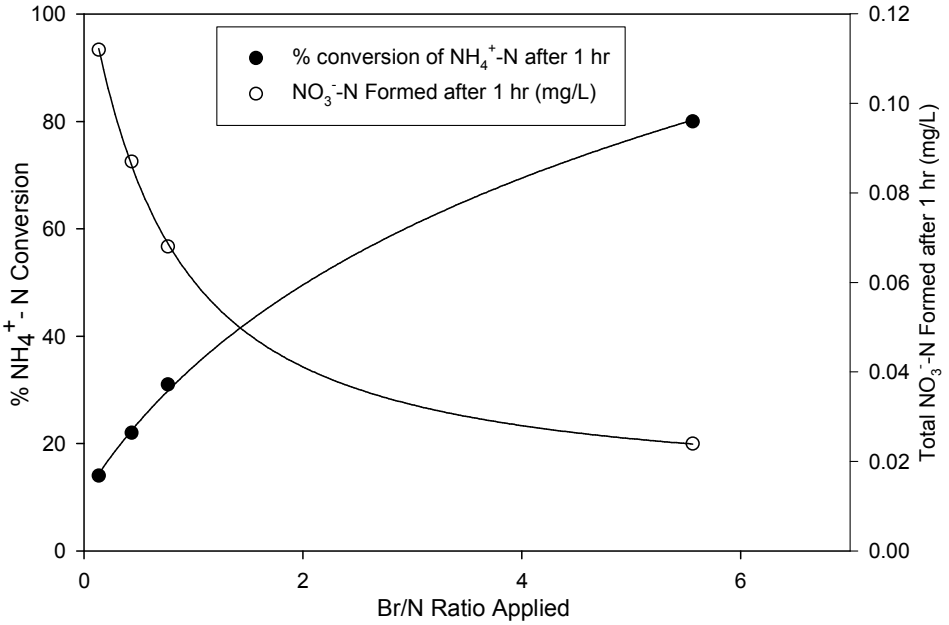

Figure 6.33. Relationship between the Br/N Ratio Applied and % Conversion of NH_4^+- N to NO_3^- - N after 1 hr

7.0. REACTION SCHEME AND SIMULATION OF THE CL^- / NH_3 SYSTEM

7.1. Development of Reaction Scheme for Cl^- / NH_3 System

Based on the foregoing discussion of the results the following summary is reiterated in the development of a reaction scheme:

- Ammonia oxidation with low-pressure mercury lamps take place in alkaline solutions, implying that only the NH_3 species of ammonia is oxidized and/or reaction of the NH_4^+ species is very slow.
- Ammonia oxidation occurred in the presence of Cl^- and Br^- at pH 5.5 – 5.8 and oxidation was enhanced at alkaline pH. The bromide ion was observed to be more effective in the enhancement process than chloride.
- Oxygen is consumed during NH_3 oxidation to nitrite/nitrate
- Protons are generated during the process and may depress the pH of the irradiating solution, depending on the extent of NH_3 oxidation occurring.
- Electrons are generated (available) during NH_3 oxidation, but are not aqueous (free) electrons and are therefore only important in the presence of scavengers.

The literature reports hundreds of reactions for NH_3 photo-oxidation. These reactions involve both water photolysis as well as redox and equilibrium reactions involving the formation and decay of nitrogen-based intermediates. In order to select a reasonable number of reactions that could adequately be used for simulation purposes without compromising the result, the literature was scrutinized for information pertaining to the important and influential reactions involved in ammonia oxidation with UV irradiation. No one published article provided this

information, so the reaction scheme was compiled on the basis of the following conclusions drawn from the literature:

- Reactions were identified in Garret et al. (2005) as important reactions used in the simulation of irradiated aerated water.
- Gonzalez and Braun (1996) reported that the complete oxidation of NH_3 to NO_3^- /NO_2^- occurs only in oxygen-saturated solution and approximately 30% re-oxidation takes place in air-saturated solutions. This results in the formation of gaseous nitrogen products with N_2 being the most likely product.
- Several studies have indicated that only the NH_3 species of ammonia is oxidized and the final stable products are generated via the intermediate, peroxynitrite. The yields of NO_3^-/NO_2^- are pH dependent.
- Kirsch et al. (2003) have identified the influential reactions involved in peroxynitrite decay using overall sensitivity coefficients derived from kinetic simulation.

In light of the above, a list of reactions that describe the ammonia oxidation process in aerated solutions was compiled, to incorporate:

- Radical generation and interaction during UV irradiation of water with low-pressure lamps emitting at 254 nm and 185 nm.
- NH_3 oxidation via radical (sourced from the irradiated water) attack. The OH and O_2^- radicals were found to be the major pathway for NH_3 decomposition to NO_x.
- NH_3 re-oxidation to N_2 via hydrazine formation and decay.

- The influential reactions involved in peroxynitrite decay (identified by Kirsch et al., 2003).
- The photolysis effect of UV light on peroxynitrite, nitrite and nitrate decay.

Sections 1 and 2 of Table I in Appendix A lists the reactions that describe the oxidation of ammonia under UV irradiation, along with the rate constants for each reaction. Section 3 of Table I are the proposed reactions that may be responsible for the increase in the rate of NH_3 oxidation observed in the presence of halide ions.

7.2. Simulation and Sensitivity Analysis

The objective of the simulation was to determine the reaction mechanism that is mainly responsible for the increased rate of NH_3 oxidation when irradiated in the presence of halide ions. The Chemical Kinetics Simulator (CKS) version 1.0 (freeware by IBM Almaden Research Center, San Jose, CA) was utilized for the simulations. This program is based on the numerical simulation of chemical reactions using a stochastic approach in solving the general problem:

> Given a fixed volume V containing a spatially uniform mixture of N chemical species that interact through M chemical reactions, what are the time-dependent levels of the molecular species in V given the initial conditions in V.

The algorithm employed in CKS uses a Monte Carlo procedure to determine the time evolution of the species in V. In simulating the time evolution of species, probability density

functions are employed to specify when the next reaction will occur and what kind of reaction it will be (Gillespie, 1977). These functions are determined from the reaction rate constants, reaction conditions and the generation of random numbers from a unit-interval uniform random number generator.

7.2.1. Simulation of Reaction Scheme for Ammonia System

Prior to the simulation of the reaction scheme for the NH_3/Cl^- system, it was necessary to simulate the ammonia oxidation process to ensure that the scheme compiled in Table I (sections 1 and 2) reliably predicts ammonia oxidation with low-pressure mercury lamps. In this regard, the literature-complied reaction scheme for ammonia oxidation under the influence of UV light as presented in sections 1 and 2 of Table I in Appendix A was utilized for this simulation. These reactions and their rate constants, along with the reaction and initial conditions employed for the experiments conducted at initial solution pH 8.16 and 10.05 were inputted into the CKS program.

A comparison of the simulated and experimental results (Figure 7.1) show that the reactions outlined in sections 1 and 2 of Table I/Appendix A adequately describes ammonia oxidation under the influence of low-pressure UV lamps. The simulated kinetic profile for ammonia and nitrite sufficiently match the experimental concentration values at both pH conditions, showing that NO_2^- / NO_3^- are the major stable reaction product at pH 10 while nitrate is the major product at pH 8. However, the simulated profile for nitrate does not always exactly correspond with the experimental values. At initial solution pH 10, slightly higher

concentration levels were obtained for NO_2^- during the initial stages of the simulation, but levels soon became close to the experimental values, the reverse occurred at solution pH 8.

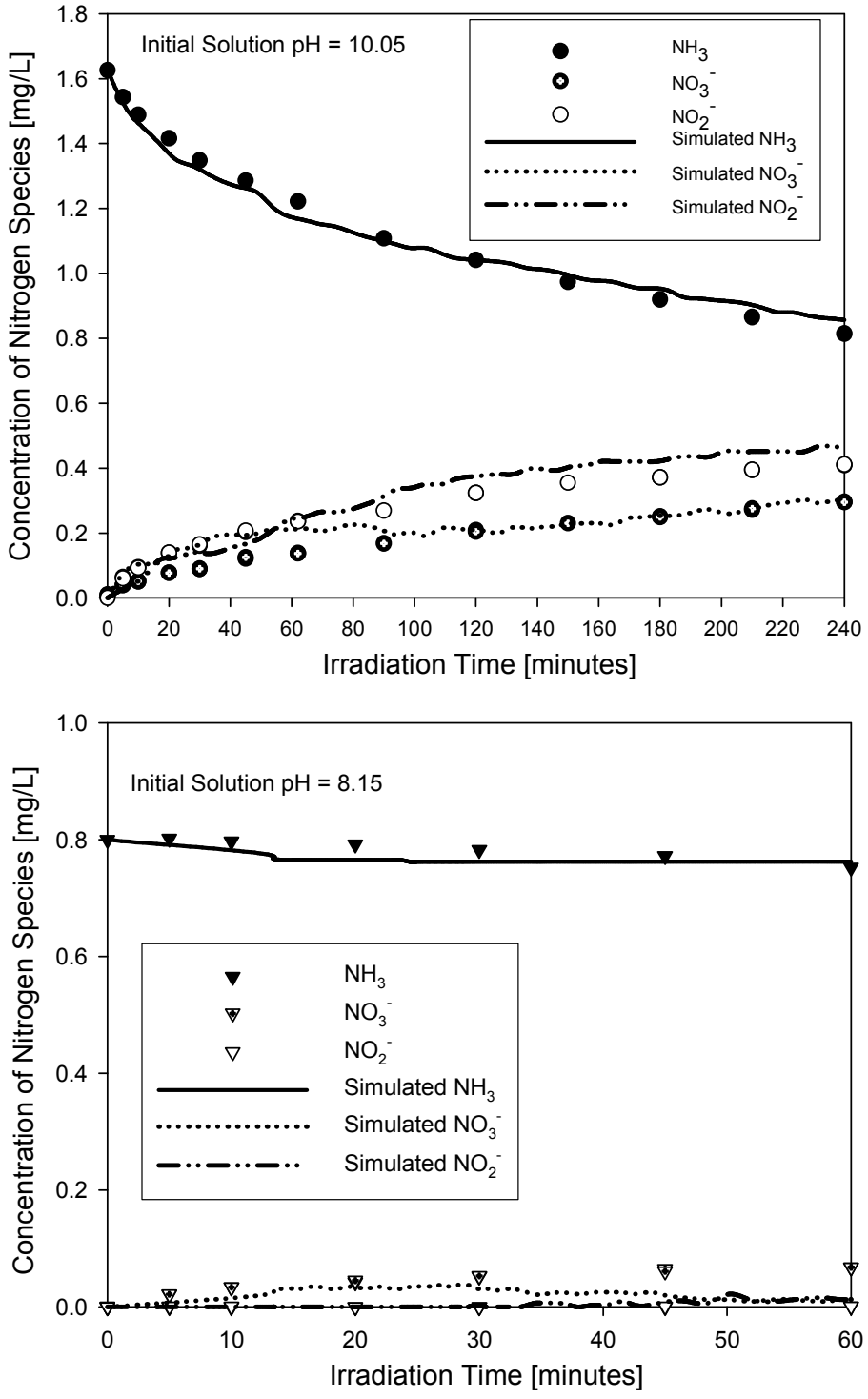

Figure 7.1. Simulated and Experimental Kinetic Profiles for UV Irradiated Ammonia Solutions

7.2.2. Simulation and Sensitivity Analysis of Reaction Scheme for NH_3/Cl^- System

Based on the experimental results and evidence from the literature of a CTTS state created when halide ions are exposed to UV irradiation, it is proposed that capable electron scavengers in the irradiated water may be responsible for the increased rate of ammonia photo-oxidation observed. This idea will be investigated through simulation. Studies on electron scavengers have revealed that:

- Scavengers of hydrated electrons (e_{aq}^-) are also scavengers of dry electrons (e^-) except for the hydrated hydrogen ion, H_3O^+ (Steen, 1970).
- The rates at which dry electrons react with scavengers are generally faster than those for hydrated electrons (Wolff et al., 1975).
- The ability of electron scavengers to remove electrons from the photochemical (or CTTS state) is dependent on the mass and radius of the scavenger (Braden et al., 2001)

Wolff et al, 1975 studied the reaction rate of H_2O_2 and NO_3^- (formed during NH_3 oxidation) with e^- and found that the relative increase in reaction rate were respectively 1.6 and 1.4 times the rate at which e_{aq}^- reacts with these compounds. The reaction rate of NH_4^+ with e^- was also determined as 2.3×10^9 $M^{-1}s^{-1}$ (Horvath and Stevenson, 1989) compared with 1.6×10^6 $M^{-1}s^{-1}$ for its reaction with e_{aq}^- (Ross et al., 1998).

An analysis of the reactions involving hydrated electrons in Table I suggests that the following scavengers may also be capable of scavenging dry electrons from the CTTS well of irradiated chloride ions, according to the following reactions. It should be noted that only

scavengers with a mass greater than the hydrated hydrogen ion (H_3O^+) was considered as potential electron scavengers of dry electrons (Steen, 1970; Braden et al., 2001).

1. $Cl^- + h\nu \rightarrow [Cl + e^-]_{CTTS}$
2. $O_2 + e^- \rightarrow O_2^{\bullet -}$
3. $e^- + O_2^{\bullet -} + H_2O \rightarrow HO_2^- + OH^-$ $\qquad$ $HO_2^- + H_2O \rightarrow H_2O_2 + OH^-$
4. $HO_2^- + e^- \rightarrow {}^{\bullet}OH + 2OH^-$
5. $H_2O_2 + e^- \rightarrow OH^- + {}^{\bullet}OH$
6. $HO_2 + e^- \rightarrow HO_2^-$
7. $O_3 + e^- \rightarrow O_3^{\bullet -}$
8. $e^- + NH_4^+ \rightarrow NH_3 + H^{\bullet}$
9. $e^- + NO_3^- \rightarrow NO_3^{2-}$
10. $e^- + ONOO^- \rightarrow ONOO^{2-}$

Section 3 of Table I lists these potential reactions which are assumed to contribute to the increased rate of ammonia oxidation in the presence of halide ions by adding additional OH and O_2^- to the system. These reactions were incorporated into the ammonia (no halide) simulation. However, due to the excessive computer time required to execute the additional ten reactions, CKS was unable to simulate the total number of reactions. Reactions 6 and 7 were therefore eliminated. The simulation was conducted for:

(i) Initial solution pH = 5.58, NH_3-N = 4.91 mg/L and Cl = 20 mg/L and

(ii) Initial solution pH =10.15, NH_3-N = 1.6 mg/L and Cl = 20 mg/L.

Rate constants for the reactions 1 – 4 and 10 were assumed. The nitrate kinetic profile for simulation conditions (i) is shown in Figure 7.2 below. The NH_4^+ species was in excess at pH 5.58 and the simulated results were very inconsistent, and showed that only minute amounts of this species was depleted by scavenging electrons from the CTTS state of the irradiated Cl^-.

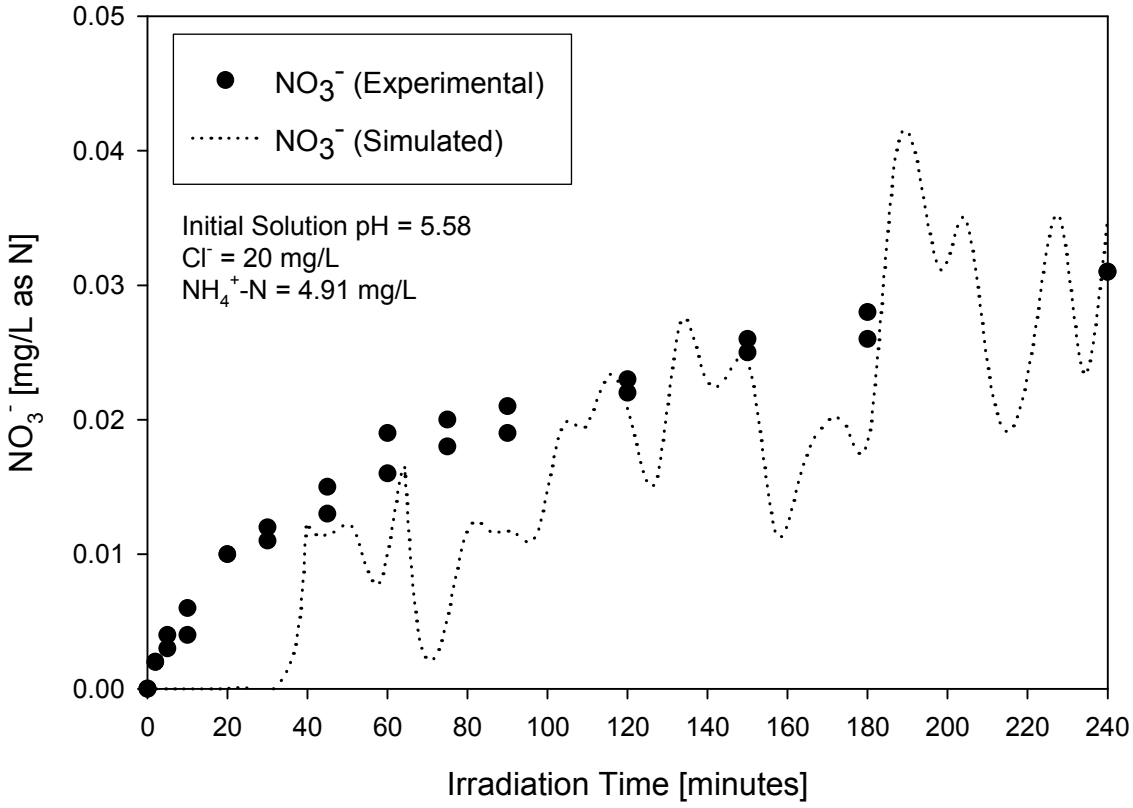

Figure 7.2. Comparison of Simulated and Experimental NO_3^- Formed during UV Irradiation of Ammonia and Chloride Ions

A sensitivity analysis of the assumed reaction rates was conducted by determining whether a change in the rate constants will impact the model prediction capability. The simulated

results of (ii) are presented in Figure 7.3 for different CTTS scavenging rates (from Cl^-) for the species: O_2, O_2^- and HO_2^-. These species contribute to the formation of OH, which together with O_2^- are required for NH_3 oxidation to NO_2^-/NO_3^-. As can be seen in the figure, the rate of NH_3 oxidation increased (over that in the absence of halide ions) when these reactions were employed in the simulation, however, changing the CTTS scavenging rates had no effect on increasing the rate of NH_3 oxidation any further. It should be noted that the simulation curves of Figure 7.3 employed a CTTS formation rate of 2.5×10^{-6} s^{-1} for the chloride ions (equation 1 above), which resulted in only a diminutive loss of Cl^- from solution. In comparing the simulated curves with the experimental results for the NH_3/Cl^- system, it can be seen that these reactions do not totally account for the increased rate of NH_3 oxidation taking place in the system. Other reaction(s) therefore play a role in increasing the rate of NH_3 oxidation in the presence of halide ions.

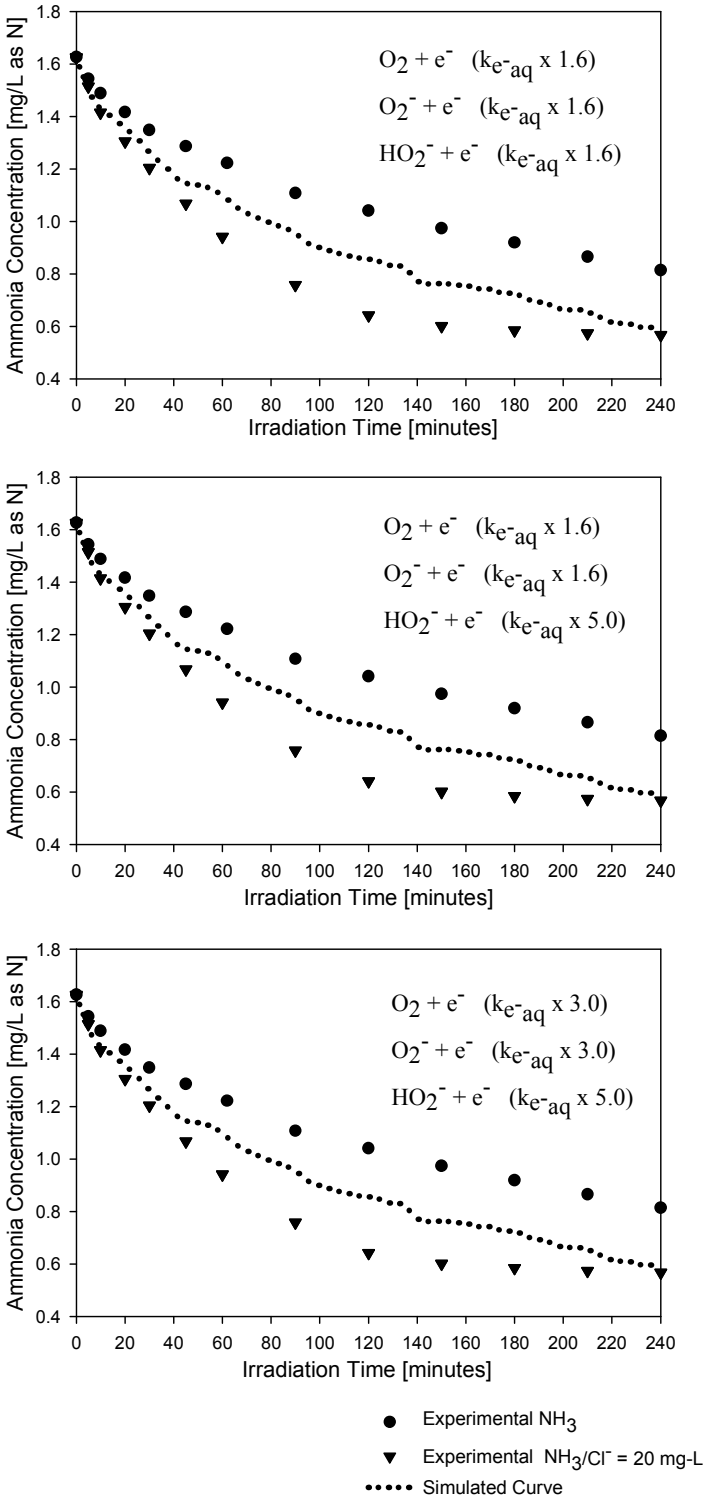

Figure 7.3. Comparison of Experimental and Simulated Kinetic Profiles of NH_3-N (1.6 mg/L) Oxidation in the Presence of Cl^- = 20 mg/L for Different Scavenger Rates

It has been observed that hydroxide ions exhibit CTTS states when exposed to irradiation (Blandamer and Fox, 1970). This may be another possible supply route for OH radicals whereby the chlorine atoms (released after scavenging from the CTTS state by O_2 and other radicals) remove electrons from the CTTS state of the hydroxide ions (Ross et al., 1998).

$$Cl + OH^- \rightarrow {}^{\bullet}OH + Cl^- \qquad k = 1.8 \times 10^{10}\ M^{-1}s^{-1}$$

This reaction was added to the scavenging reactions of Figure 7.3 and the results for estimated rates of CTTS formation by Cl^- are presented in Figure 7.4. The Chi-squared Goodness-of-Fit parameter (χ^2) shows that the null hypothesis, H_0 cannot be rejected for any of the chloride ion CTTS formation rate constants employed, however, the rate constant $2.0 \times 10^{-4}\ s^{-1}$ seems to fit the data best.

In Figure 7.4 it is seen that as the rate at which the chloride ion CTTS state is formed increases, the simulated curve moves away from the first portion of the plotted experimental points, but the simulation draws nearer to the latter experimental points. Another phenomenon involving NO_2^- may explain this behavior. Ross et al., 1998, presented a reaction for the scavenging of electrons from NO_2^- by iodine atoms:

$$I + NO_2^- \rightarrow I^- + NO_2 \qquad k = 8.8 \times 10^{9}\ M^{-1}s^{-1}$$

This reaction may be important for chlorine atoms as well and was included in the simulations (Figure 7.5). It should be remembered that the reactions involved in the pH dependent conversion of NO_2^- to NO_3^- in the presence of halide ions was not included in the simulations (mechanism unknown) and therefore the reaction of the chlorine atoms with NO_2^- might be important only during the initial stages of NH_3 oxidation when NO_2^-

is being generated. As NO_2^- starts to deplete due to declining pH (i.e. when pH ≤ pK_a for ammonia) the reaction of Cl with NO_2^- becomes redundant. The simulated nitrite/nitrate profiles obtained were therefore similar to that in the absence of halide ions. Again, the null hypothesis, H_0 cannot be rejected for any of the chloride ion CTTS formation rate constants employed and the rate constant 2.0 x 10^{-4} s^{-1} fit the data the best.

The simulated results of Figures 7.4 and 7.5 were combined for the CTTS formation rates, 2.0 x 10^{-4} s^{-1}, 2.4 x 10^{-4} s^{-1} and 2.8 x 10^{-4} s^{-1} to show the kinetics when electron scavenging from NO_2^- is important during the initial stages of NH_3 oxidation (i.e. when the solution pH > pKa of NH_3 = 9.4 @ 20^0C) and when this reaction becomes redundant (i.e. when the solution pH < pKa of NH_3). Figure 7.6 shows the combined simulated curves. In this instance, the chloride ion CTTS formation rate constant of 2.4 x 10^{-4} s^{-1} fits the data best.

The proposed mechanism whereby halide ions enhance the rate of NH_3 oxidation under low-pressure UV can thus be summarized as follows:

- Dissolved oxygen scavenges electrons out of the CTTS state of halide ions forming the superoxide ion, O_2^-.
- O_2^- is also an electron scavenger and scavenges e^- from the CTTS state of halide ions forming HO_2^-, which readily dissolves in water generating H_2O_2.
- H_2O_2 is a dry electron scavenger (Wolfe et al,) that scavenges CTTS electrons, generating OH radicals.

- The chlorine atoms released as a result of electron scavenging by (O_2, O_2^-, HO_2^- and H_2O_2) in turn scavenges electrons from hydroxide ions in solution, forming OH radicals and returning the concentration of Cl^- back to its original level. This accounts for the unchanged concentration of halide ions observed during NH_3 oxidation in the presence of bromide and chloride ions.
- As NO_2^- is formed during NH_3 oxidation, chlorine atoms also scavenge their electrons. This reaction competes with the formation of OH radicals from chlorine atoms reducing the amount of OH radicals available for NH_3 oxidation.
- When the pH of the irradiating solution is depressed to the point where ONOOH builds up, NO_2^- is converted to NO_3^- via OH^+ formed from ONOOH. Thereafter, the reaction of chlorine atoms with NO_2^- becomes gratuitous.

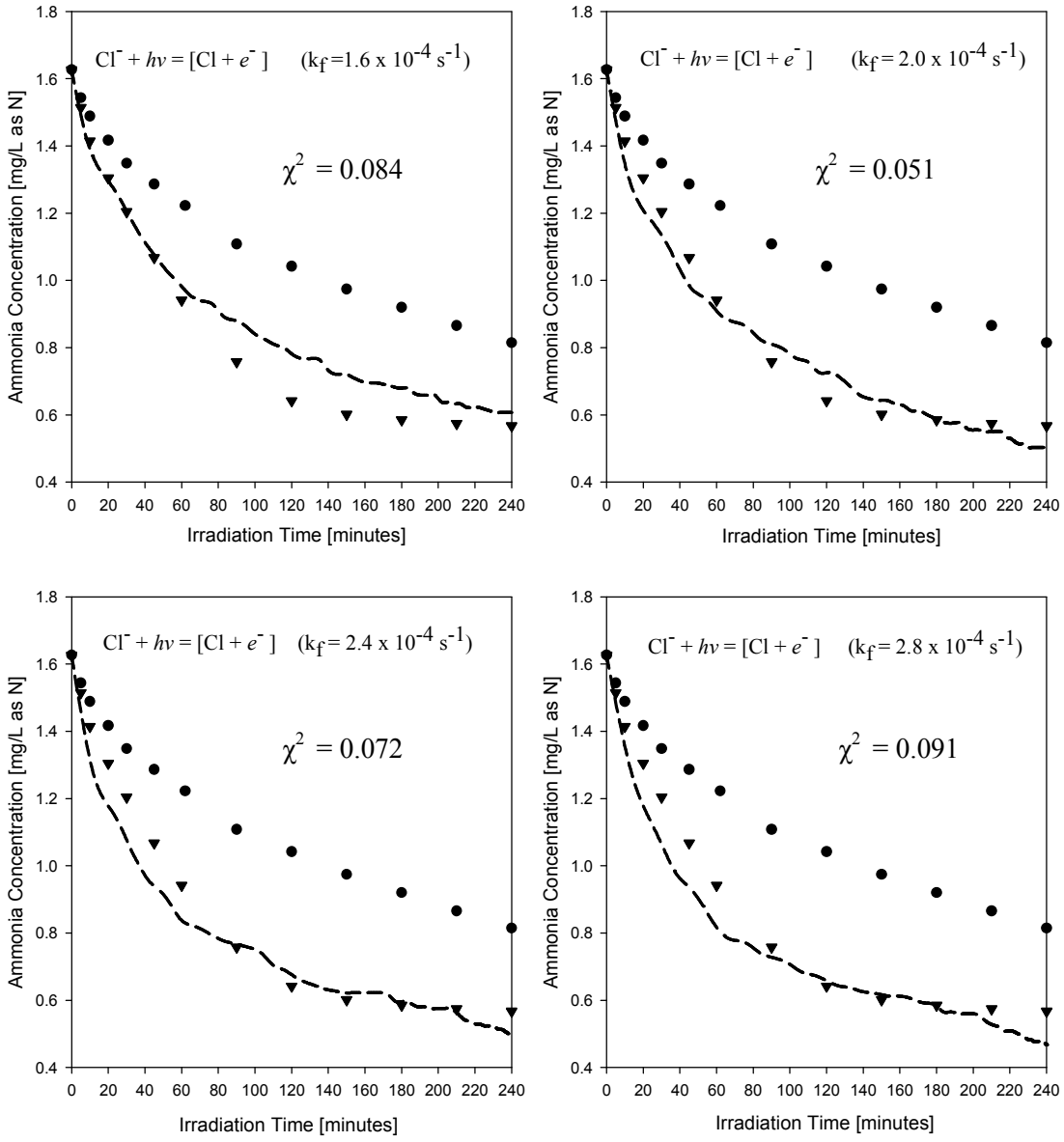

Note: a. Null hypothesis, H_0 = Fit is good.
b. H_0 is rejected if $\chi^2 > \chi_\alpha^2 = 19.675$ at the 5% level of significance and 11 degrees of freedom.

Figure 7.4. Comparison of Experimental and Simulated Kinetic Profiles of NH_3-N (1.6 mg/L) Oxidation in the Presence of Cl^- = 20 mg/L for Different CTTS Formation Rates

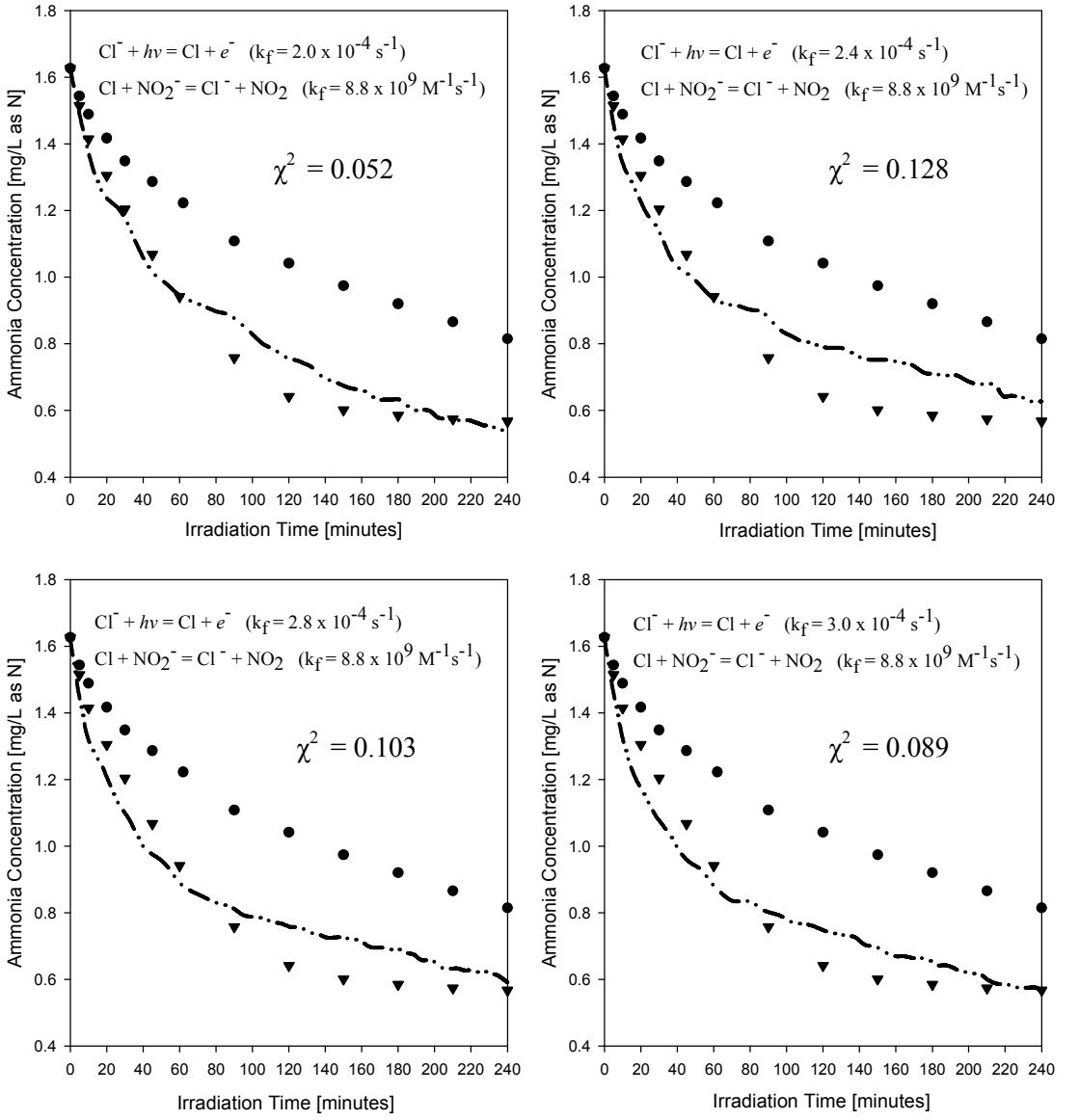

Note: a. Null hypothesis, H_0 = Fit is good.
b. H_0 is rejected if $\chi^2 > \chi_\alpha^2 = 19.675$ at the 5% level of significance and 11 degrees of freedom.

Figure 7.5. Comparison of Experimental and Simulated Kinetic Profiles of NH_3-N (1.6 mg/L) Oxidation in the Presence of Cl^- = 20 mg/L for Different CTTS Formation Rates and Cl scavenging from NO_2^-

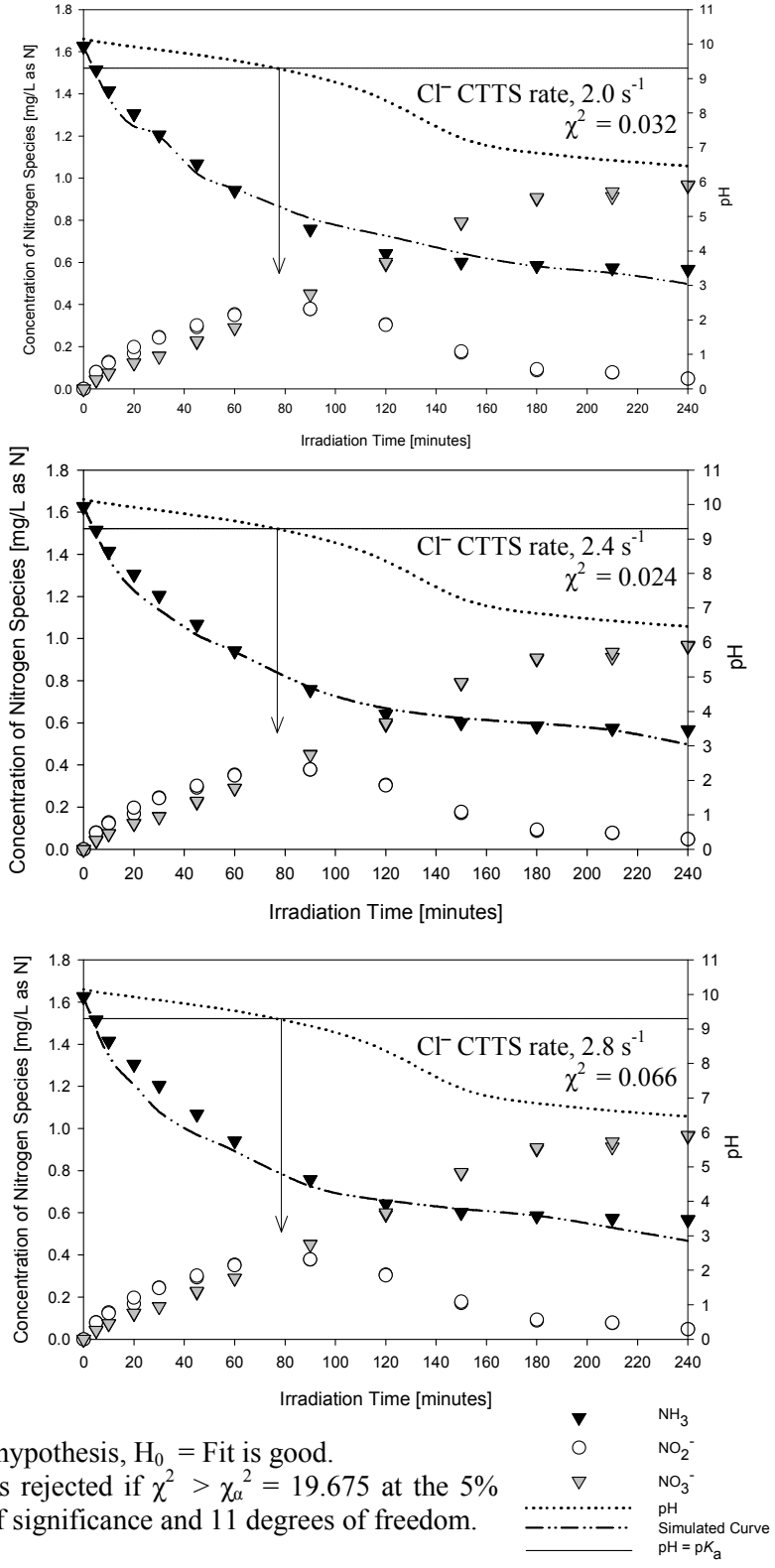

Note: a. Null hypothesis, H_0 = Fit is good.
b. H_0 is rejected if $\chi^2 > \chi_\alpha^2 = 19.675$ at the 5% level of significance and 11 degrees of freedom.

Figure 7.6. Comparison between Combined Simulated and Experimental Results for NH_3-N (1.6 mg/L) Oxidation in the Presence of Cl^- = 20 mg/L for Different CTTS Scavenging Rates

8.0 CONCLUSIONS

The following conclusions are drawn based on the preceding experimental and simulated results:

(i) The halide ions Cl^- and Br^- enhance the rate of NH_3 oxidation in both acidic (5.5 – 5.8) and alkaline (8 – 11) solutions. The extent to which these ions will promote ammonia oxidation is dependent on the concentrations of ammonia and halide ions present as well as the type of halide ion employed.

(ii) I^- did not enhance the rate of NH_3 oxidation under the light intensity applied. Based on the results, it is apparent that iodide was ionized forming free radicals, instead of a CTTS state like Cl^- and Br^-. This suggests that a CTTS state is required in order to achieve enhanced NH_3 oxidation.

(iii) Electrons are generated (available) during NH_3 oxidation and can be accessed by electron scavengers like bromate. BrO_3^- decayed at a faster rate in the presence of ammonia than in its absence. In addition, when chloride ions were added to encourage even greater NH_3 oxidation, bromate decayed the fastest under these conditions.

(iv) Table I in Appendix A adequately describes the NH_3 oxidation process as determined by simulation of these reactions.

(v) The reasons for the increased rate of NH_3 oxidation in the presence of halide ions are:

   a. Electron scavenging from the CTTS state of irradiated halides.

   b. There is an increase in the radicals formed as a result of (a) in the system, (i.e. O_2^-, HO_2^- and H_2O_2) which are all electron scavengers and lead to an

additional supply of OH and O_2^- radicals, which are necessary for NH3, decay.

c. The halide ions are another source of OH radicals since their atoms formed after scavenging by O_2, can scavenge electrons from the hydroxide ions (in significant quantities at alkaline pH) thus generating more OH radicals in the system. Halide atoms can also scavenge electrons from NO_2^- generated during NH_3 oxidation and this competes with the supply of OH radicals for NH_3 oxidation. However, NO_2^- eventually decays in the presence of the halide ions and thereafter its reaction with halide atoms is no longer of consequence.

APPENDICES

APPENDIX A

TABLE I REACTION SCHEME DESCRIBING NH_3 OXIDATION IN THE PRESENCE OF HALIDE IONS WITH UV LOW PRESSURE LAMPS

NO.	*Reaction*	k_x (s^{-1}; M^{-1} s^{-1})	Ref.
	1.0 UV Irradiation of water: Quantum yields (Φ) are given $H_2O + h\nu \rightarrow H^{\bullet} + OH^{\bullet}$ $\Phi\ (e_{aq}^{-}) = 0.0127$		88
1	$H_2O \rightleftharpoons H^+ + OH^-$	$pK_W = 14.17$ @ 20 ^{0}C	33
2	$H^{\bullet} + OH^{\bullet} \rightarrow H_2O$	2.5×10^{10}	33
3	$^{\bullet}OH + {}^{\bullet}OH \rightarrow H_2O_2$	5.0×10^{9}	33
4	$^{\bullet}OH + e_{aq}^{-} \rightarrow OH^-$	3.0×10^{10}	33
5	$e_{aq}^{-} + H_3O^+ \rightarrow H^{\bullet} + H_2O$	2.2×10^{10}	33
6	$OH^- + H^{\bullet} \rightarrow H_2O + e_{aq}^{-}$	2.0×10^{7}	33
7	$H^{\bullet} + O_2 \rightarrow HO_2^{\bullet}$	2.0×10^{10}	33
8	$O_2 + e_{aq}^{-} \rightarrow O_2^{\bullet -}$	1.9×10^{10}	33
9	$H_2O_2 + H^{\bullet} \rightarrow H_2O + {}^{\bullet}OH$	5.0×10^{7}	29
10	$H_2O_2 + e_{aq}^{-} \rightarrow OH^- + {}^{\bullet}OH$	1.2×10^{10}	33
11	$HO_2^- + H_2O \rightarrow H_2O_2 + OH^-$	1.0×10^{4}	33
12	$O^{\bullet -} + H_2O \rightarrow {}^{\bullet}OH + OH^-$	1.7×10^{6}	56
13	$e_{aq}^{-} + O_2^{\bullet -} + H_2O \rightarrow HO_2^- + OH^-$	2.0×10^{10}	33
14	$^{\bullet}OH + OH^- \rightarrow O^{\bullet -} + H_2O$	1.3×10^{10}	86
15	$O^{\bullet -} + O_2 \rightleftharpoons O_3^{\bullet -}$	3.8×10^{9} 4.0×10^{3}	56
16	$O_3^{\bullet -} + O^{\bullet -} \rightarrow 2\ O_2^{\bullet -}$	7×10^{8}	68

17	$^{\bullet}OH + O_3^{\bullet-} \rightarrow OH^- + O_3$	2.5×10^{9}	56
18	$^{\bullet}OH + O_2^{\bullet-} \rightarrow O_2 + OH^-$	1.5×10^{10}	33
19	$HO_2^{\bullet} + {}^{\bullet}OH \rightarrow O_2 + H_2O$	1.2×10^{10}	33
20	$HO_2^{\bullet} + H^{\bullet} \rightarrow H_2O_2$	2.0×10^{10}	33
21	$HO_2^{\bullet} \rightleftharpoons O_2^{\bullet-} + H^+$	1.4×10^{4} (p*K*s = 4.8) 5.0×10^{10}	68
22	$^{\bullet}OH + H_2O \rightarrow H_3O^+ + O^{\bullet-}$	1.13×10^{-3} (p*K*s = 11.9) 5.0×10^{10}	56
23	$H_2O_2 \rightleftharpoons H_3O^+ + HO_2^{\bullet-}$	2.01×10^{-3} (p*K*s = 11.65) 5.0×10^{10}	56
24	$O_3 + e_{aq}^- \rightarrow O_3^{\bullet-}$	3.6×10^{10}	86
25	$HO_2 + e_{aq}^- \rightarrow HO_2^-$	2.0×10^{10}	86
26	$HO_2^- + e_{aq}^- \rightarrow {}^{\bullet}OH + 2OH^-$	3.5×10^{9}	86
2.0 UV Irradiation of ammonia in water			
27	$NH_4^+ \rightleftharpoons NH_3 + H^+$	$k_f = 6.9\times10^{9}$ $k_r = 4.3\times10^{-2}$ (p*K*s = 9.456 @ 20°C)	19
28	$NH_4^+ + e_{aq}^- \rightarrow NH_3 + H^{\bullet}$	1.6×10^{6}	86
29	$NH_3 + {}^{\bullet}OH \rightarrow {}^{\bullet}NH_2 + H_2O$	1.0×10^{8}	86
30	$^{\bullet}NH_2 + {}^{\bullet}NH_2 \rightarrow {}^{\bullet}N_2H_4$	2.2×10^{9}	86
31	$^{\bullet}N_2H_4 + {}^{\bullet}OH \rightarrow {}^{\bullet}N_2H_3 + H_2O$	4.5×10^{9}	86
32	$^{\bullet}N_2H_3 + {}^{\bullet}N_2H_3 \rightarrow 2\ NH_3 + N_2$	2.2×10^{9}	86
33	$^{\bullet}NH_2 + H \rightarrow NH_3$	5.7×10^{7}	86
34	$^{\bullet}NH_2 + {}^{\bullet}OH \rightarrow {}^{\bullet}NH_2OH$	9.5×10^{9}	86
35	$^{\bullet}NH_2OH + e_{aq}^- \rightarrow {}^{\bullet}NH_2 + OH^-$	9.2×10^{8}	86
36	$^{\bullet}NH_2 + O_2 \rightarrow NH_2O_2^{\bullet}$	3.0×10^{8}	86
37	$NH_2O_2^{\bullet} \rightarrow {}^{\bullet}NO + H_2O$	$9.0\times10^{-2}[O_2]$	63
38	$NO^{\bullet} + O_2^{\bullet-} \rightarrow ONOO^-$	6.7×10^{9}	56

39	$ONOO^- + {}^{\bullet}OH \rightarrow O_2 + NO^{\bullet} + OH^-$	4.8×10^9	56
40	$ONOO^- + e_{aq}^- \rightarrow ONOO^{2-}$	1.2×10^{10}	63
41	$ONOO^- \rightarrow NO_2^{\bullet} + O^{\bullet-}$	5×10^{-6}	63
42	$ONOOH \rightleftharpoons ONOO^- + H^+$	1.4×10^2 (pKs = 6.8) 5.0×10^{10}	56
43	$ONOOH \rightarrow HNO_3$	0.94	56
44	$ONOOH \rightarrow NO_2^{\bullet} + {}^{\bullet}OH$	0.36	56
45	$ONOOH + {}^{\bullet}OH \rightarrow O_2 + NO^{\bullet} + H_2O$	2×10^7	56
46	$NO_2^- + {}^{\bullet}OH \rightarrow OH^- + NO_2^{\bullet}$	5.3×10^9	73
47	$^{\bullet}OH + NO^{\bullet} \rightarrow HNO_2$	1×10^{10}	86
48	$^{\bullet}OH + NO_2^{\bullet} \rightarrow HNO_3$	4.5×10^9	70
49	$HO_2^{\bullet} + NO^{\bullet} \rightarrow ONOOH$	1.9×10^9	75
50	$HO_2^{\bullet} + NO_2^{\bullet} \rightarrow O_2NOOH$	1.8×10^9	70
51	$O_2^{\bullet-} + NO_2^{\bullet} \rightarrow O_2NOO^-$	4.5×10^9	56
52	$HNO_2 \rightleftharpoons H^+ + NO_2^-$	7.2×10^5 (pKs = 5.8) 5.0×10^{10}	56
53	$O_2NOOH \rightleftharpoons O_2NOO^- + H^+$	1.43×10^3 (pKs = 5.8) 5.0×10^{10}	56
54	$NO^{\bullet} + NO_2^{\bullet} \rightarrow N_2O_3$	1.1×10^9	56
55	$N_2O_3 \rightarrow NO^{\bullet} + NO_2^{\bullet}$	8.0×10^4	56
56	$2\ NO_2^{\bullet} \rightarrow N_2O_4$	4.5×10^8	56
57	$N_2O_4 \rightarrow 2\ NO_2^{\bullet}$	6.9×10^3	56
58	$O_2NOO^- \rightarrow NO_2^- + O_2$	1.4	56
59	$O_2NOOH \rightarrow HNO_2 + O_2$	7.0×10^{-4}	56
60	$N_2O_3 + H_2O \rightarrow 2NO_2^- + 2H^+$	5.3×10^2	56
61	$N_2O_4 + H_2O \rightarrow NO_3^- + NO_2^- + 2H^+$	1×10^3	56

62	$N_2O_3 + ONOO^- \rightarrow NO_2^- + 2\ NO_2$	3.1×10^8	56
63	$O_3^{\bullet-} + NO_2^{\bullet} \rightarrow NO_3^- + O_2$	3.5×10^9	56
64	$ONOOH + H_3O^+ \rightarrow NO_2^+ + 2H_2O$	6.22	56
65	$NO_2^+ + 2\ H_2O \rightarrow HNO_3 + H_3O^+$	9×10^6	56
66	$HNO_2 + H_3O^+ \rightarrow NO^+ + 2\ H_2O$	5.9×10^1	56
67	$O_2NOO^- \rightarrow NO_2^{\bullet} + O_2^{\bullet-}$	1.05	56
68	$NO^+ + 2\ H_2O \rightarrow HNO_2 + H_3O^+$	2×10^8	56
69	$HNO_3 + H_2O \rightleftharpoons H_3O^+ + NO_3^-$	1.97×10^{10} (pKs = –1.34) 5.0×10^{10}	56
70	$O_2NOO^- + {}^{\bullet}OH \rightarrow O_2 + NO_2^{\bullet} + OH^-$	1×10^9	56
71	$NO_2^{\bullet} + ONOO^- \rightarrow NO_2^- + NO^{\bullet} + O_2$	$< 2.5\times10^4$	56
72	$e_{aq}^- + NO_3^- \rightarrow {}^{\bullet}NO_3^{2-}$	9.7×10^9	86
73	$NO_2^{\bullet 2-} + H_2O \rightarrow NO^{\bullet} + 2\ OH^-$	1×10^3	56
74	$ONOO^{\bullet 2-} + H_2O \rightarrow NO_2^{\bullet} + 2\ OH^-$	1×10^3	56
75	$H^{\bullet} + NO_3^- \rightarrow NO_2^{\bullet} + OH^-$	4.4×10^6	86
76	$H^{\bullet} + NO_2^- \rightarrow NO^{\bullet} + OH^-$	1.6×10^9	86
77	$NO_3^- + h\nu \rightarrow NO_2^{\bullet} + O^-$	$\Phi = 0.09$	73
78	$NO_3^- + h\nu \rightarrow NO_2^- + O(^3P)$	$\Phi = 0.1$	73
79	$NO_3^- + h\nu \rightarrow ONOO^-$	$\Phi = 0.068$ (estimate)	73
80	$ONOO^- + h\nu \rightarrow NO_2^{\bullet} + O^-$	$\Phi = 0.068$ (estimate)	73
81	$NO_2^- + h\nu \rightarrow NO + O^-$	$\Phi = 0.25$ (estimate)	73
82	$ONOO^- + {}^{\bullet}OH \rightarrow ONOO^{\bullet} + OH^-$	4.8×10^9	73
83	$ONOO^{\bullet} \rightarrow {}^{\bullet}NO + O_2$	1×10^{-3} (estimate)	73
84	$O(^3P) + NO_3^- \rightarrow O_2NOO^-$	3×10^8	86
85	$O(^3P) + NO_2^- \rightarrow NO_3^-$	3×10^9	86

3.0 UV Irradiation of Chloride ions in oxygenated water			
86	$NH_4^+ + e^- \rightarrow NH_3 + H^\bullet$	2.3×10^9	49
87	$O_2 + e^- \rightarrow O_2^{\bullet-}$	3.04×10^{10} (estimate)[a]	
88	$O_2^{\bullet-} + e^- \rightarrow HO_2^{\bullet-} + OH^\bullet$	3.2×10^{10} (estimate) [a]	
89	$e^- + O_2^{\bullet-} + H_2O \rightarrow HO_2^- + OH^-$	3.2×10^{10} (estimate) [a]	
90	$H_2O_2 + e^- \rightarrow OH^- + {}^\bullet OH$	1.92×10^{10}	94
91	$HO_2^- + e^- \rightarrow {}^\bullet OH + 2OH^-$	1.75×10^{10} (estimate) [a]	
92	$Cl + OH^- \rightarrow {}^\bullet OH + Cl^-$	1.8×10^{10}	86
93	$Cl + NO_2^- \rightarrow NO_2 + Cl^-$	8.8×10^9 (for I^-)	86
94	$e^- + NO_3^- \rightarrow NO_3^{2-}$	1.36×10^{10}	94
95	$e^- + ONOO^- \rightarrow ONOO^{2-}$	1.68×10^{10} (estimate) [b]	
96	$Cl^- + h\nu \rightarrow [Cl + e^-]_{CTTS}$	$[2.0 - 2.4] \times 10^{-4}$ (estimate)	
97	$Cl + e^- \rightarrow Cl^-$	3.0×10^{12}	34

a – rate was estimated based on a value of 1.6 time the reaction rate for the radical reacting with solvated electrons (e_{aq}^-).

b - rate was estimated based on a value of 1.4 time the reaction rate for the radical reacting with solvated electrons (e_{aq}^-).

APPENDIX B

TABLES OF SIMULATION RESULTS FOR NH_3, NO_3^- AND NO_2^-

SIMULATED DATA FOR NH_3 OXIDATION AT pH 8
--- Simulation data for file "c:\docume~1\admini~1\desktop\nh3.rxn"
--- This table was created on Mon Dec 11 20:25:09 2006

Time min	NH3 mole/l	NH4 mole/l	NO2- mole/l	NO3- mole/l
0.0000e+00	2.6669e-06	5.4449e-05	0.0000e+00	0.0000e+00
1.1906e+01	1.1112e-06	5.4449e-05	0.0000e+00	1.3334e-06
1.3348e+01	4.4448e-07	5.4449e-05	0.0000e+00	2.0002e-06
1.4127e+01	2.2224e-07	5.4449e-05	0.0000e+00	2.2224e-06
1.4870e+01	2.2224e-07	5.4449e-05	0.0000e+00	2.2224e-06
1.5610e+01	2.2224e-07	5.4449e-05	0.0000e+00	2.2224e-06
1.6343e+01	2.2224e-07	5.4449e-05	0.0000e+00	2.4447e-06
1.7076e+01	2.2224e-07	5.4449e-05	0.0000e+00	2.4447e-06
1.7817e+01	2.2224e-07	5.4449e-05	0.0000e+00	2.2224e-06
1.8549e+01	2.2224e-07	5.4449e-05	0.0000e+00	2.2224e-06
1.9282e+01	2.2224e-07	5.4449e-05	0.0000e+00	2.4447e-06
2.0016e+01	2.2224e-07	5.4449e-05	0.0000e+00	2.4447e-06
2.0749e+01	2.2224e-07	5.4449e-05	0.0000e+00	2.2224e-06
2.1481e+01	2.2224e-07	5.4449e-05	0.0000e+00	2.4447e-06
2.2221e+01	2.2224e-07	5.4449e-05	0.0000e+00	2.4447e-06
2.2959e+01	2.2224e-07	5.4449e-05	0.0000e+00	2.2224e-06
2.3692e+01	2.2224e-07	5.4449e-05	0.0000e+00	2.2224e-06
2.4365e+01	0.0000e+00	5.4449e-05	0.0000e+00	2.4447e-06
2.4953e+01	0.0000e+00	5.4449e-05	0.0000e+00	2.4447e-06
2.5549e+01	0.0000e+00	5.4449e-05	0.0000e+00	2.6669e-06
2.6138e+01	0.0000e+00	5.4449e-05	0.0000e+00	2.4447e-06
2.6727e+01	0.0000e+00	5.4449e-05	0.0000e+00	2.6669e-06
2.7316e+01	0.0000e+00	5.4449e-05	0.0000e+00	2.4447e-06
2.7905e+01	0.0000e+00	5.4449e-05	0.0000e+00	2.6669e-06
2.8495e+01	0.0000e+00	5.4449e-05	0.0000e+00	2.6669e-06
2.9083e+01	0.0000e+00	5.4449e-05	0.0000e+00	2.6669e-06
2.9775e+01	0.0000e+00	5.4449e-05	2.2224e-07	2.2224e-06
3.0597e+01	0.0000e+00	5.4449e-05	0.0000e+00	2.2224e-06
3.1488e+01	0.0000e+00	5.4449e-05	0.0000e+00	2.0002e-06
3.2416e+01	0.0000e+00	5.4449e-05	0.0000e+00	2.2224e-06
3.3344e+01	0.0000e+00	5.4449e-05	0.0000e+00	2.0002e-06
3.4425e+01	0.0000e+00	5.4449e-05	4.4448e-07	1.5557e-06
3.5291e+01	0.0000e+00	5.4449e-05	4.4448e-07	1.5557e-06
3.6633e+01	0.0000e+00	5.4449e-05	4.4448e-07	1.7779e-06
3.7950e+01	0.0000e+00	5.4449e-05	0.0000e+00	1.5557e-06

3.9125e+01	0.0000e+00	5.4449e-05	2.2224e-07	1.7779e-06
4.0343e+01	0.0000e+00	5.4449e-05	2.2224e-07	1.7779e-06
4.1522e+01	0.0000e+00	5.4449e-05	6.6672e-07	1.7779e-06
4.2518e+01	0.0000e+00	5.4449e-05	2.2224e-07	1.5557e-06
4.3784e+01	0.0000e+00	5.4449e-05	2.2224e-07	1.7779e-06
4.5198e+01	0.0000e+00	5.4449e-05	6.6672e-07	1.3334e-06
4.6811e+01	0.0000e+00	5.4449e-05	6.6672e-07	1.1112e-06
4.8429e+01	0.0000e+00	5.4449e-05	4.4448e-07	8.8896e-07
5.0146e+01	0.0000e+00	5.4449e-05	1.5557e-06	8.8896e-07
5.1805e+01	0.0000e+00	5.4449e-05	8.8896e-07	6.6672e-07
5.3577e+01	0.0000e+00	5.4449e-05	6.6672e-07	8.8896e-07
5.5367e+01	0.0000e+00	5.4449e-05	8.8896e-07	8.8896e-07
5.7626e+01	0.0000e+00	5.4449e-05	1.1112e-06	6.6672e-07
5.9238e+01	0.0000e+00	5.4449e-05	8.8896e-07	8.8896e-07
6.1009e+01	0.0000e+00	5.4449e-05	1.1112e-06	8.8896e-07
6.3276e+01	0.0000e+00	5.4449e-05	8.8896e-07	6.6672e-07

SIMULATED DATA FOR NH_3 OXIDATION AT pH 10
--- Simulation data for file "e:\simula~1\nh3.rxn"
--- This table was created on Thu Dec 07 21:39:03 2006

Time	NH3	NO2-	NO3-
min	mole/l	mole/l	mole/l
0.0000e+00	9.2508e-05	0.0000e+00	0.0000e+00
5.7202e+00	8.4452e-05	2.2224e-06	5.8339e-06
1.1328e+01	8.0007e-05	4.4448e-06	7.5007e-06
1.6847e+01	7.6396e-05	8.3341e-06	7.7785e-06
2.2295e+01	7.2784e-05	8.8897e-06	1.0556e-05
2.7689e+01	7.1395e-05	1.0001e-05	1.1112e-05
3.3034e+01	6.9451e-05	9.7231e-06	1.3057e-05
3.8317e+01	6.7784e-05	1.0556e-05	1.3890e-05
4.3583e+01	6.6673e-05	1.1668e-05	1.3890e-05
4.8799e+01	6.5561e-05	1.2779e-05	1.4168e-05
5.3964e+01	6.2228e-05	1.5001e-05	1.5279e-05
5.9057e+01	6.0283e-05	1.7224e-05	1.5001e-05
6.4117e+01	5.9450e-05	1.7779e-05	1.5279e-05
6.9141e+01	5.8616e-05	1.8891e-05	1.4724e-05
7.4150e+01	5.8061e-05	1.8891e-05	1.5279e-05
7.9114e+01	5.6950e-05	1.9446e-05	1.6113e-05
8.4049e+01	5.5838e-05	2.0557e-05	1.5835e-05
8.8966e+01	5.5005e-05	2.1946e-05	1.5001e-05
9.3854e+01	5.4171e-05	2.3891e-05	1.3890e-05

9.8723e+01	5.3338e-05	2.4169e-05	1.4446e-05
1.0357e+02	5.3338e-05	2.5002e-05	1.3612e-05
1.0838e+02	5.2227e-05	2.5002e-05	1.5279e-05
1.1319e+02	5.1116e-05	2.6113e-05	1.5279e-05
1.1796e+02	5.0838e-05	2.6669e-05	1.5001e-05
1.2272e+02	5.0560e-05	2.6947e-05	1.4724e-05
1.2748e+02	5.0282e-05	2.7225e-05	1.4724e-05
1.3222e+02	4.9727e-05	2.7225e-05	1.5557e-05
1.3693e+02	4.8893e-05	2.8336e-05	1.5279e-05
1.4162e+02	4.8615e-05	2.8336e-05	1.5557e-05
1.4631e+02	4.8060e-05	2.8058e-05	1.5835e-05
1.5097e+02	4.7226e-05	2.8891e-05	1.6390e-05
1.5560e+02	4.6393e-05	2.9169e-05	1.6390e-05
1.6021e+02	4.6115e-05	3.0003e-05	1.6390e-05
1.6481e+02	4.5837e-05	3.0003e-05	1.6113e-05
1.6940e+02	4.5004e-05	3.0003e-05	1.7502e-05
1.7395e+02	4.4448e-05	3.0003e-05	1.7779e-05
1.7850e+02	4.4448e-05	3.0003e-05	1.8057e-05
1.8302e+02	4.3893e-05	3.0558e-05	1.8057e-05
1.8752e+02	4.2504e-05	3.1114e-05	1.8335e-05
1.9198e+02	4.2226e-05	3.1114e-05	1.9168e-05
1.9643e+02	4.1948e-05	3.1114e-05	1.9446e-05
2.0088e+02	4.1670e-05	3.2225e-05	1.8613e-05
2.0532e+02	4.1393e-05	3.2225e-05	1.8891e-05
2.0974e+02	4.0837e-05	3.2225e-05	1.9446e-05
2.1412e+02	4.0004e-05	3.2225e-05	2.0280e-05
2.1849e+02	3.9170e-05	3.2225e-05	2.0835e-05
2.2283e+02	3.9170e-05	3.2225e-05	2.1113e-05
2.2716e+02	3.8615e-05	3.2225e-05	2.1669e-05
2.3147e+02	3.8059e-05	3.3336e-05	2.0835e-05
2.3575e+02	3.7781e-05	3.3336e-05	2.1391e-05
2.4000e+02	3.7503e-05	3.3058e-05	2.1391e-05

SIMULATED DATA FOR NH_3 /Cl^- OXIDATION AT pH 5.58
--- Simulation data for file "e:\simula~1\nh3-cl-pH5.rxn"
--- This table was created on Fri Dec 08 11:39:03 2006

Time min	NH3 mole/l	NO2- mole/l	NO3- mole/l
0	0	1.38E-04	0
7.38E-01	0	1.38E-04	0
1.09E+00	0	1.38E-04	0

1.35E+00	0	1.38E-04	0
1.60E+00	0	1.38E-04	0
1.90E+00	0	1.38E-04	0
2.90E+00	0	1.38E-04	0
8.17E+00	0	1.38E-04	0
1.39E+01	2.78E-07	1.38E-04	0.00E+00
1.98E+01	0.00E+00	1.38E-04	2.78E-07
2.57E+01	5.56E-07	1.38E-04	2.78E-07
3.15E+01	5.56E-07	1.38E-04	2.78E-07
3.75E+01	2.78E-07	1.38E-04	2.78E-07
3.96E+01	0.00E+00	1.38E-04	0.00E+00
4.10E+01	0.00E+00	1.38E-04	0.00E+00
4.69E+01	0.00E+00	1.38E-04	0.00E+00
5.20E+01	0.00E+00	1.38E-04	0.00E+00
5.79E+01	0.00E+00	1.38E-04	2.78E-07
6.31E+01	0.00E+00	1.37E-04	0.00E+00
6.45E+01	0.00E+00	1.37E-04	0.00E+00
6.45E+01	0.00E+00	1.37E-04	0.00E+00
6.79E+01	0.00E+00	1.37E-04	8.33E-07
7.39E+01	2.78E-07	1.37E-04	5.56E-07
7.98E+01	2.78E-07	1.37E-04	2.78E-07
8.57E+01	2.78E-07	1.37E-04	2.78E-07
9.17E+01	2.78E-07	1.37E-04	2.78E-07
9.76E+01	5.56E-07	1.37E-04	2.78E-07
1.04E+02	2.78E-07	1.36E-04	2.78E-07
1.09E+02	2.78E-07	1.36E-04	2.78E-07
1.15E+02	0.00E+00	1.36E-04	2.78E-07
1.21E+02	8.33E-07	1.36E-04	2.78E-07
1.27E+02	1.11E-06	1.35E-04	5.56E-07
1.33E+02	1.11E-06	1.35E-04	0.00E+00
1.39E+02	1.39E-06	1.35E-04	0.00E+00
1.45E+02	1.67E-06	1.35E-04	0.00E+00
1.51E+02	1.94E-06	1.34E-04	0.00E+00
1.57E+02	1.67E-06	1.34E-04	1.67E-06
1.63E+02	1.94E-06	1.34E-04	1.39E-06
1.69E+02	2.22E-06	1.34E-04	1.11E-06
1.75E+02	1.94E-06	1.34E-04	1.39E-06
1.81E+02	1.39E-06	1.33E-04	1.67E-06
1.87E+02	1.39E-06	1.33E-04	8.33E-07
1.93E+02	1.39E-06	1.33E-04	8.33E-07
1.99E+02	1.39E-06	1.33E-04	1.11E-06
2.04E+02	1.39E-06	1.33E-04	1.11E-06
2.10E+02	1.67E-06	1.33E-04	1.67E-06
2.16E+02	1.67E-06	1.33E-04	1.67E-06
2.22E+02	1.67E-06	1.33E-04	1.67E-06

2.28E+02	1.67E-06	1.33E-04	8.33E-07
2.34E+02	1.67E-06	1.33E-04	1.94E-06
2.40E+02	1.94E-06	1.33E-04	1.11E-06

SIMULATED DATA FOR NH_3 /Cl^- OXIDATION For CTTS FORMATION RATE 1.6 X 10^{-4} S^{-1}

--- Simulation data for file "e:\simula~1\n-cl.rxn"
--- This table was created on Tue Dec 19 04:15:07 2006

Time	NH3	NH4	NO2-	NO3-
min	mole/l	mole/l	mole/l	mole/l
0.0000e+00	9.6676e-05	1.9632e-05	0.0000e+00	0.0000e+00
8.3123e+00	8.2230e-05	1.9261e-05	5.1857e-06	9.6306e-06
1.6230e+01	7.5933e-05	1.8520e-05	7.4081e-06	1.4075e-05
2.3902e+01	7.2229e-05	1.8150e-05	9.6306e-06	1.6298e-05
3.1345e+01	6.7044e-05	1.8150e-05	1.1112e-05	2.0002e-05
3.8527e+01	6.2228e-05	1.8150e-05	1.4816e-05	2.0743e-05
4.5444e+01	5.8524e-05	1.8150e-05	1.6298e-05	2.2965e-05
5.2082e+01	5.5191e-05	1.8150e-05	1.6668e-05	2.5188e-05
5.8619e+01	5.2968e-05	1.7780e-05	1.8520e-05	2.7040e-05
6.4964e+01	5.0746e-05	1.7409e-05	1.9261e-05	2.8892e-05
7.1105e+01	5.0375e-05	1.6668e-05	2.1484e-05	2.7781e-05
7.7126e+01	4.9635e-05	1.6668e-05	2.3706e-05	2.6299e-05
8.3038e+01	4.7412e-05	1.6298e-05	2.4447e-05	2.7781e-05
8.8807e+01	4.6671e-05	1.6298e-05	2.6669e-05	2.6669e-05
9.4490e+01	4.5560e-05	1.6298e-05	2.8521e-05	2.5558e-05
1.0003e+02	4.3708e-05	1.6298e-05	3.1114e-05	2.4817e-05
1.0544e+02	4.2967e-05	1.5928e-05	3.2596e-05	2.4447e-05
1.1072e+02	4.2226e-05	1.5557e-05	3.3707e-05	2.4447e-05
1.1590e+02	4.1486e-05	1.5557e-05	3.4448e-05	2.4076e-05
1.2095e+02	4.0004e-05	1.5557e-05	3.5559e-05	2.5188e-05
1.2588e+02	3.9634e-05	1.5187e-05	3.6670e-05	2.4447e-05
1.3076e+02	3.9634e-05	1.5187e-05	3.6300e-05	2.4817e-05
1.3560e+02	3.9634e-05	1.4816e-05	3.5559e-05	2.6299e-05
1.4027e+02	3.7782e-05	1.4446e-05	3.5929e-05	2.7410e-05
1.4477e+02	3.7041e-05	1.4446e-05	3.7041e-05	2.7781e-05
1.4923e+02	3.7041e-05	1.4446e-05	3.7782e-05	2.7040e-05
1.5367e+02	3.6300e-05	1.4446e-05	3.9263e-05	2.5928e-05
1.5800e+02	3.5559e-05	1.4446e-05	3.9634e-05	2.6299e-05
1.6229e+02	3.5189e-05	1.4446e-05	4.0745e-05	2.5928e-05
1.6653e+02	3.5189e-05	1.4446e-05	4.0745e-05	2.5558e-05
1.7077e+02	3.4818e-05	1.4446e-05	4.2967e-05	2.4076e-05
1.7494e+02	3.4448e-05	1.4446e-05	4.4078e-05	2.2965e-05
1.7902e+02	3.4818e-05	1.3705e-05	4.5190e-05	2.2595e-05

1.8303e+02	3.5189e-05	1.3335e-05	4.5560e-05	2.1854e-05
1.8698e+02	3.4077e-05	1.3335e-05	4.5560e-05	2.2965e-05
1.9078e+02	3.4077e-05	1.2964e-05	4.6671e-05	2.2595e-05
1.9455e+02	3.4448e-05	1.2594e-05	4.6301e-05	2.2595e-05
1.9829e+02	3.4818e-05	1.2223e-05	4.6671e-05	2.2595e-05
2.0185e+02	3.3337e-05	1.2223e-05	4.6671e-05	2.4076e-05
2.0530e+02	3.3707e-05	1.1853e-05	4.6301e-05	2.4076e-05
2.0870e+02	3.3707e-05	1.1483e-05	4.6671e-05	2.4447e-05
2.1204e+02	3.3707e-05	1.1483e-05	4.6671e-05	2.4447e-05
2.1535e+02	3.2966e-05	1.1483e-05	4.7412e-05	2.4447e-05
2.1858e+02	3.2966e-05	1.1483e-05	4.7412e-05	2.4447e-05
2.2181e+02	3.2966e-05	1.1483e-05	4.6671e-05	2.4447e-05
2.2502e+02	3.2596e-05	1.1483e-05	4.6671e-05	2.5558e-05
2.2815e+02	3.2596e-05	1.1112e-05	4.7042e-05	2.4817e-05
2.3116e+02	3.2225e-05	1.1112e-05	4.7412e-05	2.5558e-05
2.3414e+02	3.2596e-05	1.0742e-05	4.7042e-05	2.5558e-05
2.3710e+02	3.2596e-05	1.0742e-05	4.7412e-05	2.5188e-05
2.4000e+02	3.2596e-05	1.0742e-05	4.6671e-05	2.6299e-05

SIMULATED DATA FOR NH_3 /Cl^- OXIDATION For CTTS FORMATION RATE 2.0 X 10^{-4} S^{-1}

--- Simulation data for file "f:\simula~1\n-cl.rxn"

--- This table was created on Mon Dec 18 10:30:43 2006

Time	NH3	NH4	NO2-	NO3-
min	mole/l	mole/l	mole/l	mole/l
0.0000e+00	9.6676e-05	1.9632e-05	0.0000e+00	0.0000e+00
1.0444e+01	7.6304e-05	1.9261e-05	5.1857e-06	1.4816e-05
2.0076e+01	6.7414e-05	1.8891e-05	9.6306e-06	2.0372e-05
2.9331e+01	6.2969e-05	1.8520e-05	1.5557e-05	1.8520e-05
3.8127e+01	5.6672e-05	1.8520e-05	1.7039e-05	2.4076e-05
4.6437e+01	5.1116e-05	1.8520e-05	2.1484e-05	2.4817e-05
5.4440e+01	4.8894e-05	1.8520e-05	2.2224e-05	2.6669e-05
6.2127e+01	4.6301e-05	1.7780e-05	2.2595e-05	2.8892e-05
6.9542e+01	4.5190e-05	1.7409e-05	2.5188e-05	2.8521e-05
7.6767e+01	4.5190e-05	1.6298e-05	2.5928e-05	2.8521e-05
8.3725e+01	4.2597e-05	1.6298e-05	2.7781e-05	2.9262e-05
9.0486e+01	4.1486e-05	1.6298e-05	2.8892e-05	2.9633e-05
9.7111e+01	4.0745e-05	1.5928e-05	2.8892e-05	3.0744e-05
1.0356e+02	3.8893e-05	1.5928e-05	3.1485e-05	2.9633e-05
1.0982e+02	3.8152e-05	1.5928e-05	3.3337e-05	2.8521e-05
1.1579e+02	3.6670e-05	1.5187e-05	3.5929e-05	2.7410e-05
1.2163e+02	3.6670e-05	1.5187e-05	3.6670e-05	2.7410e-05

1.2735e+02	3.5559e-05	1.5187e-05	3.5929e-05	2.9262e-05
1.3290e+02	3.3707e-05	1.5187e-05	3.7411e-05	2.9633e-05
1.3815e+02	3.1855e-05	1.5187e-05	3.7782e-05	3.1485e-05
1.4320e+02	3.1485e-05	1.4816e-05	3.8522e-05	3.1114e-05
1.4807e+02	3.1485e-05	1.4446e-05	3.8522e-05	3.1485e-05
1.5285e+02	3.2225e-05	1.3705e-05	3.8152e-05	3.1855e-05
1.5746e+02	3.1855e-05	1.3335e-05	4.0745e-05	3.0003e-05
1.6194e+02	3.1855e-05	1.2964e-05	4.1486e-05	3.0003e-05
1.6618e+02	3.1114e-05	1.2594e-05	4.0745e-05	3.0003e-05
1.7034e+02	3.1114e-05	1.2594e-05	4.2226e-05	3.0373e-05
1.7440e+02	3.0373e-05	1.2594e-05	4.1856e-05	3.0744e-05
1.7837e+02	2.9633e-05	1.2594e-05	4.1856e-05	3.1855e-05
1.8216e+02	2.9262e-05	1.2223e-05	4.2226e-05	3.1485e-05
1.8575e+02	2.8892e-05	1.2223e-05	4.1856e-05	3.2966e-05
1.8931e+02	2.8892e-05	1.2223e-05	4.2967e-05	3.1855e-05
1.9289e+02	2.8892e-05	1.2223e-05	4.3708e-05	3.1485e-05
1.9640e+02	2.7781e-05	1.2223e-05	4.4449e-05	3.1485e-05
1.9967e+02	2.7410e-05	1.2223e-05	4.4819e-05	3.1485e-05
2.0293e+02	2.7410e-05	1.2223e-05	4.5930e-05	3.0373e-05
2.0608e+02	2.7781e-05	1.1483e-05	4.5190e-05	3.1114e-05
2.0910e+02	2.7781e-05	1.1483e-05	4.5930e-05	3.1114e-05
2.1208e+02	2.8151e-05	1.1112e-05	4.5560e-05	3.0744e-05
2.1503e+02	2.8151e-05	1.1112e-05	4.6671e-05	3.0373e-05
2.1788e+02	2.7040e-05	1.1112e-05	4.6301e-05	3.1485e-05
2.2053e+02	2.7040e-05	1.0742e-05	4.5930e-05	3.1855e-05
2.2292e+02	2.6299e-05	1.0742e-05	4.6301e-05	3.2596e-05
2.2523e+02	2.5928e-05	1.0742e-05	4.6301e-05	3.2966e-05
2.2748e+02	2.5928e-05	1.0742e-05	4.7042e-05	3.2225e-05
2.2973e+02	2.5188e-05	1.0742e-05	4.7412e-05	3.2596e-05
2.3178e+02	2.5188e-05	1.0742e-05	4.7042e-05	3.2966e-05
2.3385e+02	2.5188e-05	1.0742e-05	4.8153e-05	3.2225e-05
2.3592e+02	2.5188e-05	1.0742e-05	4.7042e-05	3.2596e-05
2.3798e+02	2.5188e-05	1.0742e-05	4.8894e-05	3.1114e-05
2.4000e+02	2.4817e-05	1.0742e-05	4.9635e-05	3.1114e-05

SIMULATED DATA FOR NH_3 /Cl^- OXIDATION For CTTS FORMATION RATE 2.4 X 10^{-4} S^{-1}

--- Simulation data for file "e:\simula~1\n-cl.rxn"
--- This table was created on Mon Dec 18 20:43:34 2006

Time	NH3	NH4	NO2-	NO3-
min	mole/l	mole/l	mole/l	mole/l
0.0000e+00	9.6676e-05	1.9632e-05	0.0000e+00	0.0000e+00

1.1857e+01	7.1859e-05	1.9261e-05	7.0377e-06	1.7409e-05
2.2726e+01	6.4080e-05	1.8520e-05	1.1853e-05	2.1854e-05
3.2925e+01	5.6302e-05	1.8150e-05	1.5557e-05	2.5928e-05
4.2329e+01	5.1116e-05	1.7039e-05	1.7409e-05	3.0373e-05
5.1214e+01	4.8153e-05	1.6668e-05	2.1854e-05	2.9262e-05
5.9550e+01	4.4819e-05	1.5187e-05	2.4817e-05	3.1114e-05
6.7338e+01	4.3708e-05	1.4816e-05	2.6669e-05	3.1114e-05
7.4959e+01	4.2597e-05	1.4446e-05	2.8892e-05	3.0003e-05
8.2303e+01	4.1486e-05	1.4075e-05	3.0373e-05	3.0373e-05
8.9458e+01	4.0745e-05	1.4075e-05	3.1855e-05	2.9262e-05
9.6470e+01	4.0004e-05	1.4075e-05	3.1485e-05	3.0003e-05
1.0331e+02	3.9263e-05	1.3705e-05	3.2966e-05	3.0003e-05
1.0977e+02	3.6670e-05	1.3705e-05	3.6300e-05	2.9633e-05
1.1591e+02	3.5559e-05	1.3705e-05	4.0004e-05	2.7040e-05
1.2187e+02	3.4077e-05	1.3705e-05	4.2226e-05	2.6299e-05
1.2755e+02	3.2966e-05	1.3705e-05	4.2226e-05	2.7410e-05
1.3304e+02	3.2225e-05	1.3705e-05	4.2226e-05	2.8151e-05
1.3837e+02	3.1855e-05	1.3335e-05	4.3338e-05	2.7040e-05
1.4360e+02	3.1485e-05	1.3335e-05	4.5560e-05	2.5188e-05
1.4857e+02	3.1855e-05	1.2594e-05	4.5560e-05	2.5928e-05
1.5353e+02	3.1855e-05	1.2594e-05	4.6671e-05	2.5188e-05
1.5841e+02	3.2596e-05	1.1853e-05	4.7042e-05	2.4076e-05
1.6321e+02	3.2966e-05	1.1483e-05	4.7042e-05	2.4447e-05
1.6793e+02	3.3337e-05	1.1112e-05	4.8153e-05	2.3706e-05
1.7249e+02	3.3707e-05	1.0371e-05	4.7783e-05	2.4076e-05
1.7673e+02	3.2225e-05	1.0371e-05	4.7783e-05	2.5558e-05
1.8080e+02	3.2596e-05	1.0001e-05	4.7042e-05	2.6299e-05
1.8478e+02	3.2225e-05	1.0001e-05	4.7412e-05	2.6669e-05
1.8854e+02	3.1855e-05	9.6306e-06	4.7783e-05	2.6669e-05
1.9219e+02	3.1855e-05	9.6306e-06	4.7783e-05	2.6669e-05
1.9583e+02	3.1485e-05	9.6306e-06	4.7412e-05	2.7781e-05
1.9940e+02	3.1855e-05	9.2602e-06	4.7042e-05	2.7781e-05
2.0287e+02	3.2225e-05	8.8898e-06	4.7783e-05	2.7040e-05
2.0625e+02	3.2225e-05	8.8898e-06	4.8153e-05	2.6299e-05
2.0952e+02	3.1485e-05	8.8898e-06	4.8153e-05	2.7040e-05
2.1249e+02	3.0373e-05	8.8898e-06	4.8153e-05	2.8892e-05
2.1522e+02	3.0003e-05	8.5194e-06	4.8153e-05	2.9633e-05
2.1777e+02	3.0003e-05	8.5194e-06	4.8153e-05	2.8521e-05
2.2031e+02	2.9262e-05	8.5194e-06	4.7783e-05	3.0003e-05
2.2263e+02	2.9262e-05	8.5194e-06	4.7783e-05	3.0373e-05
2.2494e+02	2.8892e-05	8.5194e-06	4.8153e-05	3.0744e-05
2.2715e+02	2.8892e-05	8.5194e-06	4.8894e-05	3.0003e-05
2.2925e+02	2.9262e-05	7.7785e-06	4.8894e-05	3.0373e-05
2.3110e+02	2.9633e-05	7.4081e-06	4.8894e-05	3.0373e-05
2.3282e+02	2.9262e-05	7.4081e-06	4.8153e-05	3.0744e-05
2.3446e+02	2.9262e-05	7.4081e-06	4.8523e-05	3.0744e-05

2.3597e+02 2.8892e-05 7.4081e-06 4.8523e-05 3.0744e-05
2.3748e+02 2.8521e-05 7.4081e-06 4.8153e-05 3.2225e-05
2.3877e+02 2.8151e-05 7.4081e-06 4.8894e-05 3.1485e-05
2.4000e+02 2.8151e-05 7.4081e-06 4.8894e-05 3.1855e-05

SIMULATED DATA FOR NH_3 /Cl^- OXIDATION For CTTS FORMATION RATE 2.8 X 10^{-4} S^{-1}

--- Simulation data for file "c:\docume~1\admini~1\desktop\n-cl.rxn"
--- This table was created on Mon Dec 18 22:38:32 2006

Time	NH3	NH4	NO2-	NO3-
min	mole/l	mole/l	mole/l	mole/l
0.0000e+00	9.6676e-05	1.9632e-05	0.0000e+00	0.0000e+00
1.3660e+01	7.1859e-05	1.9261e-05	7.0377e-06	1.7780e-05
2.6115e+01	6.0376e-05	1.8891e-05	1.3335e-05	2.2965e-05
3.7543e+01	5.1857e-05	1.8150e-05	1.6668e-05	2.9262e-05
4.7954e+01	4.8153e-05	1.7409e-05	1.9632e-05	3.0373e-05
5.7755e+01	4.2597e-05	1.7039e-05	2.5928e-05	3.0744e-05
6.6666e+01	4.0004e-05	1.5928e-05	2.7410e-05	3.2966e-05
7.5218e+01	3.9634e-05	1.5557e-05	2.8151e-05	3.2596e-05
8.3489e+01	3.7782e-05	1.5187e-05	2.7781e-05	3.4818e-05
9.1314e+01	3.7041e-05	1.4816e-05	2.9633e-05	3.4818e-05
9.8898e+01	3.6670e-05	1.4075e-05	3.1855e-05	3.3707e-05
1.0614e+02	3.4818e-05	1.4075e-05	3.6300e-05	3.1114e-05
1.1309e+02	3.4077e-05	1.4075e-05	3.7411e-05	3.0373e-05
1.1977e+02	3.3337e-05	1.3705e-05	3.7782e-05	3.1485e-05
1.2608e+02	3.2966e-05	1.2964e-05	3.8522e-05	3.1855e-05
1.3213e+02	3.2966e-05	1.2594e-05	3.8893e-05	3.1485e-05
1.3795e+02	3.2596e-05	1.2223e-05	3.9634e-05	3.1485e-05
1.4362e+02	3.2225e-05	1.2223e-05	3.9634e-05	3.1485e-05
1.4928e+02	3.2225e-05	1.1853e-05	4.1856e-05	2.9633e-05
1.5461e+02	3.2596e-05	1.1112e-05	4.2967e-05	2.9633e-05
1.5984e+02	3.2596e-05	1.1112e-05	4.2967e-05	2.9633e-05
1.6499e+02	3.2596e-05	1.0742e-05	4.4449e-05	2.8521e-05
1.6999e+02	3.1855e-05	1.0742e-05	4.4819e-05	2.8521e-05
1.7473e+02	3.1485e-05	1.0742e-05	4.5560e-05	2.8151e-05
1.7937e+02	3.1485e-05	1.0371e-05	4.4819e-05	2.9262e-05
1.8367e+02	3.0003e-05	1.0371e-05	4.4819e-05	3.0744e-05
1.8776e+02	3.0003e-05	1.0371e-05	4.3708e-05	3.1485e-05
1.9179e+02	3.0003e-05	1.0001e-05	4.5560e-05	3.0373e-05
1.9565e+02	3.0373e-05	9.6306e-06	4.5930e-05	3.0003e-05
1.9942e+02	3.0373e-05	9.6306e-06	4.4078e-05	3.1114e-05
2.0315e+02	3.0003e-05	9.6306e-06	4.4819e-05	3.1485e-05
2.0647e+02	2.9633e-05	8.8898e-06	4.5560e-05	3.1855e-05

2.0948e+02	2.8892e-05	8.8898e-06	4.5930e-05	3.2596e-05
2.1219e+02	2.8521e-05	8.8898e-06	4.6671e-05	3.1855e-05
2.1476e+02	2.8521e-05	8.5194e-06	4.6301e-05	3.1855e-05
2.1700e+02	2.7781e-05	8.5194e-06	4.7412e-05	3.2596e-05
2.1915e+02	2.7781e-05	8.5194e-06	4.7783e-05	3.1855e-05
2.2130e+02	2.7781e-05	8.5194e-06	4.8153e-05	3.1855e-05
2.2332e+02	2.7410e-05	8.5194e-06	4.8894e-05	3.1485e-05
2.2529e+02	2.7040e-05	8.5194e-06	4.8153e-05	3.1485e-05
2.2703e+02	2.6669e-05	8.5194e-06	4.8523e-05	3.2225e-05
2.2862e+02	2.6299e-05	8.5194e-06	4.9635e-05	3.1855e-05
2.3016e+02	2.5928e-05	8.5194e-06	4.9635e-05	3.2225e-05
2.3159e+02	2.5928e-05	8.5194e-06	4.8894e-05	3.2966e-05
2.3297e+02	2.5558e-05	8.5194e-06	4.8153e-05	3.3337e-05
2.3426e+02	2.5558e-05	8.5194e-06	4.9264e-05	3.2596e-05
2.3555e+02	2.5558e-05	8.5194e-06	4.8894e-05	3.2966e-05
2.3673e+02	2.5188e-05	8.5194e-06	4.7783e-05	3.3337e-05
2.3786e+02	2.5188e-05	8.5194e-06	4.9264e-05	3.2966e-05
2.3899e+02	2.5188e-05	8.5194e-06	4.9635e-05	3.2966e-05
2.4000e+02	2.4817e-05	8.5194e-06	4.8894e-05	3.4077e-05

SIMULATED DATA FOR NH_3 /Cl^- OXIDATION: CTTS FORMATION (RATE 2.0 X 10^{-4} S^{-1}) AND Cl SCAVENGING FROM NO_2^-

--- Simulation data for file "f:\simula~1\n-cl.rxn"

--- This table was created on Mon Dec 18 08:12:20 2006

Time	NH3	NH4	NO2-	NO3-
min	mole/l	mole/l	mole/l	mole/l
0.0000e+00	9.6676e-05	1.9632e-05	0.0000e+00	0.0000e+00
9.7401e+00	7.9638e-05	1.8891e-05	4.0745e-06	1.3335e-05
1.8858e+01	7.0007e-05	1.8891e-05	7.7785e-06	1.8150e-05
2.7626e+01	6.7044e-05	1.8520e-05	1.1853e-05	1.8520e-05
3.6036e+01	6.0747e-05	1.8150e-05	1.3705e-05	2.2965e-05
4.3993e+01	5.4820e-05	1.8150e-05	1.6298e-05	2.7040e-05
5.1595e+01	5.2598e-05	1.7780e-05	1.9261e-05	2.6299e-05
5.9005e+01	5.0375e-05	1.7409e-05	2.1113e-05	2.6299e-05
6.6200e+01	5.0005e-05	1.6298e-05	2.2965e-05	2.6669e-05
7.3253e+01	4.9264e-05	1.5928e-05	2.3706e-05	2.7410e-05
8.0134e+01	4.9635e-05	1.4446e-05	2.3706e-05	2.8151e-05
8.6853e+01	4.8894e-05	1.4446e-05	2.5558e-05	2.7040e-05
9.3461e+01	4.7042e-05	1.4446e-05	2.8151e-05	2.6669e-05
9.9827e+01	4.4819e-05	1.4446e-05	2.8892e-05	2.8151e-05
1.0593e+02	4.2967e-05	1.4075e-05	2.9262e-05	2.9633e-05
1.1180e+02	4.2226e-05	1.3705e-05	3.0744e-05	2.8892e-05
1.1739e+02	4.1856e-05	1.2594e-05	3.2225e-05	2.9262e-05

1.2285e+02	4.1115e-05	1.2594e-05	3.3707e-05	2.8151e-05
1.2820e+02	4.0374e-05	1.2594e-05	3.4077e-05	2.8892e-05
1.3347e+02	3.9263e-05	1.2594e-05	3.4448e-05	2.8892e-05
1.3851e+02	3.7411e-05	1.2594e-05	3.4818e-05	3.1485e-05
1.4325e+02	3.7411e-05	1.1853e-05	3.6300e-05	3.0373e-05
1.4787e+02	3.6670e-05	1.1853e-05	3.6300e-05	3.0744e-05
1.5240e+02	3.5929e-05	1.1853e-05	3.6670e-05	3.1114e-05
1.5680e+02	3.5929e-05	1.1483e-05	3.7782e-05	3.1114e-05
1.6107e+02	3.5929e-05	1.1112e-05	3.9263e-05	3.0003e-05
1.6518e+02	3.4818e-05	1.1112e-05	4.0004e-05	3.0373e-05
1.6911e+02	3.4448e-05	1.0742e-05	3.9634e-05	3.0744e-05
1.7295e+02	3.4448e-05	1.0742e-05	3.9263e-05	3.1114e-05
1.7679e+02	3.4448e-05	1.0742e-05	4.0745e-05	3.0373e-05
1.8063e+02	3.4448e-05	1.0742e-05	4.1115e-05	2.9262e-05
1.8432e+02	3.3337e-05	1.0742e-05	4.1486e-05	3.0744e-05
1.8791e+02	3.2225e-05	1.0742e-05	4.1856e-05	3.1114e-05
1.9128e+02	3.2596e-05	1.0371e-05	4.1856e-05	3.1114e-05
1.9463e+02	3.2596e-05	1.0371e-05	4.2967e-05	3.0373e-05
1.9795e+02	3.2225e-05	1.0371e-05	4.3708e-05	2.9633e-05
2.0112e+02	3.1114e-05	1.0371e-05	4.5190e-05	2.9262e-05
2.0413e+02	3.0744e-05	1.0371e-05	4.5560e-05	2.8892e-05
2.0712e+02	3.0744e-05	1.0371e-05	4.5930e-05	2.9262e-05
2.1006e+02	3.0373e-05	1.0371e-05	4.5190e-05	3.0003e-05
2.1297e+02	3.0373e-05	1.0371e-05	4.5930e-05	2.9262e-05
2.1589e+02	3.0373e-05	1.0371e-05	4.5190e-05	2.9633e-05
2.1880e+02	3.0373e-05	1.0371e-05	4.5930e-05	2.8892e-05
2.2167e+02	3.0003e-05	1.0371e-05	4.5190e-05	3.0003e-05
2.2443e+02	2.9633e-05	1.0371e-05	4.6671e-05	2.9633e-05
2.2715e+02	2.9262e-05	1.0371e-05	4.6301e-05	3.0003e-05
2.2981e+02	2.9262e-05	1.0371e-05	4.6671e-05	3.0003e-05
2.3247e+02	2.8892e-05	1.0371e-05	4.7042e-05	2.9633e-05
2.3507e+02	2.8892e-05	1.0371e-05	4.7412e-05	2.8892e-05
2.3759e+02	2.8151e-05	1.0371e-05	4.8153e-05	2.9633e-05
2.4000e+02	2.8151e-05	1.0371e-05	4.7412e-05	3.0373e-05

SIMULATED DATA FOR NH_3 /Cl^- OXIDATION: CTTS FORMATION (RATE 2.4 X 10^{-4} S^{-1}) AND Cl SCAVENGING FROM NO_2^-

--- Simulation data for file "c:\docume~1\admini~1\desktop\n-cl.rxn"
--- This table was created on Mon Dec 18 04:14:37 2006

Time	NH3	NH4	NO2-	NO3-
min	mole/l	mole/l	mole/l	mole/l
0.0000e+00	9.6676e-05	1.9632e-05	0.0000e+00	0.0000e+00

8.0584e+00	7.9267e-05	1.9261e-05	7.4081e-06	9.6306e-06
1.5717e+01	7.1859e-05	1.9261e-05	8.5194e-06	1.5187e-05
2.3065e+01	6.5932e-05	1.9261e-05	1.1112e-05	2.0002e-05
3.0163e+01	6.2228e-05	1.8891e-05	1.4446e-05	2.0372e-05
3.6970e+01	5.6672e-05	1.8520e-05	1.6298e-05	2.4447e-05
4.3494e+01	5.4079e-05	1.8520e-05	1.7780e-05	2.5928e-05
4.9861e+01	5.2227e-05	1.8520e-05	2.1854e-05	2.3336e-05
5.6100e+01	4.9635e-05	1.8520e-05	2.5188e-05	2.2224e-05
6.2142e+01	4.8523e-05	1.7780e-05	2.6669e-05	2.2965e-05
6.8064e+01	4.7783e-05	1.7780e-05	2.6669e-05	2.3706e-05
7.3951e+01	4.7412e-05	1.7780e-05	2.8151e-05	2.2595e-05
7.9811e+01	4.6671e-05	1.7780e-05	2.7781e-05	2.3336e-05
8.5608e+01	4.6671e-05	1.7409e-05	2.9633e-05	2.2595e-05
9.1300e+01	4.4819e-05	1.7409e-05	3.0373e-05	2.3706e-05
9.6821e+01	4.2967e-05	1.7039e-05	3.0744e-05	2.5188e-05
1.0218e+02	4.2226e-05	1.6668e-05	3.0744e-05	2.5928e-05
1.0739e+02	4.1856e-05	1.5928e-05	3.1855e-05	2.6299e-05
1.1251e+02	4.1486e-05	1.5928e-05	3.1855e-05	2.6669e-05
1.1756e+02	4.1486e-05	1.5187e-05	3.1855e-05	2.7040e-05
1.2253e+02	4.1486e-05	1.4816e-05	3.3337e-05	2.6669e-05
1.2744e+02	4.1856e-05	1.4446e-05	3.4077e-05	2.5928e-05
1.3233e+02	4.1486e-05	1.4446e-05	3.6300e-05	2.3706e-05
1.3712e+02	4.1115e-05	1.3705e-05	3.5929e-05	2.5188e-05
1.4179e+02	4.0745e-05	1.3335e-05	3.5189e-05	2.6669e-05
1.4636e+02	4.0374e-05	1.3335e-05	3.7041e-05	2.5188e-05
1.5091e+02	4.0374e-05	1.3335e-05	3.7782e-05	2.4817e-05
1.5547e+02	4.0745e-05	1.2964e-05	3.8152e-05	2.4076e-05
1.5997e+02	4.0374e-05	1.2964e-05	3.9263e-05	2.3706e-05
1.6441e+02	4.0374e-05	1.2594e-05	3.9634e-05	2.3336e-05
1.6881e+02	4.0004e-05	1.2594e-05	3.9634e-05	2.3706e-05
1.7310e+02	3.9263e-05	1.2223e-05	4.0374e-05	2.4076e-05
1.7720e+02	3.8522e-05	1.2223e-05	4.2226e-05	2.3336e-05
1.8125e+02	3.9263e-05	1.1483e-05	4.2597e-05	2.2595e-05
1.8526e+02	3.8893e-05	1.1483e-05	4.1856e-05	2.3706e-05
1.8925e+02	3.8893e-05	1.1483e-05	4.1856e-05	2.3706e-05
1.9325e+02	3.8893e-05	1.1483e-05	4.1856e-05	2.3706e-05
1.9717e+02	3.8152e-05	1.1483e-05	4.2967e-05	2.3706e-05
2.0103e+02	3.7782e-05	1.1112e-05	4.4449e-05	2.2595e-05
2.0474e+02	3.7782e-05	1.0742e-05	4.5560e-05	2.1854e-05
2.0835e+02	3.8522e-05	1.0001e-05	4.5930e-05	2.1854e-05
2.1194e+02	3.8522e-05	1.0001e-05	4.5930e-05	2.1854e-05
2.1546e+02	3.7782e-05	1.0001e-05	4.7042e-05	2.1113e-05
2.1879e+02	3.6300e-05	9.6306e-06	4.7412e-05	2.2595e-05
2.2196e+02	3.6300e-05	9.6306e-06	4.8153e-05	2.1854e-05
2.2513e+02	3.6300e-05	9.6306e-06	4.8153e-05	2.2224e-05
2.2831e+02	3.6300e-05	9.6306e-06	4.7042e-05	2.2965e-05

2.3129e+02	3.6300e-05	8.8898e-06	4.7412e-05	2.3706e-05
2.3421e+02	3.5929e-05	8.8898e-06	4.7042e-05	2.4076e-05
2.3711e+02	3.5929e-05	8.8898e-06	4.7783e-05	2.3336e-05
2.4000e+02	3.5929e-05	8.8898e-06	4.8153e-05	2.3336e-05

SIMULATED DATA FOR NH_3 /Cl^- OXIDATION: CTTS FORMATION (RATE 2.8 X 10^{-4} S^{-1}) AND Cl SCAVENGING FROM NO_2^-

--- Simulation data for file "c:\docume~1\admini~1\desktop\n-cl.rxn"
--- This table was created on Sun Dec 17 23:44:00 2006

Time	NH3	NH4	NO2-	NO3-
min	mole/l	mole/l	mole/l	mole/l
0.0000e+00	9.6676e-05	1.9632e-05	0.0000e+00	0.0000e+00
8.8174e+00	7.7045e-05	1.8891e-05	6.2969e-06	1.3705e-05
1.7120e+01	7.0377e-05	1.8520e-05	8.1490e-06	1.8520e-05
2.5061e+01	6.2969e-05	1.8520e-05	1.3335e-05	2.1113e-05
3.2637e+01	5.9636e-05	1.7409e-05	1.6298e-05	2.2595e-05
3.9819e+01	5.4450e-05	1.7039e-05	1.9261e-05	2.4447e-05
4.6662e+01	5.2227e-05	1.7039e-05	2.1484e-05	2.5188e-05
5.3324e+01	5.0005e-05	1.7039e-05	2.1854e-05	2.7040e-05
5.9731e+01	4.7042e-05	1.6668e-05	2.4076e-05	2.7781e-05
6.5936e+01	4.5560e-05	1.6298e-05	2.5188e-05	2.8521e-05
7.1944e+01	4.5190e-05	1.5557e-05	2.8521e-05	2.6669e-05
7.7832e+01	4.4819e-05	1.4816e-05	2.8521e-05	2.7410e-05
8.3599e+01	4.4078e-05	1.4816e-05	2.9633e-05	2.7781e-05
8.9237e+01	4.3338e-05	1.4816e-05	3.0003e-05	2.7781e-05
9.4774e+01	4.2226e-05	1.4446e-05	3.2596e-05	2.6669e-05
1.0018e+02	4.2226e-05	1.4075e-05	3.2596e-05	2.7410e-05
1.0552e+02	4.2226e-05	1.3705e-05	3.2596e-05	2.7781e-05
1.1078e+02	4.1486e-05	1.3705e-05	3.4077e-05	2.7040e-05
1.1593e+02	4.1486e-05	1.3335e-05	3.4818e-05	2.6669e-05
1.2098e+02	4.0745e-05	1.3335e-05	3.7782e-05	2.4447e-05
1.2601e+02	4.1115e-05	1.2964e-05	3.8522e-05	2.3706e-05
1.3098e+02	4.0374e-05	1.2594e-05	3.8522e-05	2.4817e-05
1.3581e+02	4.0004e-05	1.2594e-05	3.8893e-05	2.4447e-05
1.4052e+02	3.9634e-05	1.2223e-05	3.9634e-05	2.4076e-05
1.4519e+02	3.9634e-05	1.2223e-05	4.0745e-05	2.3706e-05
1.4986e+02	3.9634e-05	1.2223e-05	4.2226e-05	2.2224e-05
1.5453e+02	3.9263e-05	1.2223e-05	4.2967e-05	2.1854e-05
1.5914e+02	3.8893e-05	1.2223e-05	4.2967e-05	2.2224e-05
1.6366e+02	3.8152e-05	1.1853e-05	4.3708e-05	2.2595e-05
1.6800e+02	3.7782e-05	1.1853e-05	4.4449e-05	2.1854e-05
1.7229e+02	3.8152e-05	1.1483e-05	4.4078e-05	2.2224e-05

1.7652e+02	3.8522e-05	1.0742e-05	4.4078e-05	2.2595e-05
1.8067e+02	3.8893e-05	1.0371e-05	4.4449e-05	2.2595e-05
1.8475e+02	3.8152e-05	1.0371e-05	4.5190e-05	2.2595e-05
1.8869e+02	3.8152e-05	1.0001e-05	4.4449e-05	2.2965e-05
1.9252e+02	3.7411e-05	9.6306e-06	4.6301e-05	2.2595e-05
1.9616e+02	3.7782e-05	9.2602e-06	4.7042e-05	2.1854e-05
1.9973e+02	3.7411e-05	9.2602e-06	4.7783e-05	2.1484e-05
2.0319e+02	3.6300e-05	9.2602e-06	4.8894e-05	2.1484e-05
2.0653e+02	3.5929e-05	9.2602e-06	4.8894e-05	2.2224e-05
2.0979e+02	3.6300e-05	8.8898e-06	4.8523e-05	2.2224e-05
2.1304e+02	3.6300e-05	8.8898e-06	4.8153e-05	2.2224e-05
2.1625e+02	3.6300e-05	8.5194e-06	4.8523e-05	2.2224e-05
2.1939e+02	3.6300e-05	8.5194e-06	4.9264e-05	2.1854e-05
2.2246e+02	3.5929e-05	8.5194e-06	4.8523e-05	2.2224e-05
2.2553e+02	3.5929e-05	8.5194e-06	4.9635e-05	2.2224e-05
2.2859e+02	3.5929e-05	8.5194e-06	4.9264e-05	2.2224e-05
2.3165e+02	3.5559e-05	8.5194e-06	4.9635e-05	2.2595e-05
2.3457e+02	3.5559e-05	8.1490e-06	5.0005e-05	2.2224e-05
2.3741e+02	3.4818e-05	8.1490e-06	5.0746e-05	2.2224e-05
2.4000e+02	3.4077e-05	8.1490e-06	5.0005e-05	2.3706e-05

TABLES OF SELECTED EXPERIMENTAL RESULTS

1.0 UV IRRADIATION OF HALIDE IONS IN THE ABSENCE OF AMMONIA

UV IRRADIATION OF Br^- = 2.2 mg/L

IRRADIATION TIME (MINUTES)	pH	Br^- CONCENTRATION (MG/L)	
0.0000	5.7500	2.2470	2.2710
10.0000	5.7500	2.1760	LC
20.5000	5.7400	2.2760	2.2360
30.0000	5.7400	LC	LC
45.0000	5.7300	2.1500	2.1760
60.0000	5.7200	2.2520	2.2680
60.0000	9.9700	2.2540	2.2510
81.0000	9.9600	LC	2.1430
100.0000	9.9500	2.1790	2.1770
120.0000	9.9400	2.2220	2.2390

UV IRRADIATION OF Cl^- = 23 mg/L

IRRADIATION TIME (MINUTES)	pH	Cl^- CONCENTRATION	
0.0000	5.9800	23.0080	LC
10.0000	5.9800	LC	LC
20.0000	5.9700	22.1820	22.9360
30.0000	5.9600	22.9770	LC
45.0000	5.9400	LC	LC
60.0000	5.9300	22.1740	22.8720
60.0000	10.0800	22.7890	LC
80.0000	10.0600	LC	LC
100.0000	10.0400	22.1880	22.5370
120.0000	10.0200	22.9430	LC

LC – Lost chromatogram

UV IRRADIATION OF $I^- \approx 2.2$ mg/L

TIME (MINUTES)	pH	I^- CONCENTRATION	
0.0000	5.7200	2.2130	2.2140
5.0000	5.9500	2.1830	2.1840
10.0000	6.1100	2.1190	2.1170
20.0000	6.3500	1.9260	1.9280
30.0000	6.5300	1.7090	1.7120
45.0000	6.7000	1.6220	1.6260
60.0000	6.8500	1.3610	1.3650
60.0000	9.7900	1.8420	1.8450
65.0000	9.7700	1.8320	1.8290
80.0000	9.7400	1.6220	1.6260
100.0000	9.7200	1.5210	1.5240
120.0000	9.7000	1.3450	1.3450

2.0 UV IRRADIATION OF HALIDE IONS IN THE PRESENCE OF AMMONIA

UV IRRADIATION OF Br^- = 0.635 mg/L IN THE PRESENCE OF NH_3-N = 0.03 mg/L

TIME (MINUTES)	pH	Br^- CONCENTRATION	NO_3^-
0.0000	5.57	0.635	-
5.0000	5.54	0.635	-
15.0000	5.47	0.634	0.004
25.0000	5.41	0.635	0.008
40.5000	5.34	0.635	0.011
60.0000	5.27	0.634	0.015

UV IRRADIATION OF Br^- = 0.635 mg/L IN THE PRESENCE OF NH_3-N = 0.19 mg/L

TIME (MINUTES)	pH	Br^- CONCENTRATION	NO_3^-
0.0000	5.57	0.634	-
5.0000	5.51	0.634	-
15.0000	5.41	0.634	0.009
25.0000	5.34	0.634	0.015
40.5000	5.24	0.633	0.021
60.0000	5.14	0.635	0.025

UV IRRADIATION OF Br^- = 0.635 mg/L IN THE PRESENCE OF NH_3-N = 0.8 mg/L

TIME (MINUTES)	pH	Br^- CONCENTRATION	NO_3^-
0.0000	5.64	0.633	-
5.0000	5.54	0.635	-
15.0000	5.38	0.636	0.013
25.0000	5.26	0.635	0.022
40.5000	5.13	0.634	0.033
60.0000	5.00	0.634	0.046

UV IRRADIATION OF Br^- = 2.22 mg/L IN THE PRESENCE OF NH_3-N = 1.6 mg/L

TIME (MINUTES)	pH	Br^- CONCENTRATION	NO_3^-
0.0000	5.58	2.2220	1.0000e-3
5.0000	5.20	2.2200	4.0000e-3
10.0000	4.96	2.2270	0.0100
20.0000	4.71	2.2290	0.0160
30.0000	4.55	2.2340	0.0240
45.5000	4.42	2.2230	0.0350
60.0000	4.33	2.2100	0.0440

UV IRRADIATION OF Br^- = 0.1 mg/L IN THE PRESENCE OF NH_3-N = 1.6 mg/L

TIME (MINUTES)	pH	DO (%)	NO_3^-	$NO3^-$
0.0000	5.70	88.6	1.0000e-3	2.0000e-3
5.0000	5.68	86.4	2.0000e-3	1.0000e-3
10.0000	5.65	85.5	3.0000e-3	3.0000e-3
20.0000	5.59	84.7	7.0000e-3	6.0000e-3
30.0000	5.55	84.2	8.0000e-3	0.0110
45.0000	5.49	83.8	0.0120	0.0120
60.0000	5.44	83.5	0.0160	0.0160
90.0000	5.37	83.0	0.0210	0.0190
120.0000	5.32	82.4	0.0220	-
150.0000	5.27	82.1	0.0260	0.0250

UV IRRADIATION OF Br^- = 2.28 mg/L IN THE PRESENCE OF NH_3-N = 1.6 mg/L and SF_6

Time (min.)	DO [%]	pH	Br^- [mg/L]		NO_3^- [mg/L]		NO_2^- [mg/L]		F^- [mg/L]		SO_4^{2-} [mg/L]	
0	97.3	5.58	2.288	2.266	0.000	1.0000e-3	0.0000	0.0000	0.0000	0.0000	6.6540	6.5760
5	97.7	5.20	2.275	2.267	6.000e-3	5.0000e-3	9.0000e-3	4.0000e-3	0.0300	0.0410	6.7980	6.6510
10	97.3	4.96	2.273	2.287	9.000e-3	8.0000e-3	4.0000e-3	7.0000e-3	0.0840	0.0980	6.7140	6.8840
20	96.6	4.71	2.229	2.289	0.0130	0.0180	1.0000e-3	9.0000e-3	0.1530	0.1930	6.7730	6.9060
30.5	96.0	4.55	2.263	2.273	0.0200	0.0250	5.0000e-3	7.0000e-3	0.2770	0.2930	6.9290	7.0680
45	95.6	4.42	2.273	2.280	0.0310	0.0340	5.0000e-3	7.0000e-3	0.3820	0.4320	7.1870	7.0880
60	95.3	4.33	2.266	2.228	0.0400	0.0410	6.0000e-3	9.0000e-3	0.4760	0.5220	7.2020	-
90	95.1	4.22	2.289	2.304	0.0580	0.0600	8.0000e-3	8.0000e-3	0.6970	0.6930	7.4930	7.5380
120	95.2	4.15	2.266	2.293	0.0730	0.0740	8.0000e-3	0.0110	0.8140	0.8000	7.6250	7.6360
150	95.4	4.10	2.285	2.284	0.0910	0.0880	9.0000e-3	0.0110	0.8840	0.9140	7.6890	7.6940

UV IRRADIATION OF Br^- = 2.28 mg/L IN THE PRESENCE OF NH_3-N = 1.6 mg/L and SF_6

Time (min.)	DO [%]	pH	Ammonia [mg/L]		Br^- [mg/L]		NO_3^- [mg/L]		NO_2^- [mg/L]		F^- [mg/L]		SO_4^{2-} [mg/L]	
0	80.2	8.64	0.87	0.80	2.3230	2.3240	0.0000	0.0000	1.0000e-3	1.0000e-3	0.0000	0.0000	5.38640	5.40840
5	78.8	8.29	0.79	0.82	2.3230	2.3520	0.0200	0.0210	0.0250	0.0240	0.0640	0.0660	5.36700	5.42670
15	77.4	6.41	0.75	0.73	2.3210	2.3400	0.0550	0.0560	0.0170	0.0180	0.2110	0.2320	5.41750	5.41750
30	77.4	5.01	0.85	0.77	2.3050	2.3210	0.0840	0.0860	8.0000e-3	8.0000e-3	0.4370	0.4560	5.43600	5.38860
45	78.3	4.65	0.95	0.80	2.3250	-	0.0950		0.0100		0.6040		5.46340	
60	79.2	4.48	0.76	0.75	2.2860	2.2990	0.1050	0.1030	0.0120	9.0000e-3	0.7310	0.7680	5.42580	5.58760
90	81.5	4.31	0.76	0.74	2.3400	2.3480	0.1260	0.1270	0.0130	0.0110	0.9570	0.9740	5.45570	5.50670
120	84.5	4.23	0.72	0.76	2.3230	2.3220	-	0.1400	1.0000e-3	0.0150	-	1.0520	5.38640	5.50010

UV IRRADIATION OF Cl^- = 1 mg/L IN THE PRESENCE OF NH_3-N = 1.6 mg/L and SF_6

Time (min.)	DO [%]	pH	Cl^- [mg/L]		NO_3^- [mg/L]		F^- [mg/L]		SO_4^{2-} [mg/L]	
0	86.4	5.69	0.965	0.966	0.0000	0.0000	0	0	6.588	6.657
2	84.9	5.62	0.968	0.968	3.0000e-3	3.0000e-3	0.003	0.004	6.637	6.699
5	85.1	5.51	0.966	1.008	3.0000e-3	3.0000e-3	0.01	0.011	6.653	6.739
10	86.0	5.37	0.96	0.961	4.0000e-3	3.0000e-3	0.035	0.032	6.659	6.621
20	86.1	5.15	0.962	0.958	4.0000e-3	3.0000e-3	0.069	0.071	6.677	6.694
30	85.7	5.01	0.961	0.96	6.0000e-3	4.0000e-3	0.106	0.116	6.75	6.742
45	85.4	4.86	0.968	0.945	5.0000e-3	5.0000e-3	0.159	0.154	6.798	6.778
60	85.3	4.76	1.008	0.964	6.0000e-3	5.0000e-3	0.211	0.21	6.804	6.851
75	85.5	4.69	0.968	0.961	5.0000e-3	9.0000e-3	0.232	0.251	6.844	6.979
90	86.0	4.64	0.966	0.967	6.0000e-3	6.0000e-3	0.283	0.284	6.978	6.951
120	86.4	4.58	0.964	0.969	7.0000e-3	7.0000e-3	0.325	0.329	6.996	7.212
150	86.8	4.55	0.972	0.968	9.0000e-3	0.0100	0.357	0.359	7.091	7.047
180	86.6	4.54	0.973	0.963	9.0000e-3	0.0100	0.373	0.375	7.102	7.061
240	86.4	4.52	1.008	0.968	0.0110	9.0000e-3	0.39	0.394	7.212	7.121

UV IRRADIATION OF Cl^- = 20 mg/L IN THE PRESENCE OF NH_3-N = 4.91 mg/L and SF_6

Time (min.)	DO [%]	pH	Cl^- [mg/L]		NO_3^- [mg/L]		F^- [mg/L]		SO_4^{2-} [mg/L]	
0	83.7	5.58	19.896	19.708	0.0000	0.0000	0.0000	0.0000	0.0000	0.0000
2	84.1	5.33	19.773	19.499	2.0000e-3	2.0000e-3	0.0330	0.0280	0.0410	0.0500
5	84.6	5.02	19.604	19.795	3.0000e-3	4.0000e-3	0.1070	0.0980	0.1130	0.1460
10	84.3	4.74	19.799	19.845	4.0000e-3	6.0000e-3	0.2380	0.2180	0.2320	0.2540
20	83.6	4.47	19.631	19.570	0.0100	0.0100	0.4430	0.4320	0.4210	0.4300
30	83.5	4.33	19.785	19.737	0.0110	0.0120	0.6090	0.5950	0.6150	0.5860
45	83.5	4.21	19.571	19.585	0.0130	0.0150	0.8010	0.8040	0.7800	0.7900
60	83.5	4.14	19.584	19.837	0.0160	0.0190	0.9940	0.9650	0.9400	0.9850
75	83.5	4.09	19.757	19.869	0.0180	0.0200	1.1260	1.1060	1.0940	1.1220
90	83.7	4.06	19.875	19.803	0.0210	0.0190	1.2180	1.2170	1.1810	1.2120
120	85.3	4.02	19.808	19.613	0.0220	0.0230	1.3440	1.3490	1.3110	1.3040
150	86.2	4.00	19.716	19.672	0.0260	0.0250	1.4060	1.3830	1.3580	1.3740
180	86.7	4.00	19.931	19.653	0.0280	0.0260	1.4270	1.4370	1.4290	1.4490
240	87.1	3.99	19.856	19.882	0.0310	0.0310	1.4530	1.4600	1.4680	1.4680

UV IRRADIATION OF Br^- = 2.2 mg/L IN THE PRESENCE OF NH_3-N = 0.7 mg/L

Time (min.)	pH	NH3 [mg/L]		NO_2^- [mg/L]		NO_3^- [mg/L]	
0	10.11	0.7180	1.6237	0.0000	0.0000	0.0000	0.0000
5	10.07	0.6580	1.5138	0.0430	0.0420	0.0180	0.0190
10	10.05	0.6300	1.4140	0.0520	0.0540	0.0310	0.0320
20	10.01	0.5520	1.3043	0.0790	0.0870	0.0550	0.0550
30	9.99	0.5030	1.2033	0.0850	0.0980	0.0680	0.0720
45	9.95		1.0677	0.1110	0.1060	0.0880	0.0880
60	9.92	0.4050	0.9413	0.1240	0.1300	0.1080	0.1050
90	9.86	0.3650	0.7577	0.1450	0.1350	0.1330	0.1320
120	9.80	0.2980	0.6418	0.1570	0.1570	0.1550	0.1560
150	9.74	0.2650	0.6006	0.1760	0.1690	0.1770	0.1690
184	9.65	0.2160	0.5847	0.1720	0.1680	0.1920	0.1940
210	9.58	0.2040	0.5738	0.1730	0.1830	0.2080	0.2050
240	9.49	0.1690	0.5680	0.1620	0.1760	0.2200	0.2190

UV IRRADIATION OF Cl^- = 20 mg/L IN THE PRESENCE OF NH_3-N = 1.6 mg/L

Time (min.)	DO [%]	pH	NH3 [mg/L]		NO_2^- [mg/L]		NO_3^- [mg/L]	
0	95.4	10.15	1.6265	1.6237	0.0000	0.0000	0.0000	0.0000
5	91.3	10.07	1.5141	1.5138	0.0800	0.0790	0.0410	0.0430
10	89.5	10.02	1.4146	1.4140	0.1270	0.1230	0.0730	0.0740
20	86.5	9.92	1.3052	1.3043	0.1680	0.1980	0.1220	0.1240
30	84.1	9.83	1.2042	1.2033	0.2450	0.2430	0.1560	0.1540
45	81.5	9.68	1.0670	1.0677	0.2930	0.3010	0.2230	0.2280
60	80.7	9.52	0.9410	0.9413	0.3530	0.3500	0.2890	0.2900
90	81.7	9.08	0.7579	0.7577	0.3780	0.3790	0.4510	0.4490
120	83.9	8.36	0.6415	0.6418	0.3060	0.3030	0.5920	0.6000
150	86.4	7.27	0.6016	0.6006	0.1720	0.1780	0.7870	0.7920
180	88.4	6.84	0.5851	0.5847	0.0880	0.0930	0.9020	0.9090
210	89.9	6.61	0.5739	0.5738	0.0770	0.0780	0.9120	0.9360
240	90.7	6.46	0.5663	0.5680	0.0480	0.0480	0.9630	0.9680

BIBLIOGRAPHY

1. Anawar, H.M.; Akai, J.; Komaki, K.; Terao, H.; Yoshioka, T.; Ishizuka, T.; Safiullah, S.; Kato, K. (2003). Geochemical occurrence of arsenic in groundwater of Bangladesh: sources and mobilization processes. *Journal of Geochemical Exploration*, 77, 109 – 131.
2. Asmus, K. and Fendler, J. "Reaction of sulphur hexafluoride with hydrated electrons" *The Journal of Phys. Chem*. Vol. 72, (1968) 4285-4289.
3. Amy, G.; Siddiqui, M.; Zhai, W.; DeBroux, J. and Odem, W. (1993). Nation-wide survey of bromide ion concentrations in drinking water sources. Proceedings – 1993 AWWA Annual Conference, 1 – 19.
4. Bartels, D. and Crowell, R. (2000). Photoionization yield vs energy in H_2O and D_2O. *The Journal of physical Chemistry*, vol.104, no.15, pp 3349-3355.
5. Barthel, E.R.; Schwartz, B.J. (2003). *J. Chem. Phys. Lett.* 375, 435.
6. Bems, B., Jentoft, F. C. and Schlogl, R. (1999). Photoinduced decomposition of nitrate in drinking water in the presence of titania and humic acids. *Applied Catalysis B: Environmental*, vol.20, pp 155-163.
7. Blandamer, M.J; Fox, M.F. (1970). Theory and Applications of Charge-transfer-to-solvent spectra. *Chem. Rev. 70,* 59-93.
8. Bonsen, E.M.; Schroeter, S.; Jacobs, H.; Broekaert, J.A.C. (1997). Photocatalytic degradation of ammonia with TiO2 as photocatalyst in the laboratory and under the use of solar radiation. Chemosphere, 35 (7) 1431 – 1445.

9. Borgis, D.; Staib, A. (1996). Ultrafast spectroscopy of the aqueous chloride ion studied by quantum molecular dynamics simulation. *J. Phys.: Condens. Matter* 8, 9389 – 9395.

10. Bourgine, F.P.; Chapman, J.I.; Kerai, H.; Green, J.G. 1993. Ozone and formation of bromate in water treatment. *Journal of the Institute of Water and Environmental Management*, 7, 571 – 576.

11. Boyle, J., Ghormley, J. Hochanadel, C. and Riley, J. (1969). Production of hydrated electrons by flash photolysis of liquid water with light in the first continuum. *The Journal of physical Chemistry*, vol.73, no.9, pp 2886-2890.

12. Braden, D.A., Parrack, E.E. and Tyler, D.R. (2001). Solvent cage effects. I. Effect of radical mass and size on radical cage pair recombination efficiency. II. Is geminate recombination of polar radicals sensitive to solvent polarity? *Coordination Chemistry Reviews*, vol.211, pp279-294.

13. Bravo, A.; Garcia, J.; Domenech, X.; Peral, J. (1993). Some aspects of the photocatalytic oxidation of ammonium ions by titanium dioxide. *J. Chem. Res.* 376 – 377.

14. Brezonik, P. L. and Fulkerson-Brekken, J. (1998). Nitrate-induced photolysis in natural waters: Controls on concentrations of hydroxyl radical photo-intermediates by natural scavenging agents. *Environmental Science and Technology*, vol.32, no.19, pp 3004-3010.

15. Buxton, G. and Dainton, F. (1968). The radiolysis of aqueous solutions of oxybromine compounds; the spectra and reactions of BrO and BrO_2. *Proc. Roy. Soc. A*., vol.304, pp 427-439.

16. Buxton, G.V.; Subhani, M.S. (1972). “Radiation chemistry and photochemistry of oxychlorine ions. Part 3 – Photodecomposition of aqueous solutions of chlorite ions”. *J. Chem. Soc., Faraday Trans*., 68, 970.
17. Chenthamarakshan, C.R. and Krishnan, R. (2000). Heterogeneous photocatalytic Reduction of Cr(VI) in UV-irradiated Titania Suspensions: Effect of Protons, Ammonium ions and Other Interfacial Aspects. *Langmuir*, vol.16, pp 2715-2721.
18. Christensen, H.; Sehested, K. (1983). Reaction of hydroxyl radicals with hydrogen at elevated temperatures. Determination of the activation energy. . *Phys. Chem.;* 87, 118-120.
19. Clutter, D.R.; Swift, T.J. (1968). Ammonium-ammonia proton exchange in liquid ammonia. *J. Am. Chem. Soc.; 90*; 601-607.
20. Cosson, H. and Ernst, W.R. (1994). “Photodecomposition of chlorine dioxide and sodium chlorite in aqueous solution by irradiation with ultraviolet light” *Ind. Eng. Chem. Res.* 33, 1468 – 1475.
21. Czapski, G. Ogdan, J. and Ottolenghi, M. (1969). On the photochemical cage effect in aqueous solutions of halide ions. *Chemical Physics Letters*, vol.3, iss.6, pp383-385.
22. Dainton, F.S.; Fowles, P. (1965). Proc. R. Soc. A. 287, 312.
23. Davis, S.N., Cecil, L.D., Zreda, M., Moysey, S. (2001). Chlorine-36, bromide and the origin of spring water. *Chem. Geol.* 179, 3 – 16.
24. Daw, B.C. Assessment of bromate formation in low bromide natural waters. Ph.D. Thesis, University of Colorado, Boulder, 2000.

25. *Dionex* Application Note 81. Ion Chromatographic determination of oxyhalides and bromide at trace level concentrations in drinking water using direct injection.

26. *Dionex* Application Note 133. Determination of inorganic anions in drinking water by ion chromatography.

27. Duong, H.A.; Berg, M.; Hoang, M.H.; Pham, H.V.; Gallard, H.; Giger, W.; von Gunten, U. (2003). "Trihalomethane formation by chlorination of ammonium- and bromide-containing groundwater in water supplies of Hanoi, Vietnam". *Water Research*, 37, 3242 – 3252.

28. Dwibedy, P., Kishore, K., Dey, G. and Moorthy, P. (1996). Nitrite formation in the radiolysis of aerated aqueous solutions of ammonia. *Radiation Physics and Chemistry*, vol.48, iss.6, pp 743-747.

29. Elliot, A.J. (1989). A pulse radiolysis study of the temperature dependence of reactions involving H, OH and e^-_{aq} in aqueous solutions. *International Journal of Radiation Applications and Instrumentation. Part C. Radiation Physics and Chemistry***,** 34, 753-758.

30. EU, 1998. Official J. Eur. Community L 330. Directive 98/83/EG.

31. Farkas, L. and Klein, F.S. (1948). On the Photo-Chemistry of Some Ions in Solution. *J. Chemical Physics*, Vol.16, no.9, pp 886-893.

32. Fischer, M. and Warneck, P. 1996 'Photodecomposition of Nitrite and Undissociated Nitrous Acid in Aqueous Solution' *J. Phys. Chem.* 100, 18749 – 18756.

33. Garrett, B. C.; Dixon, D. A.; Camaioni, D. M.; Chipman, D. M.; Johnson, M. A.; Jonah, C. D.; Kimmel, G. A.; Miller, J. H.; Rescigno, T. N.; Rossky, P. J.;

Xantheas, S. S.; Colson, S. D.; Laufer, A. H.; Ray, D.; Barbara, P. F.; Bartels, D. M.; Becker, K. H.; Bowen, K. H., Jr.; Bradforth, S. E.; Carmichael, I.; Coe, J. V.; Corrales, L. R.; Cowin, J. P.; Dupuis, M.; Eisenthal, K. B.; Franz, J. A.; Gutowski, M. S.; Jordan, K. D.; Kay, B. D.; LaVerne, J. A.; Lymar, S. V.; Madey, T. E.; McCurdy, C. W.; Meisel, D.; Mukamel, S.; Nilsson, A. R.; Orlando, T. M.; Petrik, N. G.; Pimblott, S. M.; Rustad, J. R.; Schenter, G. K.; Singer, S. J.; Tokmakoff, A.; Wang, L.-S.; Wettig, C.; Zwier, T. S. (2005). Role of Water in Electron-Initiated Processes and Radical Chemistry: Issues and Scientific Advances. *Chem. Rev.;* 105, 355-390.

34. Gauduel, Y.; Gelabert, H.; Ashokkumar, M. (1995). Short-lived charge-transfer-to-solvent-states and multiple electronic relaxations following femtosecond excitation of aqueous chloride ion. *Chem. Phys.;* 197, 167 – 193.
35. Gillespie, D.T. (1977). Exact Stochastic Simulation of Coupled Chemical Reactions. J. Phys. Chem. 81, 2340 – 2361.
36. Glaze, W.H.; Weinberg, H.S.; Cavanaugh, J.E. *J. Am. Water Works Assoc*. 1993, 85, 96.
37. Goldstein, S.; Lind, J.; Mereny, G. (2005). *Chem. Rev.* 105, 2457 – 2470.
38. Gonzalez, M.C. and Braun, A.M. (1996). Vacuum-UV photolysis of aqueous solutions of nitrate: effect of organic matter. I. Phenol. *Journal of Photocheistry and Photobiology A: Chemistry*, 93, 7 – 19.
39. Halfpenny, E. and Robinson, P.L. (1952). J. Chem. Soc. A 928 – 938.
40. Hamill, W.H. (1968) J. Chem. Phys., 49, 2446.
41. Hamill, W.H. (1969) J. Chem. Phys., 73, 1341.

42. Hanes, R.E., Zelazny, L.W. and Blaser, R.E. (1970). *NCHRP Report 91*: Effects of Deicing Salts on Water Quality and Biata: Literature Review and Recommended Research. HRB, National Research Council, Washington, D.C.

43. Hart, E. and Anbar, M. (1970). The Hydrated Electron. Wiley-Interscience, a division of John Wiley & Sons.

44. Heit, G., Neuner, A., Saugy, P. and Braun, A. (1998). Vacuum-UV ($\lambda < 172$ nm) Actinometry. The quantum yield of the photolysis of water. *Journal of Physical Chemistry A*, vol.102, no.28, pp 5551-5561.

45. Health Canada Website. "Bromate", October 1998. 1 – 11, http://www.hc-sc.gc.ca/.

46. Health Canada Website. "Ammonia", August 1978 (updated November 1987). 1 – 3, http://www.hc-sc.gc.ca/.

47. Hodges, G. R.; Ingold, K. U. (1999). Cage-Escape of Geminate Radical Pairs Can Produce Peroxynitrate from Peroxynitrite under a Wide Variety of Experimental Conditions[1] *J. Am. Chem. Soc.; 121*(46); 10695-10701.

48. Hofmann, R. and Andrews, R. (2001). Review Paper. Ammoniacal bromamines: a review of their influence on bromate formation during ozonation. *Water Research*, vol.35, no.3, pp 599-604.

49. Horvath, O.; Stevenson, K.L. (1989). Inorg. Chem. 28, 2548 – 2551.

50. Houghton, G.U. 1946. The bromide content of underground waters Part I. Determination and occurrences of traces of bromide in water. *Journal of the Society of Chemical Industry*, 65, 277 – 280.

51. Hutchinson, J.; Bailey, K.; Lunt, D.; Ofgen, T.; Fielding, M. (1995). Effects of disinfectants on organic substances in water. *National Centre for Environmental Toxicology, Water Research Centre*, Medmenham, UK.

52. Inman, G. Jr. and Johnson, D. (1984). Kinetics of monobromamine disproportionation – dibromamine formation in aqueous ammonia solution. *Environmental Science and Technology*, vol.18, no.4, pp219-224.

53. Jortner, J. Ottolenghi, M. and Stein, G. (1964). On the Photochemistry of Aqueous Solutions of Chloride, Bromide and Iodide Ions. *The Journal of Physical Chemistry*, vol.68, no.2, pp247-255.

54. Karpel Vel Leitner, N.; De Laat, J.; Dore, M. (1992a). "Photodecomposition of chlorine dioxide and chlorite by UV irradiation – Part 1. Kinetic Study. *Water Research,* 26, 1655.

55. Karpel Vel Leitner, N.; De Laat, J.; Dore, M. (1992b). "Photodecomposition of chlorine dioxide and chlorite by UV irradiation – Part II. Photoproducts. *Water Research,* 26, 1665.

56. Kirsch, M.; Korth, H-G.; Wensing, A.; Sustmann, R.; de Groot, H. (2003) Product formation and kinetic simulations in the pH range 1 – 14 account for a free-radical mechanism of peroxynitrite decomposition. Archives of Biochemistry and Biophysics, 418, 133 – 150.

57. Kloepfer, J. A.; Vilchiz, V.H.; Lenchenkov, V.A.; Chen, X.; Bradforth, S.E. (2002). *J. Chem. Phys.* 117, 776.

58. Kloepfer, J. A.; Vilchiz, V.H.; Germaine A.C.; Lenchenkov, V.A.; Bradforth, S.E. (2000). *J. Chem. Phys.* 113, 6288.

59. Krasner, S.W., McGuire, M.J., Jacangelo, J.G., Patania, N.L., Reagan, K.M. and Aieta, E.M. (1989), The Occurrence of disinfection by-products in US drinking water. *Journal of American Water Works Association*, 81, 41 – 53.

60. Krasner, S.W., Glaze, W.H.; Weinberg, H.S.; Daniel, P.A., and Najm, I.N. (1993). Formation and control ob bromate during ozonation of waters containing bromide. *Journal of American Water Works Association*, 85, 73 – 81.

61. Krasner, S.W., Gramith, J.T.; Means, E.G. (1991). Formation and control of brominated ozone by-products. Presented at the 1991 Annual American Water Works Association Conference, Philadelphia, PA.

62. Kurama, H.; Poetzschke, J.; Haseneder, R. (2002). The application of membrane filtration for the removal of ammonium ions from potable water. *Water Research*, 36, 2905 – 2909.

63. Laszlo, B., Alfassi, Z., Neta, P. and Huie, R. (1998). Kinetics and Mechanism of the reaction of $^{*}NH_2$ with O_2 in aqueous solutions. *Journal of Physical Chemistry A*, vol.102, no.44, pp 8498-8504.

64. Lefebvre, E., Racaud, P., Parpaillon, T., Deguin, A. 1995. Results of bromide and bromate monitoring at several water treatment plants. *Ozone: Science & Engineering*, 17, 311 – 327.

65. Legube, B. 1996. A survey of bromate ion in European drinking water. *Ozone: Science & Engineering*, 18, 325 – 328.

66. Leitner, N. and Dore, M. (1997). Mechanism of the reaction between hydroxyl radicals and glycolic, glyoxylic, acetic and oxylic acids in aqueous solution:

consequence on hydrogen peroxide consumption in H_2O_2/UV and O_3/ H_2O_2 systems. *Water Research*, vol.31, no.6, pp 1383-1397.

67. Leitner, N., Vessella, J., Dore, M. and Legube, B. 1998. Chlorination and formation of organoiodinated compounds: The important role of ammonia. *Environmental Science and Technology*, 32, 1680 – 1685.
68. Lind, J.; Merenyi, G.; Johansson, E.; Brinck, T. (2003). Reaction of Peroxyl Radicals with Ozone in Water. *J. Phys. Chem. A.;* 107, 676-681.
69. Linder, R., Klinefelter, G. Strader, L. Suarez, J. and Dyer, C. (1994). Acute spermatogenic effects of bromoacetic acids. *Fundamental and Applied Toxicology*, vol.22, pp422-430.
70. Loegager, T.; Sehested, K. (1993**).** Formation and decay of peroxynitric acid: a pulse radiolysis study. *J. Phys. Chem.; 97*(39); 10047-10052.
71. Long, F. H., Shi, X., Lu, H. and Eisenthal, K. B. (1994). "Electron Photodetachment from Halide Ions in Solution: Excited-State Dynamics in the Polarization Well" *The Journal of Physical Chemistry*, Vol. 98, No. 30, 7252-7255.
72. Lymar, S.V.; Hurst, J.K. (1998). Radical Nature of Peroxynitrite Reactivity. *Chem. Res. Toxicol.* 11, 714 – 715.
73. Mack, J. and Bolton, J. R. 1999 'Photochemistry of nitrite and nitrate in aqueous solution: a review' *Journal of Photochemistry and Photobiology A: Chemistry* 128, 1 – 13.
74. Magazinovic, R.S.; Nicholson, B.C.; Mulcahy, D.E. and Davey, D.E. (2004). "Bromide levels in natural waters: its relationship to levels of both chloride and

total dissolved solids and the implications for water treatment". *Chemosphere*, vol. 57, 329 – 335.

75. Mahoney, L.R. (1970). Evidence for the formation of hydroxyl radicals in the isomerization of pernitrous acid to nitric acid in aqueous solution. *J. Am. Chem. Soc., 92*(17); 5262-5263.
76. Male, J. L., Lindfors, B.E., Covert, K. J. and Tyler, D.R. (1998). Effect of radical size and mass on the cage recombination efficiency of photochemically generated radical cage pairs. *Journal of the American Chemical Society*, vol.120, no.50, pp13176-13186.
77. Meunier, L.; Canonica, S.; von Gunten, U 2006, 'Implications of sequential use of UV and ozone for drinking water quality' *Water Research* 40, 1864 – 1876.
78. Michael, G.E. et al (1981). Chlorine dioxide water disinfection: a prospective epidemiology study. *Archives of Environmental Health*, 36, 20 – 27.
79. National Tap Water Quality Database. http://www.ewg.org/tapwater.
80. Noyes, R.M. (1955) *J. Am. Chem. Soc.* 77, 2042.
81. Ohtaki, H.; Radnai, T. (1993). Structure and dynamics of hydrated ions. *Chem. Rev.;* 3, 1157 – 1204.
82. Peters, R., de Leer, E. and Versteegh, J. (1994). Identification of Halogenated compounds produced by chlorination of humic acid in the presence of bromide. *Journal of Chromatography A*, vol.686, iss.2, pp253-261.
83. Pinkernell and von Gunten, 2001 'Bromate Minimization during Ozonation: Mechanistic Considerations'. *Environ. Sci. Technol*. 35, 2525 – 2531.

84. Rao, U., Hollocher, K., Sherman, J., Eisele, I. Frunzi, M.N., Swatkoski, S.J. and Hammons, A.L. (2005). The use of 36Cl and chloride/bromide ratios in discerning salinity sources and fluid mixing patterns: A case study at Saratoga Springs. *Chemical Geology*

85. Rebhun, M., Manka, J., Zilberman, A. 1988. Trihalomethane formation in high-bromide Lake Galilee water. *Journal of American Water Works Association*, 80, 84 – 89.

86. Ross, A.B.; Mallard, W.G.; Helman, W.P.; Buxton, G.V.; Neta, H.P. NDRL/NIST Solution Kinetics Database 3.0, NDRL/NIST, Gaithersburg, MD, 1998.

87. Sacher, F.; Matschi, A.; Brauch, H-J. (1995). Analysis and occurrence of bromate in raw water and drinking water. *Acta hydrochim hydrobiol*, 23, 26 – 30.

88. Sauer, M.C. Jr., Crowell, R.A. and Shkrob, I.A. (2004). "Electron Photodetachment from Aqueous Anions: 1. Quantum Yields for Generation of Hydrated Electron by 193 and 248 nm Laser Photoexcitation of Miscellaneous inorganic Anions" *Journal of Physical Chemistry A*, Vol. 108, No. 25, 5490-5502.

89. Sharpless, C.H. and Linden, K. G. (2001). UV photolysis of nitrate: effects of natural organic matter and dissolved inorganic carbon and implications for UV water disinfection. *Environmental Science and Technology*, vol.35, no.14, pp 2949-2955.

90. Sharpless, C.H. and Linden, K. G. (2003). Experimental and model comparisons of low- and medium-pressure Hg lamps for the direct and H2O2 assisted UV photodegradation of N-nitrosodimethylamine in simulated drinking water. *Environmental Science and Technology*, 37, 1933 – 1940.

91. Shiraishi, H.; Sunaryo, G.R.; Ishigure, K. (1994). J. Phys. Chem. **98**, 5164-5173

92. Siddiqui, M.S., Amy,G.L., Cooper, W.J., Kuruez, C.N., Waite, T.D. and Nickelen, M.G. (1996). Bromate ion Removal by HEEB Irradiation. *Journal AWWA*, vol.88, no.10, pp90-101.

93. Sobolewski, A. L.; Domcke, W. (2003). Photochemistry of $HCl(H_2O)_4$: Cluster Model of the Photodetachment of the Chloride Anion in Water. *J. Phys. Chem. A.; 107*(10); 1557-1562.

94. Steen, H. B. (1970). "Effect of various dry electron scavengers on the radioluminescence of indole in polar solutions." *The Journal of Physical Chemistry*, Vol. 74, No. 23, 4059-4061.

95. Stein, G., Treinin, A. (1958). Trans Faraday Soc, 55, 1086

96. Stumm, W., Morgan, J.J. 1981. Aquatic Chemistry. An Introduction Emphasizing Chemical Equilibria in Natural Waters, John Wiley and Sons, New York.

97. Talu, G. F. and Diyamandoglu, V. 2004 "Formate Ion Decomposition in Water Under UV Irradiation at 253.7 nm." *Environ. Sci. Technol. 38*(14); 3984-3993.

98. USEPA, 1998. Federal Register 63 (241) 69390-69476.

99. USEPA, EPA/625/R-98/004. Handbook of Advanced Photochemical Oxidation Processes, December, 1998.

100. van Dijk-Looijaard, A.M. and van Genderen, A. (2000). Levels of exposure from drinking water. *Food and Chemical Toxicology*, 38, S37 – S42.

101. von Gunten, Urs. (2003). Ozonation of drinking water: Part II. Disinfection and by-product formation in presence of bromide, iodide or chlorine. *Water Research*, 37, 1469-1487.

102. von Gunten, U; Salhi, E. (2000). Bromat imm Trinkwasser – ein problem in der Schweiz? *Gas Wasser Abwasser*, 80, 705 – 710.

103. von Gunten, U.; Bruchet, A.; Costentin, E. 1996. *J. Am. Water Works Assoc*., 88, 53.

104. von Gunten, U. and Oliveras, Y. (1998). Advanced oxidation of bromide-containing water: bromate formation mechanisms. *Environmental science & Technology*, vol.32, no.1, pp 63-70.

105. von Gunten, U. and Pinkernell, U. (2000). Ozonation of bromide-containing drinking waters: a delicate balance between disinfection and bromate formation. *Water Science and Tech*., Vol.41, no.7, pp53-59.

106. Westerhoff, P., Siddiqui, M., Debroux, J., Zhai, W., Ozekin, K. and Amy, G. (1994). Nation-wide bromide occurrence and bromate formation potential in drinking water supplies. *National Conference on Environmental Engineering*, Jul 11-13, pp 670-677.

107. WHO, 1993. Guideline for drinking water quality, vol. 1, Geneva.

108. Xu, Mariano, T., Laskin, J. and Weisel, C. (2002). *Toxicology and Applied Pharmacology*, vol.184, pp19-26.

109. Yamabe, S.; Kouno, H.; Matsumura, K. (2000). A Mechanism of the Ion Separation of the NaCl Microcrystal via the Association of Water Clusters. *J. Phys. Chem. B.; 104*(44); 10242-10252.

110. Zhu, X.; Castleberry, S.R.; Nanny, M.A.; Butler, E.C. (2005). Effects of pH and catalyst concentration on photocatalytic oxidation of aqueous ammonia

and nitrite in titanium dioxide suspensions. *Environmental science & Technology*, vol.39, 3784 – 3791.

111. Neta, P.; Maruthamuthu, P.; Carton, P.M.; Fessenden, R.W. (1978). *J. Phys. Chem.* 82, 1875 – 1878.

112. Maurer, P; Thomas, C.; Kissner, R.; Ruegger, H.; Greter, O.; Rothlisberger, U.; Koppenol, W. (2003). *J. Phys. Chem. A.* 107, 1763 – 1769.

113. Smith, J.E and Frailey, M.M. (1990). "On-Site Evaluation of a Teflon-Based Ultraviolet Light System and Hydrogen Peroxide for the Degradation of Color and Chlorinated Orgaincs in Pine E_0 from Kraft Mill Beach Plant Effluents" *Proceedings, 1990 TAPPI Environmental Conference, Seattle, Washington,* 101 – 110.

114. EPA Handbook, EPA/625/R-98/004. December 1998. Advanced Photochemical Oxidation Processes.